



Chulalongkorn University
จุฬาลงกรณ์มหาวิทยาลัย

การเตรียมสารประกอบเชิงซ้อนโคบอลต์ไอโคซานฟอสเฟต/ซิงก์ออกไซด์เพื่อใช้
งานด้านวัสดุปิดแผลปริทันต์

นางสาววีรนุช สระแก้ว

วิทยานิพนธ์นี้เป็นส่วนหนึ่งของการศึกษาตามหลักสูตรปริญญาวิทยาศาสตรดุษฎีบัณฑิต

สาขาวิชาวัสดุศาสตร์ ภาควิชาวัสดุศาสตร์

คณะวิทยาศาสตร์ จุฬาลงกรณ์มหาวิทยาลัย

ปีการศึกษา 2551

ลิขสิทธิ์ของจุฬาลงกรณ์มหาวิทยาลัย



Chulalongkorn University
จุฬาลงกรณ์มหาวิทยาลัย

PREPARATION OF SODIUM CHITOSAN PHOSPHATE/ZINC OXIDE COMPLEXES FOR
PERIODONTAL DRESSING APPLICATION

Miss Veeranuch Srakaew

A Dissertation Submitted in Partial Fulfillment of the Requirements
for the Degree of Doctor of Philosophy Program in Materials Science

Department of Materials Science

Faculty of Science

Chulalongkorn University

Academic year 2008

Copyright of Chulalongkorn University



Thesis Title PREPARATION OF SODIUM CHITOSAN PHOSPHATE/ZINC
OXIDE COMPLEXES FOR PERIODONTAL DRESSING
APPLICATION
By Miss Veeranuch Srakaew
Field of Study Materials Science
Advisor Wanpen Tachaboonyakiat, Ph.D.
Co-advisor Assistant Professor Kanyarat Suthin, D.D.S., Ph.D.

Accepted by the Faculty of Science, Chulalongkorn University in Partial
Fulfillment of the Requirements for the Doctoral Degree

Science Dean of the Faculty of
Science
(Professor Supot Hannongbua, Dr.rer.nat.)

THESIS COMMITTEE

..... Chairman
(Associate Professor Saowaroj Chuayjuljit)

..... Advisor
(Wanpen Tachaboonyakiat, Ph.D.)

..... Co-advisor
(Assistant Professor Kanyarat Suthin, D.D.S., Ph.D.)

..... Examiner
(Associate Professor Vimolvann Pimpan, Ph.D.)

..... External Examiner
(Associate Professor Ittipol Jangchud, Ph.D.)



วีรบุรุษ สาระแก้ว : การเตรียมสารประกอบเชิงซ้อนโซเดียมโคโตซานฟอสเฟต/ซิงก์ออกไซด์
เพื่อใช้งานด้านวัสดุปิดแผลปริทันต์. (PREPARATION OF SODIUM CHITOSAN
PHOSPHATE/ZINC OXIDE COMPLEXES FOR PERIODONTAL DRESSING
APPLICATION) อ.ที่ปรึกษาวิทยานิพนธ์หลัก : อ.ดร.วันเพ็ญ เตชะบุญเกียรติ,
อ.ที่ปรึกษาวิทยานิพนธ์ร่วม : ผศ.ดร.ทพญ.กัญยารัตน์ สุทิน, 86 หน้า.

สารประกอบเชิงซ้อนโซเดียมโคโตซานฟอสเฟต/ซิงก์ออกไซด์สามารถเตรียมได้โดยการ
ผสมผงซิงก์ออกไซด์เข้าไปในสารละลายโซเดียมโคโตซานฟอสเฟต อัตราส่วนโมลของโซเดียม
โคโตซานฟอสเฟตต่อซิงก์ออกไซด์อยู่ในช่วง 1:0.25-2 โครงสร้างที่น่าจะเป็นไปได้ของ
สารประกอบโลหะเชิงซ้อนวิเคราะห์ด้วย FTIR, XRD, TGA และ DSC ลักษณะพื้นผิวสังเกตโดย
SEM ความแข็งวัดเพื่อวิเคราะห์สมบัติเชิงกลของสารประกอบเชิงซ้อน ความเข้ากันได้ทางชีวภาพ
ของสารประกอบเชิงซ้อนทดสอบกับเซลล์ไฟโบรบลาสต์ของเหงือกโดยใช้โซเดียมโคโตซานฟอสเฟต
เป็นตัวควบคุม พบว่า สารประกอบเชิงซ้อนที่อัตราส่วนต่างๆ น่าจะเกิดเนื่องจากไนโตรเจนในหมู่
แอมีน ออกซิเจนในหมู่ฟอสเฟต และออกซิเจนในหมู่ไฮดรอกซิลของโซเดียมโคโตซานฟอสเฟตให้
อิเล็กทรอนิกส์โคออร์ดิเนชันกับโมเลกุลน้ำล้อมรอบบนพื้นผิวของซิงก์ออกไซด์ สารประกอบเชิงซ้อน
ทั้งหมดที่อัตราส่วนต่างๆ แสดงขึ้นของการสลายตัวของสารประกอบโลหะเชิงซ้อนในช่วง 200-
220 องศาเซลเซียส ซึ่งไม่พบในโซเดียมโคโตซานฟอสเฟต ความแข็งของสารประกอบเชิงซ้อน
เพิ่มขึ้นเมื่อเพิ่มปริมาณซิงก์ออกไซด์ จากการทดสอบการสัมผัสตรงกับเซลล์สารประกอบเชิงซ้อน
ที่อัตราส่วน 1:0.25 และ 1:0.5 แสดงถึงความเข้ากันได้ทางชีวภาพได้ดีเหมือนตัวควบคุม ซึ่ง
เหมาะสำหรับประยุกต์ใช้ด้านวัสดุปิดแผลทางปริทันต์ ขณะที่สารประกอบเชิงซ้อนที่อัตราส่วนโมล
1:1 และ 1:2 แสดงถึงความเป็นพิษต่อเซลล์ เนื่องจากปริมาณซิงก์ออกไซด์จำนวนมากปกคลุม
พื้นผิวของสารประกอบเชิงซ้อน จากการทดสอบการสัมผัสโดยอ้อมกับเซลล์ สารที่สกัดออกมา
จากสารประกอบเชิงซ้อนทุกอัตราส่วนแสดงความเข้ากันได้ทางชีวภาพได้ดีเหมือนตัวควบคุม

ภาควิชา วัสดุศาสตร์ ลายมือชื่อ.....
สาขาวิชา วัสดุศาสตร์ ลายมือชื่ออ.ที่ปรึกษาวิทยานิพนธ์หลัก.....
ปีการศึกษา...2551..... ลายมือชื่ออ.ที่ปรึกษาวิทยานิพนธ์ร่วม.....



4873892323 :MAJOR MATERIALS SCIENCE

KEY WORD : PERIODONTAL DRESSING/COMPLEX/SODIUM CHITOSAN PHOSPHATE/
 ZINC OXIDE

VEERANUCH SRAKAEW : PREPARATION OF SODIUM CHITOSAN
 PHOSPHATE/ZINC OXIDE COMPLEXES FOR PERIODONTAL DRESSING
 APPLICATION ADVISOR : WANPEN TACHABOONYAKIAT, Ph.D., THESIS
 COADVISOR : ASST. PROF. KANYARAT SUTHIN, D.D,S, Ph.D., 86 pp.

Sodium chitosan phosphate/zinc oxide complexes were prepared by mixing zinc oxide powder to sodium chitosan phosphate aqueous solution. Mole ratios of sodium chitosan phosphate to zinc oxide were varied in the range of 1:0.25-2. The possible structure of the metal complexes were characterized by FTIR, XRD, TGA and DSC. Surface morphology was observed by SEM. Hardness was measured to investigate the mechanical property of the complex. Cytocompatibility was tested with human gingival fibroblast to all complexes using sodium chitosan phosphate as control. It was found that the complex with various mole ratios was feasibly formed by donating lone pair electrons from nitrogen of amine groups, oxygen of phosphate groups and oxygen of hydroxyl groups of sodium chitosan phosphate to water molecules surrounding on the surface of zinc oxide. All complexes with various mole ratios exhibited the metal complex degradation stage in the range of 200-220 °C that did not found in sodium chitosan phosphate. Hardness of the complexes increased as increasing the amount of zinc oxide. For direct contact test, the complexes with sodium chitosan phosphate to zinc oxide ratios of 1:0.25 and 1:0.5 showed biocompatibility as well as the control that was suitable for applying as periodontal dressing whereas, the complexes with mole ratios of 1:1 and 1:2 exhibited cytotoxicity due to large amount of zinc oxide covering the surface of complexes. For indirect contact test, the extracted solutions from all complexes with various mole ratios showed biocompatibility as well as the control.

Department :Materials Science..... Student's Signature :
 Field of Study :Materials Science..... Advisor's Signature :
 Academic Year :2008..... Co-advisor's Signature :



Acknowledgements

First of all, the author wishes to express deepest gratitude to her advisor, Dr.Wanpen Tachaboonyakiat, Department of Materials Science, Faculty of Science, Chulalongkorn University and her co-advisor, Assistant Professor Dr.Kanyarat Suthin, Department of Conservative Dentistry, Faculty of Dentistry, and Prince of Songkla University for their vital advices, concern and encouragement throughout the research.

She also would like to express gratitude to Aj.Prapasri Runangsri, Department of Conservative Dentistry, Faculty of Dentistry, Prince of Songkla University, who gave her the advices on cell culture experiments.

She would like to appreciate to all staffs in Faculty of Dentistry, Prince of Songkla University to their support throughout her partial research work at Prince of Songkla University.

She would like to thank the chairman and members of the thesis committee for their valuable suggestions and comments. She would like to express her gratitude to Department of Materials Science, Faculty of Science, Chulalongkorn University, for providing the basis knowledge in polymer science.

She acknowledges Chandrakasem Rajabhat University for providing the scholarship for her Ph.D. study in Department of Materials Science, Faculty of Science Chulalongkorn University.

Finally, she also would like to express deeply gratitude to her father and mother for their love and encouragement.

CONTENTS

	Page
ABSTRACT IN THAI.....	iv
ABSTRACT IN ENGLISH.....	v
ACKNOWLEDGEMENTS.....	vi
CONTENTS.....	vii
LIST OF TABLES.....	x
LIST OF FIGURES.....	xi
LIST OF ABBREVIATIONS.....	xv
CHAPTER I INTRODUCTION.....	1
1.1 Objectives.....	4
1.2 Expected results.....	4
CHAPTER II LITERATER REVIEW.....	5
2.1 Periodontal dressings.....	5
2.1.1 Classification of periodontal dressings.....	5
- Hard pack.....	5
- Soft pack.....	5
- Light curable gel.....	6
2.1.2 Preparation and applications of each periodontal dressing.....	6
- Hard pack.....	6
- Soft pack.....	6
2.2 Disadvantage of periodontal dressing.....	8
2.3 Rosin and Colophony.....	14
2.4 The mechanism between rosin and phospholipids model.....	16
2.5 The main function of ingredients of some periodontal dressing	20
2.6 The reaction of zinc oxide and resin having carboxylic group.....	21
2.7 Methods of analysis of the metal complexes.....	22
2.7.1 Determination metal bound to chitosan derivatives.....	22
- Indirect determination.....	22
- Direct determination.....	22
2.7.2 Determination of sorption mechanism, structure of complex by SEM/EDX, DSC, TGA and IR, ¹³ C NMR.....	23
CHAPTER III EXPERIMENTAL PROCEDURE.....	29

3.1 Chemicals and materials.....	29
3.2 Methodology.....	30
3.2.1 Preparation of sodium chitosan phosphate/zinc oxide complexes.....	30
3.2.2 Investigation of complex formation by FTIR, XRD, TGA and DSC.....	32
3.2.2.1 Identification of functional groups.....	32
3.2.2.2 Determination of crystalline.....	33
3.2.2.3 Thermal analysis.....	34
3.2.3 Determination of setting time.....	35
3.2.4 Determination of hardness.....	35
3.2.5 Characterization of surface morphology.....	36
3.2.6 Cytocompatibility test of sodium chitosan phosphate and sodium chitosan phosphate/zinc oxide complexes with human gingival fibroblast (HGF).....	37
3.2.6.1 Harvest of healthy gingival tissue.....	37
3.2.6.2 Human gingival fibroblast cell culture.....	37
3.2.6.3 Subculture human gingival fibroblast cell.....	38
3.2.6.4 Cytocompatibility test of sodium chitosan phosphate and sodium chitosan phosphate/zinc oxide complexes with human gingival fibroblast.....	38
CHAPTER IV RESULTS AND DISCUSSION.....	41
4.1 Appearance of PCTS/ZnO complexes.....	41
4.2 Possible structure of PCTS/ZnO complexes.....	41
4.2.1 Chemical structure of PCTS/ZnO complexes.....	41
4.2.2 Crystalline structure of PCTS/ZnO complexes.....	44
4.2.3 Thermal properties of PCTS/ZnO complexes.....	45
4.3 Setting time of PCTS/ZnO complexes.....	51
4.4 Surface Morphology	52
4.5 Hardness of PCTS/ZnO complexes.....	53
4.6 Cytocompatibility of PCTS/ZnO complexes.....	54
4.6.1 Direct contact test.....	54
4.6.2 Indirect contact test.....	59
CHAPTER V CONCLUSIONS AND SUGGESTIONS.....	61
5.1 Conclusions.....	61
5.2 Suggestions.....	62
References.....	63
Appendices.....	66
Biography.....	86

LIST OF TABLES

	page	
Table 1.1	Composition of periodontal dressing materials according to the information of the manufacturers (no further details are available).....	2
Table 2.1	Growth of primary human gingival fibroblasts (HGF) with extract I and II of the periodontal dressing materials for 24 and 48 h (values are expressed as growth in % referred to controls, 100%±SD, n = 3–6).....	10
Table 2.2	Rosin components detected in 6 different “all-in-one” diapers according to GC analyses.....	15
Table 3.1	Chemicals list.....	29
Table 3.2	Instrument list.....	30
Table 3.3	Mole ratios of sodium chitosan phosphate and zinc oxide.....	32
Table 4.1	Derivative thermal gravimetric (DTG) deriving from TGA curves of PCTS and PCTS/ZnO complexes.....	47
Table 4.2	Summary of exothermic and endothermic temperature.....	48
Table 4.3	Hardness value of PCTS/ZnO complexes at different PCTS/ZnO mole ratios.....	52
Table 4.4	Optical density (OD) of PCTS, PCTS/ZnO complexes, rosin and Coe-pak [®] by MTT assay.....	59
A 1	The ratio of phosphorus pentoxide and chitosan.....	68

LIST OF FIGURES

		page
Figure 1.1	Periodontal dressing material applied on surgical wound.....	2
Figure 2.1	Inserting the periodontal pack. (a) A strip of pack is hooked around the last molar and pressed into place interiorly. (b) The lingual pack is joined to the facial strip at the distal surface of the last molar and fitted into place interiorly. (c) Gentle pressure on the facial and lingual surfaces joins the pack interproximally.....	7
Figure 2.2	Comparisons of the cytotoxic effects of dressing materials by the neutral red vital stain technique after 24-hour incubation.....	9
Figure 2.3	Ward's Wondr-pak [®] (right) and control disc (left) placing on fibroblast monolayer. Clear zone indicative of cytotoxicity was observed surrounding the sample after 6 hours.....	12
Figure 2.4	Adverse effect to woman (71 years old) whom was applied a surgical pack containing eugenol and colophony after 7 days. Swelling and redness of the face (A), sore and swollen lips (B) and swelling and redness of the oral mucosa in contact with the dressing (C).	13
Figure 2.5	Marked swelling around the interphalangeal joints.....	16
Figure 2.6	In vitro cytotoxicity expressed as ⁵¹ Cr release from PMN cells (●) and gingival fibroblasts (□) exposed to resin acids and rosins 5, 10.6, 21.2, 42.5, 85, 170, 340 and 680 μg/ml (a) Abietic acid, (b) Dehydroabietic acid, (c) Neoabietic acid (d) Levopimaric acid, (e) Isopimaric acid, (f) Oleoresin # 1, and (g) Oleoresin # 2.....	17
Figure 2.7	Chemical structures of the test compounds.....	18
Figure 2.8	Concentration-response cytotoxicity to fibroblasts as determined with the neutral red assay. Briefly, the cells were seeded to 96-well microtiter plates and incubated for (a) 1 h, (b) 4 h, (c) 24 h, or (d) 48 h in the absence (control : 0 μg/ml) or presence of different chemicals at concentrations (10, 30, 100, 300, or 1000 μg/ml) as indicated.....	19
Figure 2.9	DSC thermograms for mixtures of DPPC/abietic acid. The concentration of abietic acid in the membrane (mol fraction) is expressed on the curves.	20

Figure 2.10	Thermograms of chitosan-copper complex (below) and chitosan-ferrous iron complex (above).....	24
Figure 2.11	DTG, TG and DTA curves for silver-containing chitosan.....	25
Figure 2.12	Change in bacterial counts on the tooth surface after applying a) 0.1 % b) 0.5% chitosan derivatives.....	27
Figure 3.1	Synthesis pathway of sodium chitosan phosphate.....	31
Figure 3.2	Fourier Transform Infrared Spectrometer.....	33
Figure 3.3	X-ray Diffractometer.....	33
Figure 3.4	Thermal Gravimetric Analyzer.....	34
Figure 3.5	Differential Scanning Calorimeter.....	34
Figure 3.6	Penetrometer.....	35
Figure 3.7	Scanning Electron Microscope.....	37
Figure 4.1	FTIR spectra of (a) sodium chitosan phosphate (PCTS) (b) PCTS/ZnO, 1:0.25 (c) PCTS/ZnO, 1:0.5 (d) PCTS/ZnO, 1:1 (e) PCTS/ZnO, 1:2 equivalent mole.....	43
Figure 4.2	XRD patterns of (a) chitosan (b) sodium chitosan phosphate (c) zinc oxide (d) PCTS/ZnO, 1:0.25 (e) PCTS/ZnO, 1:0.5 (f) PCTS/ZnO, 1:1 (g) PCTS/ZnO, 1:2 equivalent mole.....	44
Figure 4.3	TGA diagrams of (a) PCTS, and its metal complexes with various PCTS/ZnO mole ratios of (b)1:0.25, (c) 1:0.5, (d)1:1 and (e) 1:2.....	46
Figure 4.5	DSC curves of (a) PCTS and its metal complexes with various PCTS/ZnO mole ratios of (b)1:0.25, (c) 1:0.5, (d)1:1 and (e) 1:2.....	49
Figure 4.6	Possible structures of sodium chitosan phosphate/zinc oxide complexes at 1:0.25, 1:0.5, 1:1 and 1:2 equivalent moles.....	50
Figure 4.6	Setting time of sodium chitosan phosphate/zinc oxide complexes at mole ratios of chitosan to zinc oxide of (a) 1:0.25, (b) 1:0.5, (c) 1:1 and (d) 1:2.....	51
Figure 4.7	SEM images in mapping mode observing ZnO dispersion on the surface of the complexes at different ratios of PCTS/ZnO of (a) 1:0.25 (b) 1:0.5 (c) 1:1 (d) 1:2.....	52
Figure 4.8	Direct contact test of materials placing on monolayer cell culture at 0 hr.....	55
Figure 4.8	(conti.) Direct contact test of materials placing on monolayer cell culture after 24 hrs.....	56

Figure 4.8	(conti.) Direct contact test of materials placing on monolayer cell culture after 48 hrs.....	57
Figure 4.8	(conti.) Direct contact test of materials placing on monolayer cell culture after 72 hrs.....	58
A 2	FTIR spectrum of chitosan.....	69
A 3	FTIR spectrum of sodium chitosan phosphate.....	69
A 4	FTIR spectrum of the complexes at 1:0.25 equivalent moles.....	70
A 5	FTIR spectrum of the complexes at 1:0.5 equivalent moles.....	70
A 6	FTIR spectrum of the complexes at 1:1 equivalent moles.....	71
A 7	FTIR spectrum of the complexes at 1:2 equivalent moles.....	71
A 8	FTIR spectrum of ZnO.....	72
A 9	XRD pattern of chitosan.....	72
A 10	XRD pattern of sodium chitosan phosphate.....	73
A 11	XRD pattern of PCTS/ZnO (1:0.25).....	73
A 12	XRD pattern of PCTS/ZnO (1:0.5).....	74
A 13	XRD pattern of PCTS/ZnO (1:1).....	74
A 14	XRD pattern of PCTS/ZnO (1:2).....	75
A 15	TGA diagram and Derivative thermal gravimetric (DTG) of sodium chitosan phosphate.....	75
A 16	TGA diagram and Derivative thermal gravimetric (DTG) of sodium chitosan phosphate/zinc oxide complexes at 1:0.25 equivalent mole.....	76
A 17	TGA diagram and Derivative thermal gravimetric (DTG) of sodium chitosan phosphate/zinc oxide complexes at 1:0.5 equivalent mole.....	76
A 18	TGA diagram and Derivative thermal gravimetric (DTG) of sodium chitosan phosphate/zinc oxide complexes at 1:1 equivalent mole.....	77
A 19	TGA diagram and Derivative thermal gravimetric (DTG) of sodium chitosan phosphate/zinc oxide complexes at 1:2 equivalent mole.....	77
A 20	DSC curve of PCTS.....	78
A 21	DSC curve of PCTS/ZnO (1:0.25).....	78
A 22	DSC curve of PCTS/ZnO (1:0.5).....	79
A 23	DSC curve of PCTS/ZnO (1:1).....	79
A 24	DSC curve of PCTS/ZnO (1:2).....	80
A 25	SEM images of the complexes at 1:0.25.....	81
A 26	SEM images of the complexes at 1:0.5.....	81

A 27	SEM images of the complexes at 1:1.....	82
A 28	SEM images of the complexes at 1:2.....	82
A 29	Human gingival fibroblast from gingival pieces.....	83
A 30	Human gingival fibroblast at passage 7.....	83
A 31	Human gingival fibroblast at passage 1 in 75 ml plastic flask.....	84
A 32	Immersion of materials into fibroblast media for 24, 48 and 72 hrs.....	84
A 33	Death cells were contacted with zinc oxide.....	85

LIST OF ABBREVIATIONS

FTIR	Fourier Transform Infrared Spectrometer
XRD	X-Ray Diffraction Spectrometer
TGA	Thermal Gravimetric Analyzer
DSC	Differential Scanning Calorimeter
SEM	Scanning Electron Microscope
HV	Vickers Hardness
HGF	Human Gingival Fibroblast

CHAPTER I

INTRODUCTION

Periodontal dressing is always used after the periodontal surgery to cover the surgical wound as shown in Figure 1.1. The pack will prevent the surface of trauma from striking against foods during mastication, control bleeding and wound healing [1]. Since normal periodontal wound healing takes about 2 weeks, thus, the periodontal dressing will be kept contacting to wound around 2 weeks [1]. Periodontal dressing consists of three main compositions including carboxylic organic acids, inorganic metal oxides, carboxylic groups available polymeric resins with other ingredients such as flavors, cohesive substances, viscosity-adding agents, therapeutic agents, and filler [2]. Carboxylic organic acid will form complex with inorganic metal oxide. Carboxylic groups available polymeric resins present as a reaction rate modifying agents [2] because of their huge steric molecules. Those resins also have ability to form complex with inorganic metal oxide. Table 1.1 showed the composition of commercial periodontal dressing according to the information of the manufacturers [3]. Coe-pak[®], Vocopac[®], Peri-pac[®] are commercial available periodontal dressing. Each commercial periodontal dressing consists of different polymeric resins. The polymeric resins utilized in Coe-pak[®], Barricaid[®] and Peri-pac[®] are rosin, polyether-urethane dimethacrylate resin and acrylic resin, respectively. Those periodontal dressings exhibit moderate to severe cytotoxic effect in cell culture system due to the release of cytotoxic substances [3]. The cytotoxic substances released from periodontal dressing may impair healing of periodontal tissues after application.

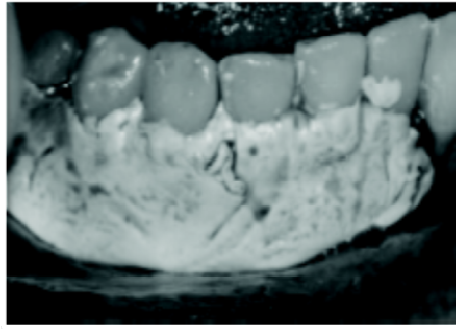


Figure 1.1 Periodontal dressing material applied on surgical wound.

Table 1.1 Composition of periodontal dressing materials according to the information of the manufacturers (no further dental are available) [3]

Material	Ingredients	Manufacturer
Coe-Pak [®] , paste-paste, chemically curing	Base : rosin, cellulose, natural gums and waxes, liquid coconut fatty acid, chlorothymol, zinc acetate, denatured alcohol, methanol, petrolatum, lorcithidol (a fungicide). Accelerator : zinc oxide, vegetable oil, mineral oil, chlorothymol (an antibacterial agent), silica, magnesium oxide, synthetic resin, coumarin	GC America Inc., Chicago, USA
Voco pac [®] (VP), paste-paste, chemically curing	Zinc oxide, magnesium oxide	Voco, Cuxhaven, Germany
Peripac [®] (PP), paste	Calcium sulphate-hemihydrate, zinc oxide, zinc sulphate, acrylic-type resin, glycol solvent, flavoring and coloring agent	De rey/Dentsply, Konstanz, Germany
Barricaid [®] (BC), Light-curable gel	Gel: polyether urethane dimethacrylate resin, silanized silica, VLC photo-initiator and accelerator, stabilizer, colorant	Caulk/Dentsply, Milford, USA

The cytotoxic substances [3] are rosin (colophonium), non-specified acrylic-type resins, and urethane dimethacrylates. Coe-pak[®], Peri-pac[®] and Barricaid[®] were consisted those carboxylic groups available polymeric resins respectively. Rosin, a derivative of abietic acid, was obtained from turpentine. There is some research studied on the interaction of abietic acid with model membranes of dipalmitoylphosphatidylcholine (DPPC) by using differential scanning calorimetry (DSC). It was found that abietic acid greatly perturbs the phase transition of DPPC by intercalating into the phospholipids palisade [4]. Soderberg and co-worker [5] studied the behavior of abietic acid derivative to human fibroblast cells by using a quantitative neutral red spectrophotometric assay. It was found that dehydroabietic acid (DHAA) was the most toxic compounds due to DHAA possessing an aromatic ring with an isopropyl group at C-13 has been shown to affect cells like a detergent, by dissolving in the lipid layers of the cellular membrane thus affecting the membrane permeability and the function of ion transporting membrane proteins [5]. Therefore, abietic acid and its derivatives were found to perturb the phospholipids membrane owing to its available carboxyl groups and aromatic rings.

Setting pathway of periodontal dressing was separated in two classifications which were light cure and chemical reaction.

For light cure setting, periodontal dressing was set by light. Basic ingredients were resin and photoinitiator. Characteristics of periodontal dressing were very elastic and non-brittle. Light cured dressing may be directly placed into the mouth from syringe or indirectly off a pad.

For chemical reaction setting, it is noted to know that periodontal dressing can be set not only by the complexation between organic carboxylic group and metal oxide, but also by the complexation between polymeric resin having carboxylic acid and metal oxide. The function of polymeric resin having carboxylic acid is a reactive rate modifying agent and body forming agent [2].

In this research, other natural polymer would be surveyed in order to replace those cytotoxic carboxylic group available polymeric resins using in commercial periodontal dressing. Sodium chitosan phosphate, a derivative of chitosan, was selected as polymeric resin. Sodium chitosan phosphate has phosphate substituted

groups. Phosphate groups are found in typical cell membrane. Therefore, sodium chitosan phosphate should also be biocompatible, biodegradable and non-toxic as chitosan. Beside, sodium chitosan phosphate is water soluble that overcame the solubility problem of chitosan in dilute acid. Owing to its own phosphate groups, amino groups and hydroxyl groups, thus, sodium chitosan phosphate is expected to form complex with metal oxide. Zinc oxide was selected as metal oxide, since it is normally found in commercial periodontal dressing materials. Therefore, the aim of this research is to prepare sodium chitosan phosphate/zinc oxide complexes and characterize the possible complex structure. Cytotoxicity of sodium chitosan phosphate/zinc oxide complexes was determined using sodium chitosan phosphate, rosin and Coe-pak[®] as control. The obtained sodium chitosan phosphate/zinc oxide complexes are expected for non-cytotoxicity which an approach for periodontal dressing component.

1.1 Objectives

1.1.1 To prepare sodium chitosan phosphate/zinc oxide complexes and determine the setting time of complexes.

1.1.2 To study the possible complex structure and the hardness of sodium chitosan phosphate/zinc oxide complexes.

1.1.3 To study the cytotoxicity of sodium chitosan phosphate and sodium chitosan phosphate/ zinc oxide complexes to human gingival fibroblast cell.

1.2 Expected results

To obtain the novel biocompatible complex between sodium chitosan phosphate and zinc oxide that can be applied for one component in periodontal dressing.

CHAPTER II

LITERATURE REVIEW

2.1 Periodontal dressings

Periodontal dressing is a protective pain relief covering of the gum and periodontal tissues used after periodontal surgery. Periodontal dressing is applied to the necks of teeth and the adjacent tissue to cover and protect the surgical wound. In general, packs or dressings have no curative properties; they assist healing by protecting the tissue rather than providing "healing factors". The pack minimizes the likelihood of postoperative infection or hemorrhage, stops bleeding, facilitates healing by preventing surface trauma during mastication [1].

2.1.1 Classification of periodontal dressings

- **Hard pack** (Zinc oxide-Eugenol Pack): Hard packs have the basis ingredients of zinc oxide powder and eugenol liquid. Hard packs setting is based on the reaction of zinc oxide and eugenol include the Wondr-pak[®] developed by Ward in 1923 [6] and several others that modified Ward's original formula. The addition of accelerators such as zinc acetate gives the dressing a better working time. Zinc oxide-Eugenol dressing is supplied as a liquid and a powder that are mixed prior to use. Eugenol in this type of pack may induce an allergic reaction that produces reddening of the area and burning pain in some patients.

- **Soft pack** (Non-eugenol Packs): Soft packs have the basis ingredients of base and accelerator supplied in two tubes separately. Base tube contains liquid coconut fatty acids thickened with colophony resin (rosin) and chlorothymol (a bacteriostatic agent). Accelerator tube contain zinc oxide, and oil (for plasticity), a gum (for cohesiveness), and lorchidol (a fungicide). The contents of which are mixed

immediately before use until a uniform color is obtained. Soft packs setting are based on the reaction between a metal oxide and fatty acid. Coe-pak[®] is one of commercial examples at most widely used periodontal dressing in Thailand and the United State of America. This dressing does not contain asbestos or eugenol, thereby avoiding the problems associated with these substances.

- **Light curable gel:** Light curable gel has the basis ingredient of acrylate resin and photoinitiator. Commercial available of light curable gel, is Barricaid[®], can be directly injected into small surgical area with syringes or indirectly injected on a plastic pad before pasting on surgical wound. It can be completely polymerized by light source. As prepared light cured pack shows very elastic property.

2.1.2 Preparation and application of each periodontal dressing [1]

- Hard pack

Zinc oxide powder are mixed with eugenol liquids on a wax paper pad with a wooden tongue depressor. The powder is gradually incorporated with the liquid until a thick paste is formed.

- Soft pack

Soft pack is prepared by mixing equal lengths of paste by accelerator and base tube, until obtaining a uniform color of mixture paste. A capsule of tetracycline powder can be added at this time. The pack is then placed in a cup of water at room temperature for 2 to 3 minutes; the paste loses its tackiness and can be handled and molded. It takes around 15 to 20 minutes to be set as solid. Solidification time can be shortened by adding a small amount of zinc oxide to the accelerator (pink paste) before mixing. As shown in Figure 2.2, the pack is then rolled into two strips approximately the length of the treated area. The end of one strip is bent into a hook shape and fitted around the distal surface of the last tooth. The remainder of the strip is brought forward along the facial surface to the midline and gently pressed into place

along the gingival margin and interproximally. The second strip is applied from the lingual surface. It is joined to the pack at the distal surface of the last tooth, and then brought forward along the gingival margin to midline. The strips are joined interproximally by applying gentle pressure on the facial and lingual surfaces of the pack. For isolated teeth separated by edentulous spaces, the pack should be made continuous from tooth to tooth, covering the edentulous areas.

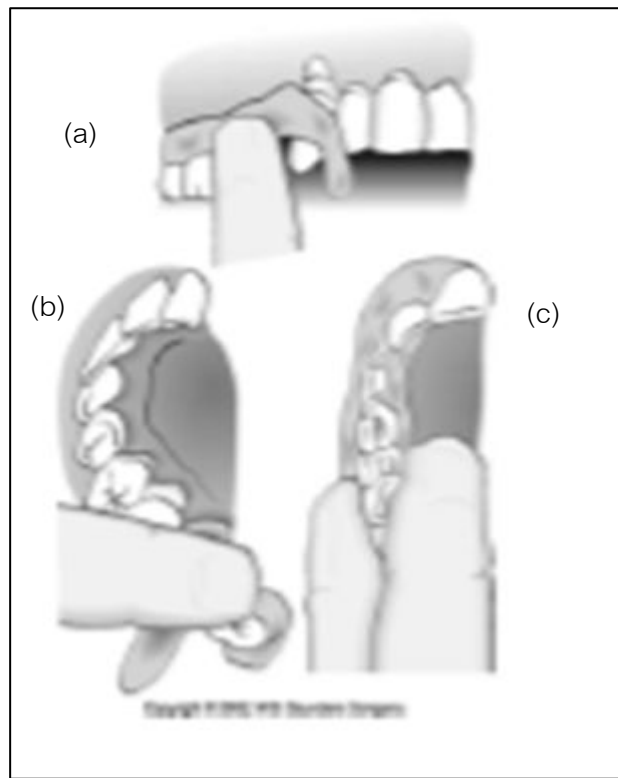


Figure 2.1 Inserting the periodontal pack. (a) A strip of pack is hooked around the last molar and pressed into place interiorly. (b) The lingual pack is joined to the facial strip at the distal surface of the last molar and fitted into place interiorly. (c) Gentle pressure on the facial and lingual surfaces joins the pack interproximally [1].

Periodontal dressing materials should reach the optimum requirements such as non-toxic or non-irritated to the tissue, minimally discomfort to patient.

2.2 Disadvantage of periodontal dressing

The disadvantage of some commercial periodontal dressing showed the report as following.

Haugen and co-workers [7] studied the cytotoxicity of Coe-pak[®], Peripac[®] and Ward's Wondrpak[®] as periodontal dressings by neutral red vital techniques. In experimental, both freshly made and stored materials were filled into plastic molds to form cones with a circular base 10 mm in diameter. The fresh materials were tested within 1 hour after preparation but the stored materials were stored in cell culture medium for 5 days and tested together with fresh material. A monolayer of human epithelial cells was treated with 2 ml of a 0.1% solution of neutral red in growth medium for 20 minutes. On each dish, a test specimen was placed together with a millipore filter as a control specimen. Then 2 ml of medium was added to the dishes. After 24 hours, cell integrity was evaluated in a microscope. It was found that, the zone of dead cells surrounded to Coe-pak[®] had increased considerably and very few cells still retained any stain granular. The course of events for stored Coe-pak[®] specimen was similar to that of fresh specimen. Fresh Peripac[®] also had caused cell lysis on the entries dish as shown in Figure 2.2 whereas, stored Peripac[®] did not cause any precipitation of medium component. The fresh material of Ward's Wondrpak[®], had increased death zone but the stored of Ward's Wondrpak[®] had the cell of normal appearance and stain were still seen. However, the variety of effects seen in the cultures indicated that the substances from each periodontal dressing differed in solubility in the cell culture medium, leach ability from the specimens with time, and the mode of action of these substances differs for the periodontal dressing tested.

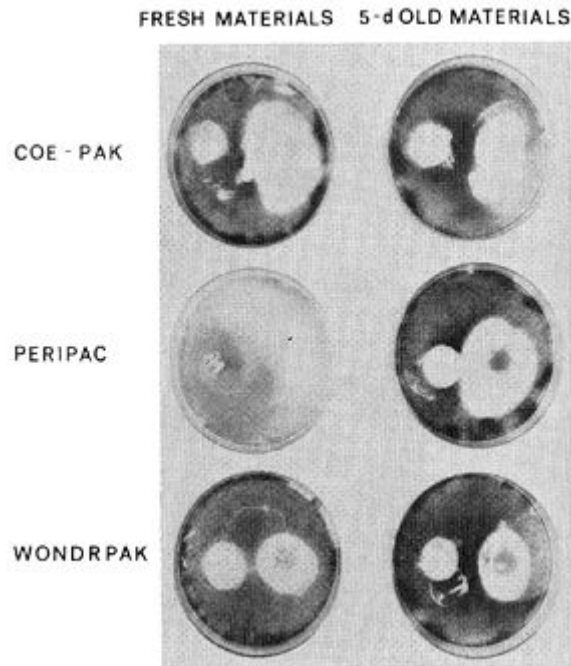


Figure 2.2 Comparisons of the cytotoxic effects of dressing materials by the neutral red vital stain technique after 24-hour incubation [7].

Alpar and co-workers [3] determined the cytocompatibility of various periodontal dressing materials with human primary gingival fibroblasts (HGF). From Coe-pak[®] (CP), Voco-pac[®] (VP), Peripac[®] (PP) and Barricaid[®] (BC) materials, equally sized specimens with a free surface of 70.7 mm², a thickness of 2 mm, and a diameter of 5 mm were prepared. After that, CP, VP and PP were allowed to set for 1 hour at 37 °C in 100% humidity. BC was polymerized for 60 s by light source. Three specimens of the investigated products were extracted at 37 °C in each 5 ml cell culture medium for 1 day (Extract I) and between day 2 and day 8 (Extract II) after setting. Cell culture medium extracts (time periods of extraction: day 1 and between day 2 and day 8 after setting) as well as solid specimens of the following materials were used to investigate the cytotoxicity. Responses of cultures exposed to Extract I or Extract II for 24 h and 48 h to these materials were monitored by the fluorescent dyes H33342 and sulforhodamin 101 as well as by light microscopy as shown in Table 2.1. It was found that Coe-Pak[®] reduced the proliferation of HGF compared to untreated controls due to CP-extracts

may be partially caused by released rosin or resin acids liberated from colophonium into aqueous media. This hypothesis is confirmed by data reported by Sunzel and co-worker [8] who observed a strong dose-related cytotoxicity of rosin and pure resin acids in human gingival fibroblasts. The effect of the periodontal dressing materials on the growth and morphology of the various cell cultures was determined by means of direct contact tests. Specimens from each material were placed in 6-well microculture dishes. Additionally, BC was tested uncured. Thereafter, 2×10^5 cells/well were seeded into the dishes and grown for 24 h. Then, cells were investigated by phase contrast microscopy. It was found that primary fibroblasts to solid specimens of CP, and PP resulted in severe changes due to cytotoxic substances segregated from CP and PP should be the main causative factor for inflammatory reactions of the gingival connective tissue.

Table 2.1 Growth of primary human gingival fibroblasts (HGF) with extract I and II of the periodontal dressing materials for 24 and 48 h (values are expressed as growth in % referred to controls, $100\% \pm SD$, $n = 3-6$) [8]

HG F	Extract I				Extract II			
	Hoechs t 33342	Sulfo 101	Hoechs t 33342	Sulfo 101	Hoechst 33342	Sulfo 101	Hoechst 33342	Sulfo 101
	24 hrs	48 hrs	24 hrs	48 hrs	24 hrs	48 hrs	24 hrs	48 hrs
CP	80.2 ± 7	62.4 ± 7	86.7 ± 9	71.1 ± 12	82.9 ± 8	70.6 ± 4	94.3 ± 6	90.4 ± 5
VP	97.7 ± 8	102.8 ± 7	97.7 ± 5	99.4 ± 11	105.5 ± 5	99.7 ± 7	98.9 ± 5	96.7 ± 3
PP	131 ± 43	99.9 ± 18	71.4 ± 12	67.4 ± 15	97.2 ± 9	63.9 ± 8	84.7 ± 6	73.1 ± 6
BC	102.2 ± 6	109.7 ± 4	99.4 ± 5	104.3 ± 10	107.8 ± 11	111.4 ± 9	101.5 ± 6	103.5 ± 3

Hildebrand and co-workers [9] evaluated the effect of four commercially available dressings such as Coe-pak[®], Ward's Wondr-pak[®], Peripac[®]-non eugenol and Peripac[®]-eugenol on monolayer of L929 fibroblast cells using assay plate assembly, designed specifically for in vitro toxicity screening as shown in Figure 2.3. Each of the four sample dressings, two of which were eugenol, and two non-eugenol (eugenol

dressing: 1.PPC-Eugenol, 2.Ward's Wondr-pak[®], non eugenol, 3. PPC-Non-Eugenol, 4. Coe-pak[®]) were mixed and placed into mold to form 8 mm discs. The cells were grown out on the cell culture assay plates and stain with a vital stain, 0.01% Neutral Red. By placing the specimens to be tested directly onto the cell monolayer, a more sensitive assay is achieved. Plate was observed microscopically at 1, 2, 6, 8 and 24 hours to determine alterations in the cells surrounding the dressing sample. At 1 hour, there were no microscopic alterations in the cells surrounding either the Coe-pak[®] or the Peripac[®]-eugenol dressing. At 2 hours the distance of cells affected around the Ward's and Peripac[®]-non eugenol discs had increased, and some of the cells around Peripac[®]-eugenol dressing had begun to lose the stain and to appear very granular. The cells near the Coe-pak[®] demonstrated slight microscopic alterations, although macroscopic changes were not yet observable. By 6 hours the cells surrounding all four discs appeared altered for some distance when viewed microscopically, while at the same time, distinct clear cytotoxic zones were seen around all samples when observed with naked eye. At the 8 hour interval a greater quantity of cells surrounding the four samples appeared to be affected upon microscopic observation than was true of the 6 hours reading. By 24 hours, Coe-pak[®] produced a more extensive zone than the other three dressings. In the early 60's, Coe-pak[®] turned out to be more cytotoxic to tissue culture cells. This finding supported in vivo observation by Perrson and co-worker that it produced the most pronounced inflammatory response, and subsequently that it produced the most potent antibacterial activity of the dressing studied.

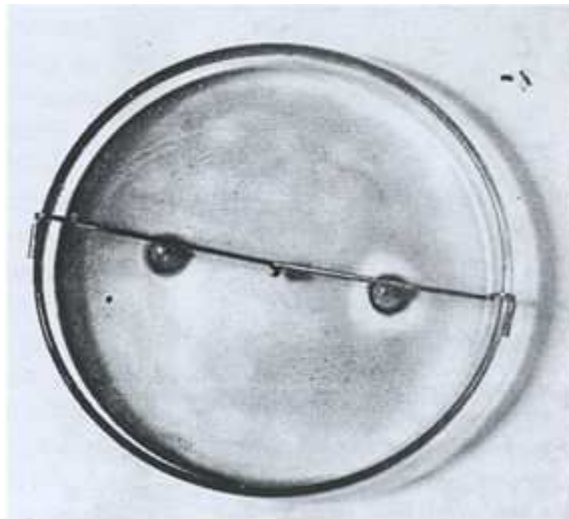


Figure 2.3 Ward's Wondr-pak[®](right) and control disc (left) placing on fibroblast monolayer [9].

Koch and co-workers [10] studied on the irritation of eugenol/colophony containing dressing. In the present study, 142 patients were underwent periodontal treatment and applied the eugenol/colophony containing dressing. Before the surgical treatment all patients were patch tested with 5 % eugenol and 20 % colophony, both in petrolatum. All test patches were used and fixed to the back of the patients with Leucosilk plaster. The patches were left on the skin for 48 hours. The reaction was tested for 24 hours after removal of the patches (72 hours after application). The criteria used for a positive reaction were redness and infiltration at the test site. These preoperative tests showed that 9 patients were sensitive to eugenol and/or colophony and therefore they were excluded from the investigation. The remaining 133 patients underwent surgical treatment. For about fourteen days the wound was covered with a surgical dressing which contained approximately 43% colophony, 7% eugenol and also zinc oxide and linseed oil. It was found that 13 patients sensitized to eugenol and/or colophony. They were complained a burning sensation in the mouth and difficulties of swallowing. They also had swelling of the oral mucosa and erythema or urticaria of the face as shown in Figure 2.4. The findings of the present study strongly indicate the

importance in periodontal surgery of using dressing which do not contain either eugenol or colophony.

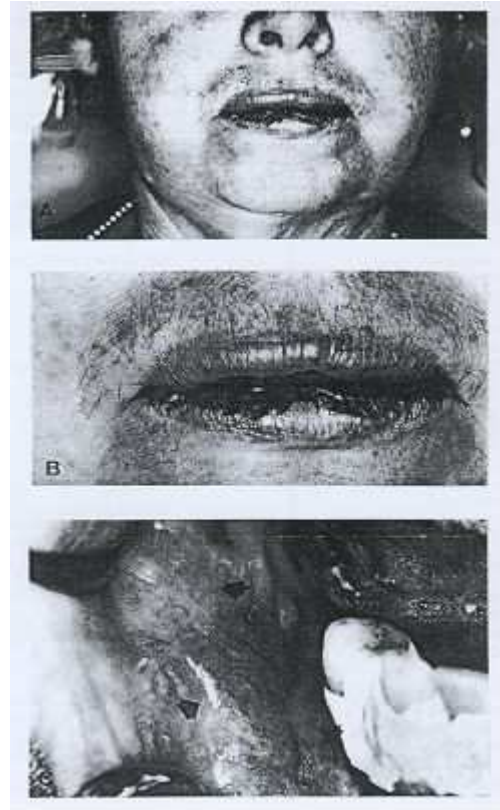


Figure 2.4 Adverse effect to woman (71 years old) whom was applied a surgical pack containing eugenol and colophony after 7 days. Swelling and redness of the face (A), sore and swollen lips (B) and swelling and redness of the oral mucosa in contact with the dressing (C) [10].

As mentioned above that periodontal dressing consisted rosin which induce to irritate tissue.

2.3 Rosin or Colophony

Rosin or colophony is solid form of resin. It obtained from pines and conifer. It is semi-transparent, brittle and variable in color from yellow to black. Rosin consists mainly of 90% resin acids and about 10% neutral materials. The resin acids are diterpene acids of the abietic type - neoabietic, palustric and dehydroabietic and the pimaric type – pimaric, isopimaric and sandaracopimaric. Rosin is insoluble in water but soluble in most organic solvent. Rosin is use in making inferior varnishes, sealing-wax and various adhesives. Several researches of rosin were shown in these reports.

Ann-Therese Karlberg and co-workers [11] analyzed rosin in diapers by using gas chromatography. Diapers from the 2 major products in Swedish market was sampling in this experiment. The diapers were divided into 3 parts: the back sheet (including glue), the fluff, and the top layer. The top layer and the fluff of diapers were extracted with acetone for the determination of rosin compounds. About 2.5 g of top layer and 12.5 g of fluff were cut into small pieces and the materials were extracted with 100 ml acetone for 10 min. Gas chromatographic (GC) analyses were performed to detect the main rosin compounds, abietic acid and dehydroabietic acid, and also the oxidation product, 7-oxodehydroabietic acid, in the diaper extracts. Prior to analysis, the extracts were methylated with diazomethane. The results of the analyses of the content of rosin components in the different diapers are shown in Table 2.2. Rosin compounds (mainly abietic acid and dehydroabietic acid) were detected in all diapers. It was found that the diapers had more rosin on the top layer, which is in close contact with skin, than in the fluff.

Table 2.2 Rosin components detected in 6 different “all-in-one” diapers according to GC analyses [11]

Diapers	Diaper parts	Rosin Components (ppm)		
		AbA ^a	DeA	7-O-DeA
A	Top layer	33	7	nd b
	Fluff	10	1	nd
B	Top layer	na	na	nd
	Fluff	20	4	nd
C	Top layer	nd	nd	nd
	Fluff	3	2	nd
D	Top layer	nd	nd	nd
	Fluff	3	2	nd
E	Top layer	25	nd	nd
	Fluff	3	nd	nd
E ₉₅ ^c	Top layer	67	225	nd
	Fluff	3	5	nd
F	Top layer	104	nd	nd
	Fluff	20	9	2
F ₉₅	Top layer	24	nd	nd

Furthermore, in 1976, Leif Lysell and co-workers [12] studied the contact allergy to rosin in a periodontal dressing. In case report, a 33 year old man was the patient for the treatment of periodontitis, after that a surgical dressing containing zinc oxide, rosin and eugenol was used for wound protection. After 1 week, the wound was applied a new surgical dressing but the patient had a burning sensation in the operated area for a few minutes. Four days later the patient came at the clinic with both oral and dermatological symptoms. There was a slight erythematic of the oral mucosa. He also had urticarial on the left lateral part of his abdomen and marked swellings on the dorsal part of both his hands, the interphalangeal joints were particularly affected as shown in Figure 2.5. The old periodontal dressing was removed and replaced with a wax packing.

After 24 hours, the results of the dermatological patch-test showed that the patient had a contact allergy to rosin. A reaction to eugenol or zinc oxide could not be found.



Figure 2.5 Marked swelling around the interphalangeal joints [12].

2.4 The mechanism between rosin and phospholipids model

Rosin is a resin having available carboxylic group, present with a reaction rate modifying agent and body forming agent [2]. It has many abietic acids that consisting of aromatic ring and carboxylic group influence to irritate with tissue. It displayed the toxic results from abietic acid and its derivatives in this reports.

Sunzel and co-workers [8] investigated toxic effects to human gingival fibroblast of two commercial rosins which comprised Nobetec[®] (oleoresins #1) and Apoteksbolaget AB (oleoresins #2). Five highly purified resin acids, which were dehydroabietic acid (DHAA), neabietic acid, isopimaric acid, levopimaric acid and abietic acid, were also studied the toxic effect. The pure resin acids were dissolved and diluted to the desired concentration in 99.5% ethanol. The concentrations of the oleoresins and the pure resin acids used in the experimental were 5, 10.6, 21.2, 42.5, 85, 170, 340 and 680 $\mu\text{g/ml}$. Fibroblast (10^4 cells/well) was cultivated in 96-well microtiter plates in medium supplemented with 100 $\mu\text{Ci/ml}$ ($\text{Na}_2^{51}\text{CrO}_4$) addition to each well. The target cells were incubated for 60 min at 37 °C. ^{51}Cr -labelled fibroblast cells were mixed with 100 μl of the test solutions. Abietic acid, Neoabietic, levopimaric, isopimaric acid

and oleoresins #2 appeared the most toxic resin acids for gingival fibroblasts due to the aromatic ring with the isopropyl at C-13.

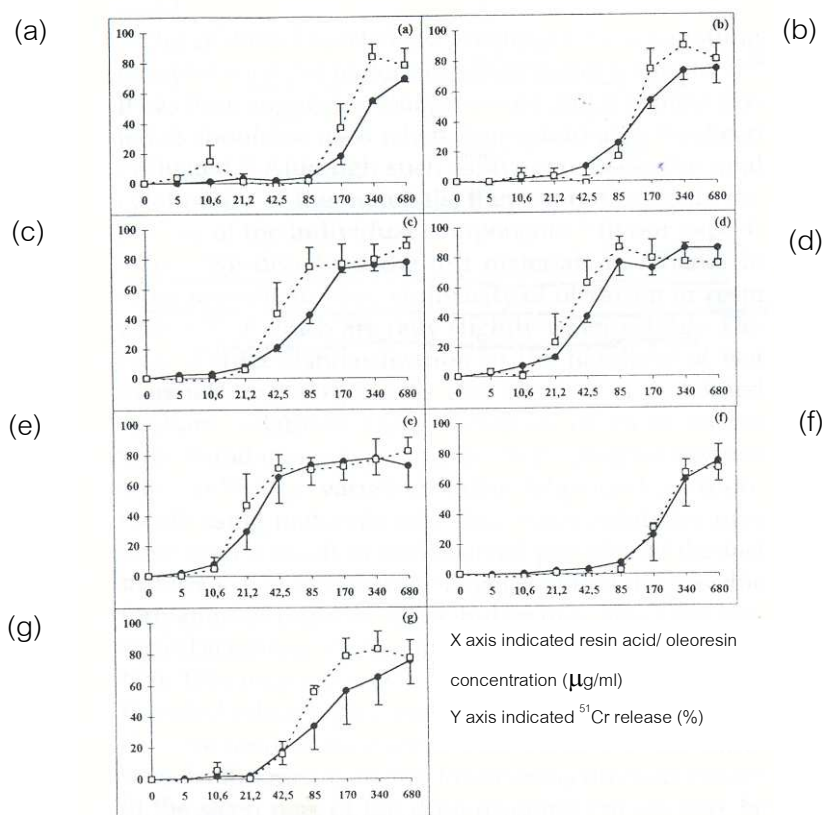


Figure 2.6 In vitro cytotoxicity expressed as ⁵¹Cr release from PMN cells (●) and gingival fibroblasts (○) exposed to resin acids and rosins 5, 10.6, 21.2, 42.5, 85, 170, 340 and 680 μg/ml (a) Abietic acid, (b) Dehydroabietic acid, (c) Neoabietic acid (d) Levopimaric acid, (e) Isopimaric acid, (f) Oleoresin # 1, and (g) Oleoresin # 2 [8].

Soderberg and co-workers [5] studied the toxic effect of dehydroabietic acid, podocarpic acid, O-methylpodocarpic acid, oleoresin and tea tree oil on fibroblast cells by using a quantitative neutral red spectrophotometric assay at 540 nm. This assay quantified the number of visible cells. The cytotoxic effect of the tested compounds on human fibroblast cells incubated for 1, 4, 24 and 48 hours at various acids concentrations (0, 10, 30, 100, 300 and 1000 μg/ml). It was found that the high concentrations and longer time caused increased cell death. Dehydroabietic acid and the oleoresin were the most toxic compound followed by O-methylpodocarpic acid,

whereas podocarpic acid and tea tree oil showed a lower level of toxicity. Because dehydroabietic acid have an aromatic ring with isopropyl group at C₁₃ which has been shown to affect cells like a detergent by dissolving in the lipid layer of the cellular membrane. Fibroblast cells exposed to the oleoresin in higher concentrations showed a rapid decline in viability.

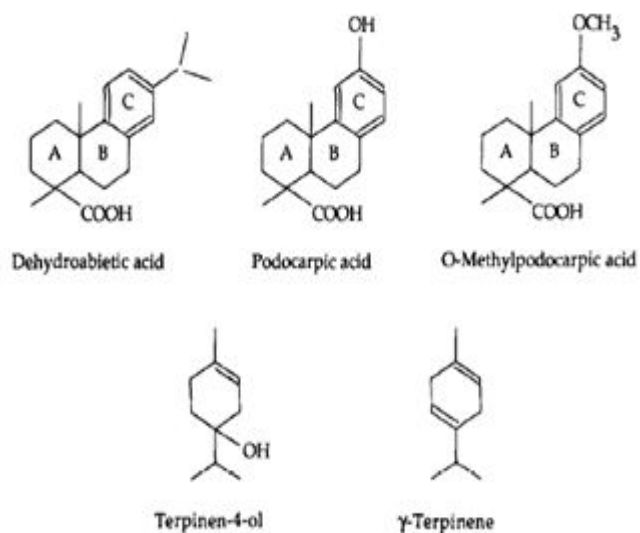


Figure 2.7 Chemical structures of the test compounds [5].

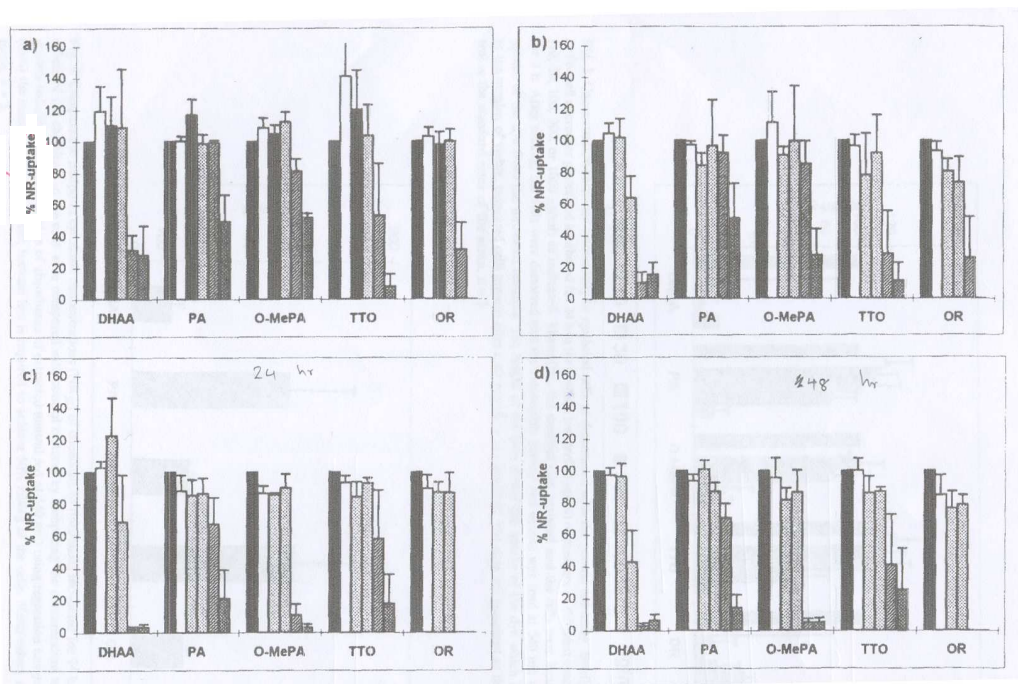


Figure 2.8 Concentration-response cytotoxicity to fibroblasts as determined with the neutral red assay. Briefly, the cells were seeded to 96-well microtiter plates and incubated for (a) 1 h, (b) 4 h, (c) 24 h, or (d) 48 h in the absence (control : 0 $\mu\text{g/ml}$) or presence of different chemicals at concentrations (10, 30, 100, 300, or 1000 $\mu\text{g/ml}$) as indicated [5].

Aranda and co-workers [4] studied the interaction of abietic acid with model membranes of dipalmitoylphosphatidylcholine (DPPC) by using DSC. It was found that abietic acid greatly affected the phase transition of DPPC. The DSC profiles for pure DPPC, when the concentration of abietic acid were increased, the lamellar liquid-crystalline phase transition temperature (T_c) were decreased. It was shown that abietic acid perturbed the cooperative behavior of phospholipids due to the carboxyl group of abietic acid was located near the polar group of phospholipids, i.e., near the water interface, where it could form hydrogen bonding with water and also established the interactions with the polar part of the phospholipids. Incorporation of increasing concentrations of abietic acid resulted in a progressive damage of phospholipids structure.

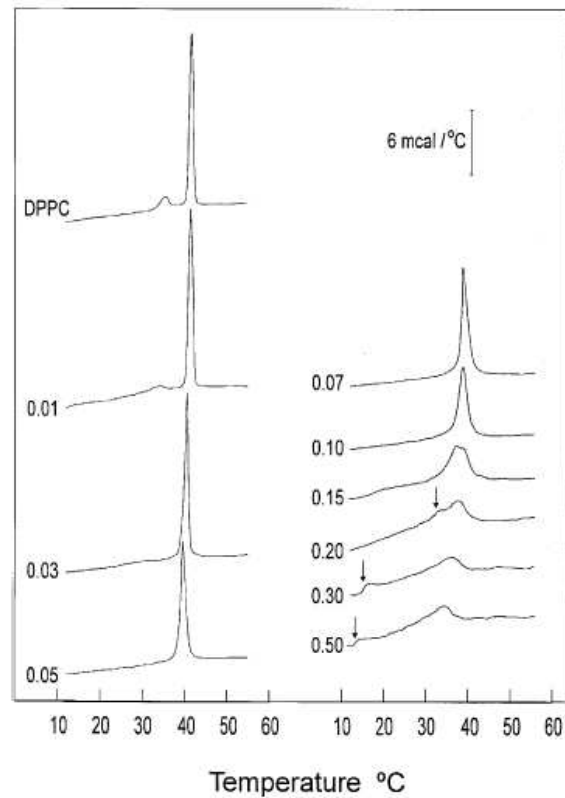


Figure 2.9 DSC thermograms for mixtures of DPPC/abietic acid [4].

2.5 The main function of ingredients of some periodontal dressing [2]

Periodontal dressing consists of three main components as follows:

2.5.1 Reactive organic carboxylic acid e.g. organic fatty acids (vegetable oils, animal fats and oils, marine fats and oils)

2.5.2 Inorganic metal compound e.g. zinc oxide, magnesium oxide

2.5.3 Polymeric resin having carboxylic group e.g. rosin

Besides other ingredient [2] e.g. flavors, cohesive substances, viscosity-adding agents, therapeutic agents, filler are also added to improve physical and mechanical properties

Most of organic fatty acids readily form salts with metal oxides to obtain metal organic salts. This reaction is very fast. In order to retard the reaction, polymeric resin having carboxylic such as rosin will also be added into periodontal dressing ingredients. Some researches studied the reaction of zinc oxide and those resin.

2.6 The reaction of zinc oxide and resin having carboxylic group

In order to understand the mechanism of complexation between carboxylic groups and metal ions, several research studies have been reviewed as follows:

Tang and co-workers [13] prepared the grafting of poly(methacrylic acid) (PMAA) to hydroxyl groups (–OH) on the surface of zinc oxide nanoparticles. The interaction at the interface of nano-ZnO was studied by TGA, FT-IR, ^{13}C NMR and XRD. First, the surface of ZnO was modified with poly(methyl methacrylate). In the spectrum of nano-ZnO particle, the peak at 3410 cm^{-1} indicates the presence of –OH. In the FT-IR spectrum of modified ZnO, the absorption bands at 1732 cm^{-1} are characteristics of C=O stretching vibration from PMMA. The strong absorption bands of 1570 cm^{-1} and 1400 cm^{-1} should correspond to COO[–] of MAA. The interaction between ZnO nanoparticles and grafted PMAA can be deduced from the shift of carboxylic peak toward low wave number. It indicated that ZnO nanoparticles were not simply encapsulated by copolymer chains, but a strong interaction existed at the interface of nano-ZnO and copolymer, implying the carboxylic acid groups of MAA changed into poly(zinc methacrylate) complex sediment. The ZnO/polymer composite were analyzed by ^{13}C NMR, respectively. Comparing the spectrum of the composite with that of the pure polymer, the chemical shift of C=O decreases from 180.7 ppm to 173.4 ppm, which implies that a strong interaction exists at nano-ZnO and the carboxyl groups of copolymer chains. It indicated that the reaction between hydroxyl groups of ZnO and carboxyl group of PMAA occurs on the surface of nanoparticles. The copolymer contents of ZnO/P(MMA–MAA) samples were determined through the weight loss at $700\text{ }^{\circ}\text{C}$ in air using TGA. The TGA curves of both pure polymer and composite particle reveal that the thermal events occur in two temperature ranges: $25\text{--}200\text{ }^{\circ}\text{C}$ and $200\text{--}700\text{ }^{\circ}\text{C}$. In the first zone, the decrease of weight is 1.68% which can be attributed to desorption of water and initiator fragments. The second weight loss corresponds to the P(MMA–MAA) decomposition. The loss value of composite particles is 68.2%. X-ray diffraction patterns of pure nano-ZnO particles and composite particles were analyzed by using XRD. Except for a weak amorphous peak appearing at 2θ from 10 to 15, the spectra of composite particles are almost the same as those of pure particles, implying that the reaction has not altered the

crystalline structure of the ZnO nanoparticles. Nevertheless, the presence of PMAA results in the decrease of the crystallite size represented by less sharp diffraction peaks. It indicates that a small amount of Zn is possibly consumed to form poly(zinc methacrylate) complex on the surface of nano-ZnO. The carboxyl groups of methacrylic acid can react with the hydroxyl groups (-OH) on the surface ZnO to form poly(zinc methacrylate) complex. The copolymer chain were grafted and encapsulated on the surface of nano-ZnO. The reaction has not altered the crystalline structure of the ZnO nanoparticles.

2.7 Methods of analysis of the metal complexes [14]

2.7.1 Determination metal bound to chitosan derivatives

- **Indirect determination:** The amount of metal adsorbed on the polymer can be determined by equilibrating the polymer in a metal ion solution of known concentration, followed by determination of the amount of metal ion in the supernatant by atomic absorption spectroscopy, (AAS), titration with EDTA, UV spectra, etc.

- **Direct determination:** The metal ion bound to the polymer can be determined by decomposing the polymer-metal complex in concentrated nitric acid and then measuring the concentration by AAS.

2.7.2 Determination of sorption mechanism, structure of complexes by SEM/EDAX, DSC, TGA, IR and ^{13}C NMR

- SEM/ EDAX

Scanning electron microscopy (SEM) is an extremely useful method for visual confirmation of surface morphology and the physical state of the surface. SEM coupled with energy dispersive analysis of X-rays (EDAX) is used to determine the metal uptake mechanism on chitosan which is a complex phenomenon involving nodule formation on the polymer surface, ion adsorption and ion absorption. It may also be used to determine the porosity of chitosan beads as well as membranes and diffusion of metal ions through them.

- DSC

Differential scanning calorimetry (DSC) is an effective tool in characterizing chitosan and its metal chelates. The DSC curve of chitosan–metal chelates shows two peaks: an endothermic peak at $100\text{ }^{\circ}\text{C}$ and an exothermic peak at $310\text{ }^{\circ}\text{C}$. The glass transition temperature of chitosan was observed to be $203\text{ }^{\circ}\text{C}$. The two peaks in the DSC curve are due to vaporization of water in the polymer and oxidative degradation as well as deacetylation [15]. Hg^{2+} , Cu^{2+} and Fe^{3+} complexes of chitosan had been characterized by DSC as shown in Figure 2.10. It was observed that there was a small increase above the chitosan in the decomposition temperature of these metal complexes. This was considered to be the effect of two opposing factors: (a) conformational changes of chitosan leading to thermal instability, and (b) additional bridging through metal ion leading to enhanced thermal stability. It was observed that chitosan does not show any endothermic transition between room temperature and $250\text{ }^{\circ}\text{C}$ indicating the lack of any crystalline or any other phase change during the heating process. The strong exothermic peak centered around $270\text{ }^{\circ}\text{C}$ is due to Hg^{2+} complex showed three endothermic transitions at 206 , 220 and $242\text{ }^{\circ}\text{C}$ while Cu^{2+} complex

showed a single peak at 203 °C, which could be due to formation of a new crystalline phase.

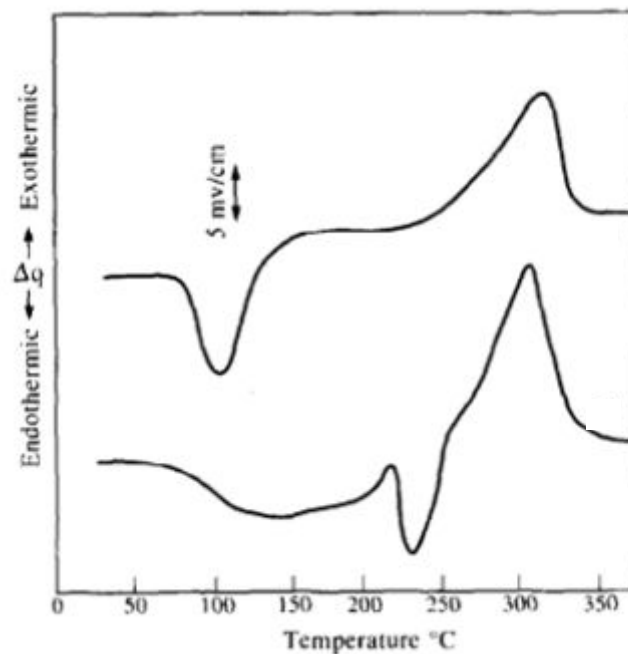


Figure 2.10 Thermograms of chitosan-copper complex (below) and chitosan-ferrous iron complex (above) [15].

- TGA

Thermogravimetric analysis (TGA) has been used to study the chitosan- Ag^+ complexes and it was observed that chitosan became thermally less stable after forming the complex [16]. It was also seen that only 52% of the Ag^+ present was complexed with chitosan while remaining was retained by sorption as shown in Figure 2.11. Chitosan- Cu^{2+} complexes at pH 5, 6 and 7 were studied by TGA. Chitosan showed three steps in thermograms while complexes showed four steps [17].

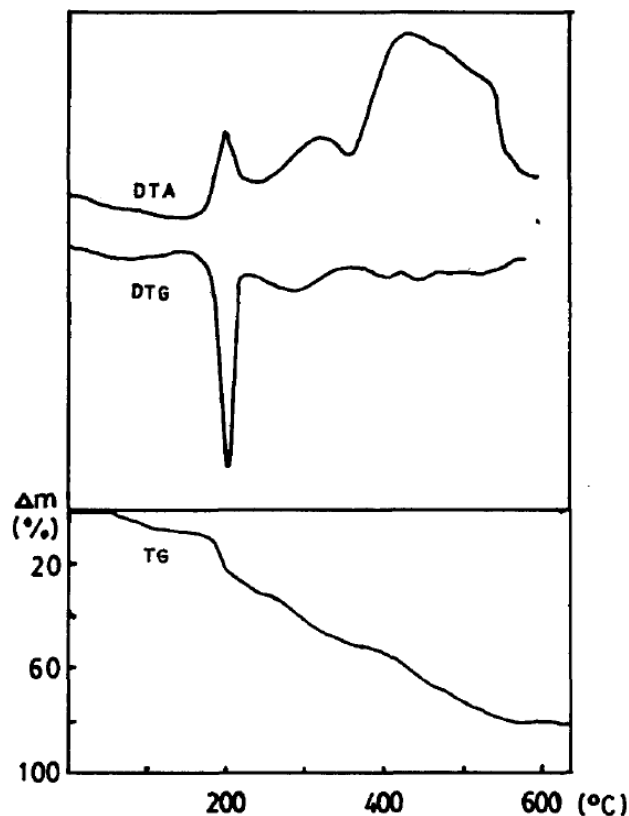


Figure 2.11 DTG, TG and DTA curves for silver-containing chitosan [16].

- IR and ^{13}C NMR

Infrared (IR) and nuclear magnetic resonance (NMR) techniques are one of the most commonly used to determine the active sites in chelate formation. A study of chitosan–Schiff's bases, viz. mixed salicylidene and benzylidene chitosan derivatives and their complexes with Cu^{2+} , showed that the carbon signals due to salicylidene chitosan disappeared and those of benzylidene chitosan were broadened significantly. This indicated that benzylidene chitosan did not take part in chelate formation. It was also shown that the presence of paramagnetic ions affected the resolution significantly [18]. Coordination of fully deacetylated chitosan with Zn^{2+} showed the involvement of amine and secondary hydroxyl groups of chitosan in chelate formation. Also shifts in the bands at 3420 cm^{-1} (OH and NH_2 groups) to 3391 cm^{-1} , at 1597 cm^{-1} band ($-\text{NH}$ stretching) to 1620 cm^{-1} , and at 1098 cm^{-1} band (sec OH stretching) to 1062 cm^{-1} supported the chelate formation of amine and hydroxyl groups

with Zn^{2+} . There was no shift in the band at 1038 cm^{-1} (primary OH), which suggested that primary hydroxyl was not involved in chelate formation. IR spectrum of chitosan– Cu^{2+} complex revealed that the secondary hydroxyl and amine coordinated to Cu^{2+} and new peaks were observed at 555, 532, 551, and 511 cm^{-1} . The peak at 550 cm^{-1} corresponds to asymmetric Cu–O vibration and 511 cm^{-1} corresponds to hydroxy-bridged complex [17].

Rosin, abietic acid and its derivatives was used in the ingredient at some commercial available periodontal dressing in order to retard the setting time i.e. to retard the reaction between organic carboxylic acids and metal, and able to be molded. From the above reports, rosin was a toxic substance. Therefore, it is our interest to find novel complexation between non-toxic polymers with metal oxide, instead of toxic carboxylic groups owning materials.

Sodium chitosan phosphated were selected in this study because of its own the amino groups, phosphate groups and hydroxyl groups that can complexation with zinc oxide.

The aim of this research was to prepare sodium chitosan phosphate/zinc oxide complexes and characterize the possible structure. Cytotoxicity of sodium chitosan phosphate/ zinc oxide complexes were determined using sodium chitosan phosphate, rosin and Coe-pak[®] as control. The obtained sodium chitosan phosphate/zinc oxide complexes were expected for non-cytotoxicity which an approach for periodontal dressing component. And other research studied the mechanism between chitosan and zinc ion which could occurred the complexation.

Furthermore, it had the reports about phosphorylated chitosan was inhibited the growth of oral bacterial. Hiroshi and co-workers [19] examined the effects of four kinds of chitosan derivatives on initial adherence of oral bacterial onto human anterior teeth surfaces. We found that the order of magnitude of the inhibitory effect on the adherence of oral bacteria was low molecular chitosan (LMCS) > phosphorylated chitosan (PPPS) > amorphous chitosan (PDAS) > carboxymethyl chitosan (PCMS). These results suggest that phosphorylated chitosan have the potential to effectively inhibit the initial adherence of oral bacteria onto human tooth surfaces due to phosphorylated chitosan contains both phosphate group and amino resides in the same glucosamine units.

These amphoteric units might interfere with the binding of a variety of plaque bacteria, which may adsorb to the enamel surface by electrostatic interactions. Therefore, the possible mechanism of the action of phosphorylated chitosan might include of formation of polyelectrolyte complexes on the tooth surface, which permit less interaction between oral bacterial and tooth enamel. Furthermore, Sodium chitosan phosphate was expected the biocompatible material.

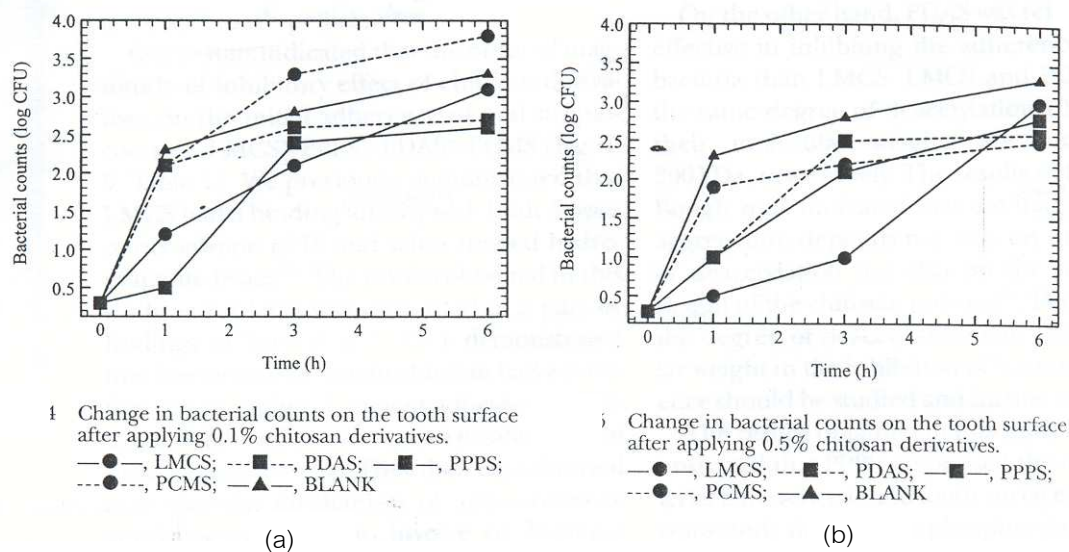


Figure 2.12 Change in bacterial counts on the tooth surface after applying a) 0.1 % b) 0.5% chitosan derivatives [19].

Nishi and co-workers [20] studied the adsorption of Ca^{2+} ions to highly phosphorylated derivatives of chitin (P-chitin) and partially deacetylated chitin (%DA = 45, 97) (high degree of substitutions) were crosslinked with adipoyl chloride. It was found that phosphoryl, hydroxyl and acetylamine groups of phosphorylated chitin and deacetylated chitin could be binding with Ca^{2+} ion due to phosphate group at $900\text{-}1000\text{ cm}^{-1}$ and around 1200 cm^{-1} changed remarkably by the binding of Ca^{2+} ion. The adsorption due to amide around 3200 cm^{-1} and around $1550\text{-}1700\text{ cm}^{-1}$ also changed. Furthermore, the amino group around 3000 cm^{-1} and hydroxyl group around 1300 cm^{-1} were also changed.

CHAPTER III

EXPERIMENTAL PROCEDURE

3.1 Chemicals and materials

Chemicals and instrument used in this study were listed in Tables 3.1 and 3.2.

Table 3.1 Chemicals list

Chemicals	Formulation	Abbreviation	Supplier
1. Chitosan (%DD = 85), high viscosity		CTS-85	Fluka (Japan)
2. Phosphorus pentoxide	P ₂ O ₅	-	Carlo Erba (Italy)
3. Methanesulfonic acid	CH ₄ SO ₃	-	Acros organic (USA)
4. Sodium hydroxide	NaOH	-	Ajax Finechem (Australia)
5. Ethanol	C ₂ H ₅ OH	-	Zen point (Thailand)
6. Acetone	C ₄ H ₉ NO	-	Zen point (Thailand)
7. Hydrochloric acid	HCl	-	Lab scan (Thailand)
8. Zinc oxide	ZnO	-	Ajax Finechem (Australia)
9. Dulbecco's Modified Eagle's Medium	-	DMEM	Gibco BRL (USA)
10. Fetal bovine serum	-	FBS	Gibco BRL (USA)
11. Penicillin/Streptomycin	-	-	Gibco BRL (USA)
12. Fungizone	-	-	Gibco GRL (USA)
13. Phosphate buffed saline, pH 7.4	-	PBS	Gibco BRL (USA)
14. Povidone Iodine solution	-	-	-
15. Vybrant [®] MTT cell proliferation assay kit	-	V-13154	Gibco BRL (USA)

Table 3.2 Instrument list

Instruments	Abbreviation	Supplier
1. Fourier Transform Infrared Spectrometer	FTIR	Perkin Elmer
2. X-ray Diffractometer	XRD	Bruker AXS Model D8
3. Thermogravimetric Analyzer	TGA	Mettler Toledo
4. Differential Scanning Calorimeter	DSC	Mettler Toledo
5. Penetrometer	-	Future-Tech
6. Microhardness	-	Amersham bioscience
7. Scanning Electron Microscope	SEM	JEOL JSM-5800LV
8. Microplate reader	TE2000-U	-
9. Inverts optical microscope	-	Nikon Eclipse
10. CO ₂ incubator	-	Thermo Forma
11. Water bath	Hiclave™ HV-50	Memmert
12. Autoclave	-	Hirayama co.
13. Microflow Laminar	-	Astec Microflow

3.2 Methodology

3.2.1 Preparation of sodium chitosan phosphate/zinc oxide complexes

Sodium chitosan phosphate with degree of phosphate substitution of 0.6 was synthesized in the laboratory according to the method presented by Netswasdi [21]. Briefly, synthesis of sodium chitosan phosphate is shown in Figure 3.1. Sodium chitosan phosphate was synthesized through 3 steps which were phosphorylation, sodium salt formation and neutralization. First, a 4 g of chitosan was reacted with 2 equivalent moles of phosphorus pentoxide (P₂O₅) 6.8 g in 28 ml of methanesulfonic acid. The reaction was allowed to proceed at room temperature for 3 hrs with stirring speed of 300 rpm. The mixture was then precipitated in acetone, washed with ethanol and dried at 40°C. Second, the obtained phosphorylated chitosan was dissolved in small amount of

distilled water, dialyzed against sodium hydroxide. The excess sodium hydroxide was neutralized with hydrochloric acid. The mixture was then dialyzed again against distilled water.

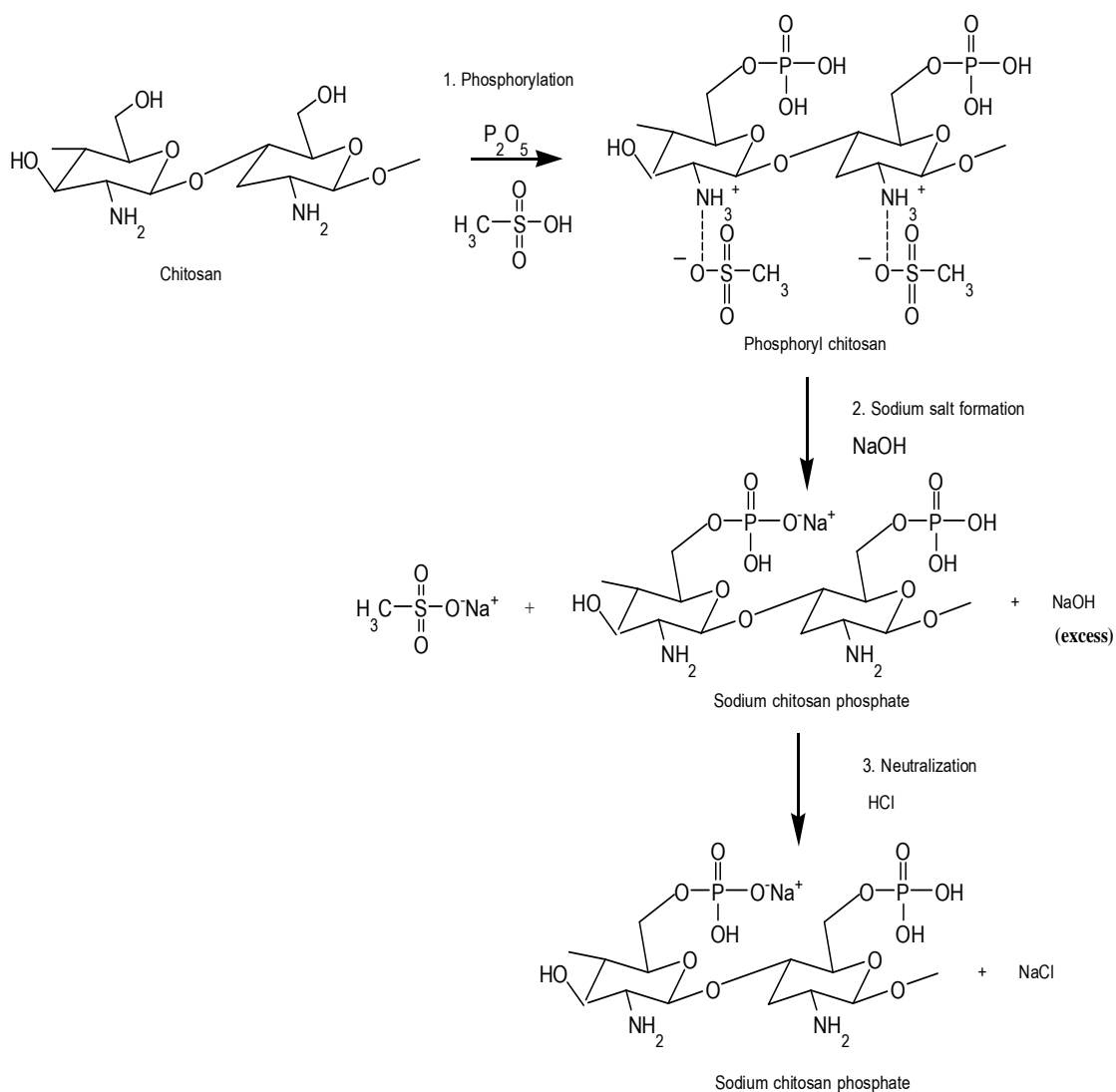


Figure 3.1 Synthesis pathway of sodium chitosan phosphate [21].

A 0.1 g of sodium chitosan phosphate was dissolved in 1.5 ml distilled water i.e. concentration of sodium chitosan phosphate of 6.67% by weight. Zinc oxide powder was then added to sodium chitosan phosphate solution in various sodium chitosan phosphate to zinc oxide ratios of 1:0.25, 1:0.5, 1:1 and 1:2 as shown in Table 3.3. The mixture was then mixed homogeneously until the solution change to be pasted. The obtained sodium chitosan phosphate/zinc oxide complexes paste was incubated at 37°C for 24 hrs.

Table 3.3 Mole ratios of sodium chitosan phosphate and zinc oxide

Mole ratios of PCTS and Zinc oxide	Content of PCTS (mmol)	Content of ZnO (mmol)	H ₂ O (ml)
1:0.25	0.474	0.1185	1.5
1:0.5		0.2370	
1:1		0.4740	
1:2		0.948	

3.2.2 Investigation of complex formation by FTIR, XRD, TGA and DSC

3.2.2.1 Identification of functional groups

The functional group and chemical structure of sodium chitosan phosphate/zinc oxide complexes were examined by FTIR. The complexes between sodium chitosan phosphate and zinc oxide at different ratios were grinded with KBr powder and then pressed to be transparent pellet. The FTIR spectra were scanned from 4000-400 cm⁻¹ with resolution of 4.0 cm⁻¹, number of scan 16 scans using DLATGS detector.



Figure 3.2 Fourier Transform Infrared Spectrometer.

3.2.2.2 Determination of crystalline

The crystalline of sodium chitosan phosphate/zinc oxide complexes were determined by XRD comparing with chitosan powder, sodium chitosan phosphate powder and zinc oxide powder. X-ray diffraction was measured by a Bruker AXS Model D8. X-ray source was originated using $\text{CuK}\alpha$ ($\lambda=0.154$ nm). Sodium chitosan phosphate/zinc oxide complexes were scanned at 2θ in the range of $5\text{-}60^\circ$ with scan speed of $0.02^\circ\text{sec}^{-1}$.



Figure 3.3 X-ray Diffractometer.

3.2.2.3 Thermal analysis

Thermograms of PCTS/ZnO complexes were recorded by using DSC and TGA with a Mettler Toledo. The decomposition temperature (T_d) and derivative thermal gravimetric (DTG) of samples were determined by TGA from 25°C to 1000°C with heating rate of 20°C/min under N₂ atmosphere. The crystalline metal complex temperature (T_c) was analyzed by DSC with the first heat scan from 50°C to 250°C with heating rate of 10°C/min.



Figure 3.4 Thermal Gravimetric Analyzer.



Figure 3.5 Differential Scanning Calorimeter.

3.2.3 Determination of setting time [22]

Setting time was defined as time to solidify sodium chitosan phosphate/zinc oxide complexes at 37°C. The setting time of sodium chitosan phosphate/zinc oxide complexes were measured followed by ISO 3107 using penetrometer as shown in Figure 3.6. The mixture of sodium chitosan phosphate and zinc oxide in various ratios was stirred 180 s before filling into mould (10 mm in diameter and 2 mm in height), then incubated at 37°C. The specimens were compressed with indented needle of mass $100\text{ g} \pm 0.5\text{ g}$ and having flat end of diameter of $2.00\text{ mm} \pm 0.1\text{ mm}$. The setting time was recorded when the needle could not penetrate into the specimens. Each specimen was measured for 5 times and reported in average values.



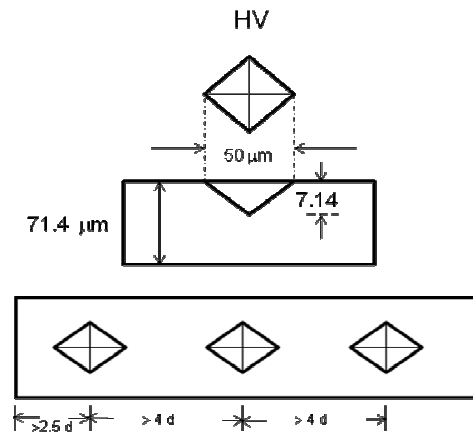
Figure 3.6 Penetrometer.

3.2.4 Determination of hardness [23]

The hardness of sodium chitosan phosphate/zinc oxide complexes were measured by the Vicker microhardness. The specimens were prepared by mixing sodium chitosan phosphate solution with zinc oxide at different mole ratios as mentioned in Table 3.3. The mixture was then paste onto one glass plate and punch at 5 mm in diameter. The mixture was then covered with another glass plate and incubated at 37°C

for 24 hours. The specimens with 2 mm. thickness were selected for the test spacer. The hardness of all specimens was measured with square-based pyramidal diamond indenter. Load of 50 g or 100 g was applied to the specimens. Vicker hardness was calculated by following equation 1 [23].

$$HV = 0.102 F/S = 0.102 [2 F \sin(\theta/2)/d^2] = 0.1891 F/d^2 \quad (1)$$



Where, HV = Vickers hardness

F = Test load (N)

S = Surface area of an indentation (mm²)

d = Average diagonal length of an indentation (mm)

θ = Face angle of the pyramidal diamond indenter (°)

3.2.5 Characterization of surface morphology

The morphology of sodium chitosan phosphate/zinc oxide complexes were observed by SEM. Zinc distribution in the complexes was observed by SEM in mapping mode as 500 magnitudes. The dispersion of zinc oxide of the complexes were observed by SEM mapping mode. The % degree of substitution (%DS) of sodium chitosan phosphate were determined for 3 times by using SEM-EDS mode [21].



Figure 3.7 Scanning Electron Microscope.

3.2.6 Cytocompatibility test of sodium chitosan phosphate and sodium chitosan phosphate/zinc oxide complexes with human gingival fibroblast (HGF) [24]

3.2.6.1 Harvest of healthy gingival tissue

Human gingival fibroblast cell (HGF) was obtained from the healthy gingival tissue attached to the removal tooth from patients whom admitted for gingival surgery at oral and maxillofacial surgery clinic in Faculty of Dentistry, Prince of Songkla University. The harvested healthy gingival tissue was placed in DMEM (Dulbacco's Modified Eagle's Medium) pH 7.2

3.2.6.2 Human gingival fibroblast cell culture

The gingival tissue sample was sterilized by immersed in providone iodine solution about 3-5 minutes. The gingival tissue sample was washed with DMEM pH 7.2 about 3 times. The gingival tissue sample was cut into thin pieces in size $1 \times 1 \text{ mm}^2$ and placed in the culture plate diameter 6 cm. Next, fibroblast culture medium pH 7.2 was added in the culture plate. Fibroblast culture medium is DMEM medium containing FBS, Peniciline and Fungizone. Gingival fibroblast cells were cultured in humidified atmosphere of 95% air and 5% CO_2 at 37°C for 48 hours. After 48

hours, cells were observed under microscope. Fibroblast culture media was changed every 2 days. When the fibroblast cells were grown up about 70-80% of the culture plate, the cells were subcultured to the next passage.

3.2.6.3 Subculture of human gingival fibroblast cell

The culture plates that had the fibroblast cells about 70-80% of culture areas were discarded. The cell culture plate was rinsed with phosphate buffer saline (PBS) pH 7.4 about 2 times. After that, a 2 ml of 0.025% trypsin - EDTA was added into culture plates to detach cell from the culture plate. The fibroblast cells were incubated in humidified atmosphere of 95% air and 5% CO₂, 37°C about 1 min. Then, the fibroblast media was added into the culture plate to suspend the detached fibroblast cells. After that, the cells suspension was transferred into the centrifuge tube, and centrifuged at 4 °C, 2000 rpm for 10 minutes. The supernatant were slowly discarded. A 1-2 ml of fresh fibroblast culture media was added. The obtained cell suspension was transferred into the plastic flask, size 25 ml. The fibroblast culture medium was added until total volume of 5 ml. Cell culture medium was changed every 2 days. When the plastic flask had the fibroblast cells about 70-80%. The fibroblast cells were subcultured again into plastic flask size 75 ml or 2 flasks of the same size. The fibroblast cells were subcultured until to the passage 7. Then this passage was used to test the cytotoxicity of the complexes materials.

3.2.6.4 Cytocompatibility of sodium chitosan phosphate and sodium chitosan phosphate/zinc oxide complexes with human gingival fibroblast (HGF)

3.2.6.4.1 Direct contact test

Cytocompatibility of sodium chitosan phosphate/zinc oxide complexes were analyzed with human gingival fibroblast cells using sodium chitosan phosphate as control. Cytocompatibility of rosin and Coe-pak[®] were also tested for comparative study. Human gingival fibroblast were cultured monolayer in 24

multi-wells plate around 2.5×10^4 cells per well. Fibroblast culture medium were filled into 24 multi-wells plate around 5 ml per well. When the fibroblast cells were grown up about 70-80% of the culture plate, the old media were removed. The fresh medium was filled into plate around 5 ml per well. Next, the sodium chitosan phosphate, sodium chitosan phosphate/zinc oxide complexes, rosin and Coe-pak[®] were cut into small pieces of 5 mm in diameter and 2 mm in height. The specimens were sterilized with 70% ethanol for 1 hr and rinsed with phosphate buffer saline 3 times. The specimens of sodium chitosan phosphate or sodium chitosan phosphate/zinc oxide complexes were placed on the monolayer of human gingival fibroblast multi-wells culture plate. After that, the human gingival fibroblast cells were incubated at 37°C in humidified atmosphere of 95% air and 5% CO₂. The fibroblast culture media was changed every 2 days. Clear zone was observed by inverted phase contrast light microscopy after 24, 48 and 72 hrs with magnification of object lens of $\times 10$, eyes lens of $\times 10$ and camera digital zoom of $\times 0.7$.

3.2.6.4.2 Indirect contact test

For indirect contact test, the samples such as sodium chitosan phosphate, the PCTS/ZnO complexes at 1:0.25, 1:0.5, 1:1, 1:2 equivalent mole, rosin and Coe-pak[®] were rinsed in ethanol for 1 hour. Next, samples were immersed in fibroblast media and incubated at 37°C in humidified atmosphere of 95% air and 5% CO₂ for 2 weeks. After remove those samples, the remaining fibroblast culture media was called later "Extract solution". After that, an indirect cytotoxic test was investigated with HGF cells culturing with each samples' extract solutions. Human gingival fibroblast were cultured around 5×10^3 cells per well in 96 multi-wells. Fibroblast medium were added into 96 multi-wells around 1 ml per well. After that, the human gingival fibroblast cells were incubated at 37°C in humidified atmosphere of 95% air and 5% CO₂ for 24 hrs. After 24 hours, cells were observed under microscope. When the fibroblast cells were grown up about 70-80% of the culture plate, the old medium were drained by suction. Next, each samples' extract solutions was filled into 96 multi-wells around 1 ml per well. Next, these multi-wells were incubated at 37°C in humidified atmosphere of

95% air and 5% CO₂ for 24 and 48 hrs. After 24 and 48 hours, the extracted solutions were replaced with 1 ml of fresh culture medium. Then, Vybrant[®] MTT Cell Proliferation Assay Kit provides a simple method for determination of cell number using standard microplate absorbance readers. Briefly of MTT assay, Component A, which are the mixture between 3-(4,5-dimethylthiazol-2-yl)-2,5-diphenyltetrazolium bromide (MTT) and phosphate-buffered saline, and Component B, which are the mixture between sodium dodecyl sulfate (SDS) and hydrochloric acid, were added into the 96 multi-wells. The MTT assay involves the conversion of the water soluble MTT to an insoluble formazan and the concentration determined by optical density (OD) at 570 nm with comparing to optical density of control. Positive control was groups of HGF cells culturing with normal fibroblast culture medium.

CHAPTER IV

RESULTS AND DISCUSSION

4.1 Appearance of PCTS/ZnO complexes

All ratios of sodium chitosan phosphate/ zinc oxide complexes were successfully prepared by mixing zinc oxide powder to sodium chitosan phosphate aqueous solution for 180 s. Sodium chitosan phosphate aqueous solution has the pH value around 6.5. Since amino groups of chitosan showed pKa around 6.5 [25], thus, amino groups of sodium chitosan phosphate are almost no electrical charged. The mixture was similarly in appearance to milky colloid solution due to the dispersion of zinc oxide in sodium chitosan phosphate aqueous solution. The mixture was dried at 37°C to obtain brittle white organic/inorganic hybrids. The solidification time is not dependent on mole ratios of sodium chitosan phosphate to zinc oxide.

4.2 Possible structure of PCTS/ZnO complexes

4.2.1 Chemical structure of PCTS/ZnO complexes

Sodium chitosan phosphate and sodium chitosan phosphate/zinc oxide complexes with various mole ratios were characterized by FTIR spectroscopy. FTIR spectra of the complexes are showed in Figure 4.1. In FTIR spectrum of sodium chitosan phosphate (Figure 4.1 (a)), the board absorption band at 3441 cm^{-1} is due to -NH_2 groups and -OH groups stretching on pyranose ring of sodium chitosan phosphate. The absorption bands at 1554 cm^{-1} and 975 cm^{-1} represent the specific peaks of N-H bending and P-OH groups, respectively. In FTIR spectra of sodium chitosan phosphate/zinc oxide complexes (Figure 4.1 b-e), all complexes with various sodium chitosan phosphate to zinc oxide mole ratios show similar FTIR spectra. The higher content of zinc oxide shows the boarder OH adsorption band at 3441 cm^{-1} due to higher amount of OH absorption of water molecules on the surface of zinc oxide. Zinc oxide also shows FTIR spectrum only one peak of OH absorption (data shown in appendix). It

indicates that surface is covered with surface hydroxyl species. According to many literatures [26] mention that hydroxyl groups are formed by dissociative chemisorptions of water molecules, and it is generally considered that hydration and hydroxylation occur at exposed lattice metal ion sites on the surface as the lattice metal ions are strong Lewis acids. With this mechanism, the surface hydroxyl site density would be different depending on the metal ion valences and the lattice planes exposed. Tamura and co-workers [26] also mentioned that hydroxyl groups were formed by the neutralization of Lewis base by the exposed water. The new mechanism, however, was verified that closely packed lattice oxide ions (rather than lattice metal ions) were exposed to water because of their size and that the surface oxide ions were strong Lewis bases as a result of insufficient coordination to the lattice metal ions. Since it was found that the surface hydroxyl site densities measured by the Grignard reagent method were not different for different oxide samples with different lattice metal ion valences [27].

The NH_2 and OH stretching peak at 3441 cm^{-1} was shifted to lower frequency for all complexes as comparing PCTS, possibly owing to transferring lone pair electrons from hydroxyl groups to surface of ZnO. The absorption band at 1554 cm^{-1} of N-H bending gradually disappeared as increasing equivalent mole of ZnO. This may be due to lone pair electron of nitrogen in N-H bending was transferred to the surface of ZnO. The specific band of P-OH stretching at 975 cm^{-1} in all complexes were not shifted, but P-OH peak may combine with the neighboring peaks. This was also possibly due to lone pair electron donating to the surface of ZnO. Since, lone pairs of electron have the ability to bind to a proton or complex with a metal ion through electron-pair sharing. A nitrogen site would have a stronger ability to donate the lone pair of electrons in sharing with a metal ion than an oxygen site since oxygen has a stronger attraction of the lone pair of electrons to its nucleus [28].

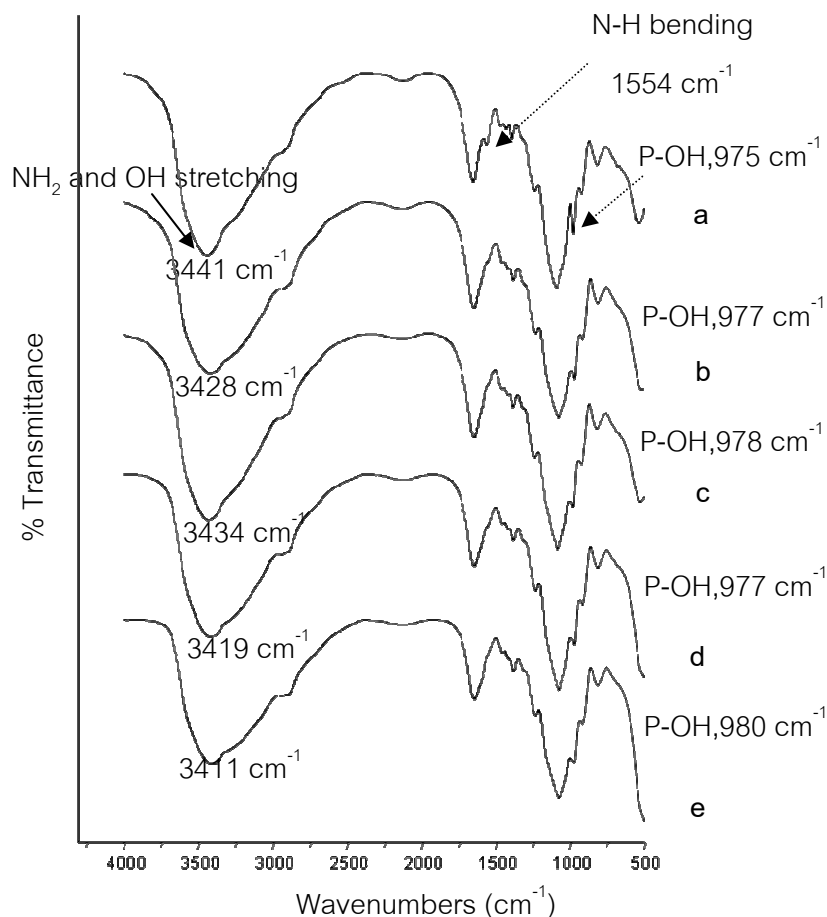


Figure 4.1 FTIR spectra of (a) sodium chitosan phosphate (PCTS) (b) PCTS/ZnO, 1:0.25 (c) PCTS/ZnO, 1:0.5 (d) PCTS/ZnO, 1:1 (e) PCTS/ZnO, 1:2 equivalent mole.

4.2.2 Crystalline structure of PCTS/ZnO complexes

The X-ray diffraction patterns of (a) chitosan (b) sodium chitosan phosphate (c) zinc oxide (d) PCTS/ZnO, 1:0.25 (e) PCTS/ZnO, 1:0.5 (f) PCTS/ZnO, 1:1 (g) PCTS/ZnO, 1:2 mole equivalent were shown in Figure 4.2. The XRD pattern of chitosan shows 2θ at 10° and 20° in Figure 4.2 a, while sodium chitosan phosphate (Figure 4.2 b) does not show any XRD pattern. This indicates that sodium chitosan phosphate is in amorphous form. Pure zinc oxide (Figure 4.2 c) shows 2θ at 31° , 34° , 35° , 47° and 56° . When sodium chitosan phosphate was reacted with zinc oxide at different sodium chitosan phosphate to zinc oxide ratio as shown in Figures 4.2 d-g, sodium chitosan phosphate/zinc oxide complexes show only 2θ peaks of zinc oxide.

The results from X-ray diffraction indicate that the complexation does not disturb crystalline of zinc oxide.

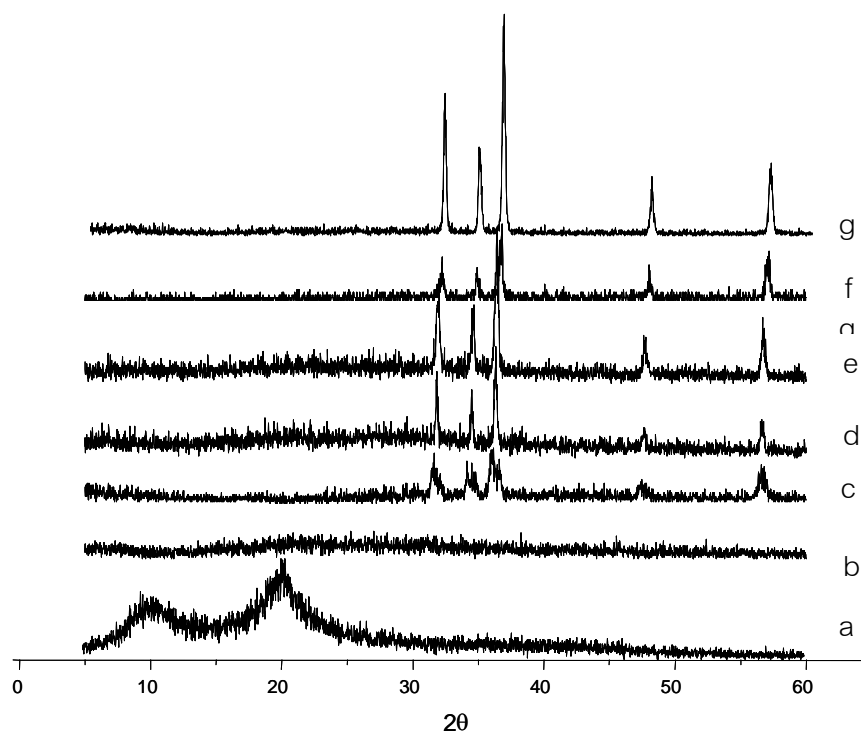


Figure 4.2 XRD patterns of (a) chitosan (b) sodium chitosan phosphate (c) zinc oxide (d) PCTS/ZnO, 1:0.25 (e) PCTS/ZnO, 1:0.5 (f) PCTS/ZnO, 1:1 (g) PCTS/ZnO, 1:2 equivalent mole.

4.2.3 Thermal properties of PCTS/ZnO complexes

Figure 4.3 shows TGA diagrams of sodium chitosan phosphate and sodium chitosan phosphate/zinc oxide complexes with various mole ratios. All samples show the initial water loss stage around 100°C . Table 4.1 shows derivative thermal gravimetric (DTG) deriving from TGA curves of PCTS and PCTS/ZnO complexes. It was found that the initial water loss temperature of the complex decreases as increasing ZnO. This may be because ZnO absorbs heat and accelerates the evaporation of the absorbed water. The degradation of sodium chitosan phosphate main chain is single stage decomposition around 255°C . Sodium chitosan phosphate/zinc oxide complexes exhibit the second stage nearly merging with the first stage i.e. the start temperature of

the second stage degradation is the same as the end temperature of the first stage with the DTG of degradation temperature being observed in Figure 4.3. This may be attributed to metal complex degradation temperature. According to thermal properties of crosslinked chitosan metal complex studied by Trimukhe and co-workers [29], ignoring the initial water loss stage, crosslinked chitosan showed single stages degradation, whereas chitosan-metal complexes exhibited two stages thermal degradation indicating the metal complex degradation and chitosan degradation, respectively. As shown in Table 4.1, metal complex degradation temperature significantly increases from around 210°C to 220°C when the equivalent mole of ZnO to PCTS reaches 1:1. This may be because of ZnO has ability to absorb heat and retard the degradation of metal complex interaction. The final stage decomposition of sodium chitosan phosphate of metal complexes exhibits DTG a bit higher than the decomposition temperature of sodium chitosan phosphate as shown in Table 4.1. Also, the degradation temperature of polymer main chain significantly increases from around 260°C to 270°C when the equivalent mole of ZnO to PCTS reaches 1:1. Since ceramic has a higher thermal conductivity as well as heat conductivity value than polymer [30] [31]. Zinc oxide will absorb the heat transmitted from the surrounding and retard the direct impart to polymer backbone, resulting in the retardation of polymer degradation. Then, the decomposition temperature of PCTS in the complexes increases as increasing zinc oxide contents. The PCTS/ZnO complexes with higher equivalent moles of zinc oxide show slighter weight loss.

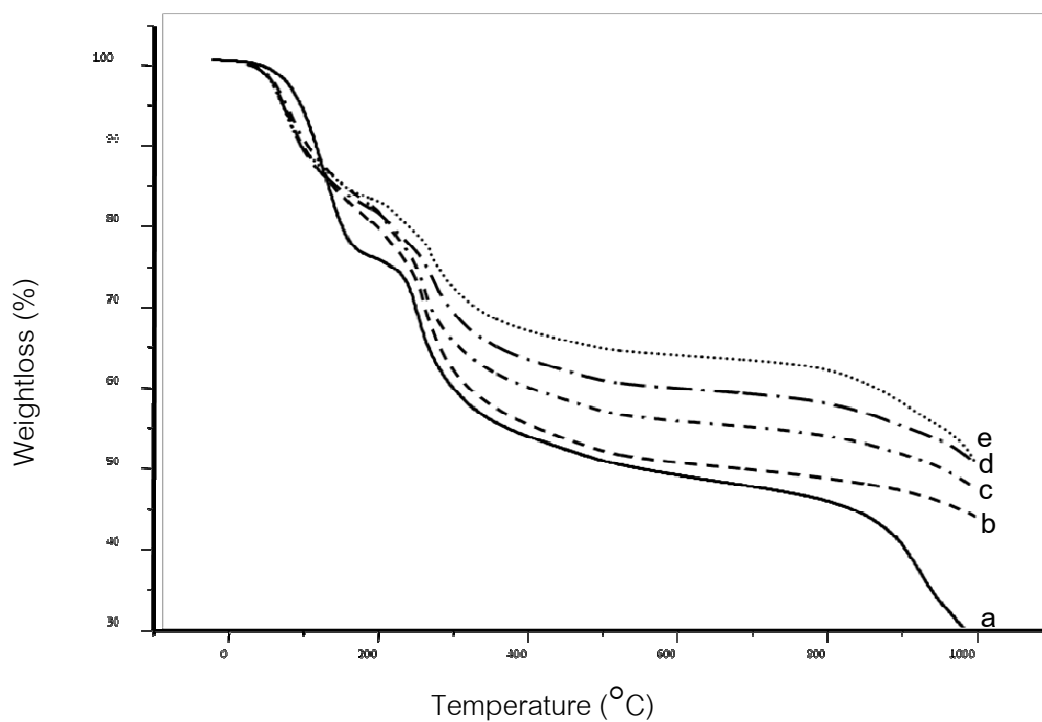


Figure 4.3 TGA diagrams of (a) PCTS, and its metal complexes with various PCTS/ZnO mole ratios of (b) 1:0.25, (c) 1:0.5, (d) 1:1 and (e) 1:2.

Table 4.1 Derivative thermal gravimetric (DTG) deriving from TGA curves of PCTS and PCTS/ZnO complexes

Sample	First stage (°C) DTG (water loss)	Second stage (°C) DTG (metal complex degradation)	Third stage (°C) DTG (Polymer decomposition)
PCTS	125	-	255
1:0.25	82	210	260
1:0.5	87	207	263
1:1	80	217	273
1:2	77	220	272

Figure 4.4 shows DSC diagrams of PCTS and its metal complexes. PCTS shows only one endothermic peak, whereas, its metal complexes show another exothermic peak. The former endothermic peak represents the evaporation of volatile [15] and the latter exothermic peak corresponds to metal complex degradation [15]. Table 4.2 summarizes volatile evaporation temperature and metal complex degradation temperature in detail. All samples appeared the evaporation of adsorbed water temperature around 100-114 °C. It is found that the evaporation temperature decreases with increasing zinc oxide contents as shown in Table 4.2. Similar reason as mentioned above that possibly due to heat absorption capacity rise when increasing in amount of ZnO and accelerate evaporation of water. Furthermore, no metal complexes degradation peak was found in PCTS. This result indicates that PCTS may form complex with zinc oxide. According to TGA results, the metal complex degradation temperature of those complexes increases as increasing zinc oxide contents. Because zinc oxide particles could adsorb heat, and stabilize PCTS backbone to degrade in higher temperature at higher zinc oxide contents.

Table 4.2 Summary of endothermic and exothermic temperature

Samples	Evaporation temperature (endothermic, °C)	Metal complex degradation temperature (exothermic, °C)
PCTS	114	-
PCTS/ZnO, 1:0.25	108	198
PCTS/ZnO, 1:0.5	104	201
PCTS/ZnO, 1:1	103	201
PCTS/ZnO, 1:2	100	210

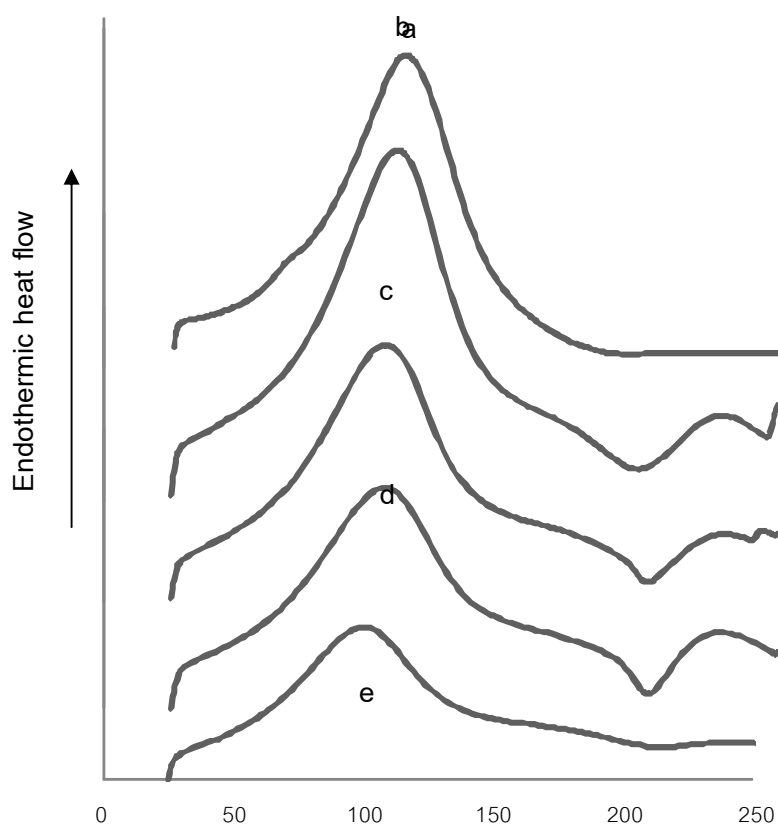


Figure 4.4 DSC thermograms of (a) PCTS and its metal complexes with various PCTS/ZnO mole ratios of (b) 1:0.25, (c) 1:0.5, (d) 1:1 and (e) 1:2.

From the FTIR, XRD, TGA, DSC results, it is found that zinc oxide form complex with sodium chitosan phosphate without changing zinc oxide crystallinity. All the complexes with various mole ratios shows the similar results, thus, the amount of zinc oxide do not influence on the complexes structure. The complex between PCTS and ZnO possibly forms by electron donating from amino groups, hydroxyl groups and phosphate groups to hydroxyl species on the surface of ZnO. In general, zinc oxide can not be dissolved in water. The complexation forms only at the surface of ZnO, thus, the crystallinity of zinc oxide does not be interfered. Therefore, the possible structure of sodium chitosan phosphate/zinc oxide complexes can be predicted as shown in Figure 4.5. Several researches had been studied the crystallinity of polymer after metal complexation [32-34]. It was found that metal oxide which dissolved in water formed the complex with polymer and changed the crystallinity of polymers.

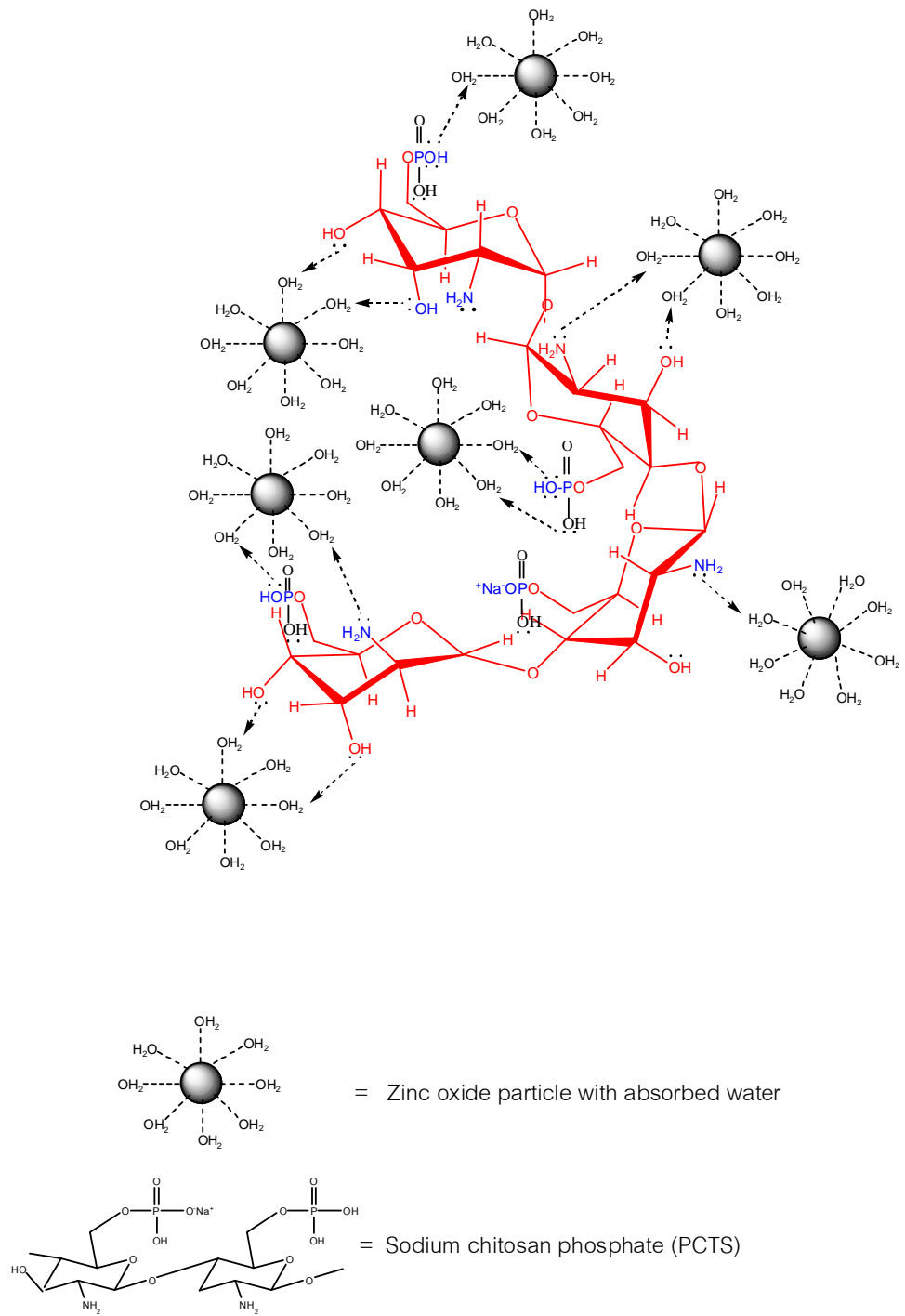


Figure 4.5 Possible structures of sodium chitosan phosphate/zinc oxide complexes at 1:0.25, 1:0.5, 1:1 and 1:2 equivalent moles.

4.3 Setting time of PCTS/ZnO complexes

The setting time of sodium chitosan phosphate/zinc oxide complexes with various mole ratios was approximately 2 hours as shown in Figure 4.6. This result indicates that the setting time of the complexes is independent on mole equivalent of zinc oxide. Rate of complex formation should be the main factor to control setting time. In order to eliminate other factors on setting time, there is no adding the additional agents in this research. On the other hand, three main ingredients which influence to the setting time of commercial periodontal dressing are organic carboxylic acid, metal oxide and polymeric resins having carboxylic groups. The setting time of some commercial periodontal dressings was about 3-5 minutes due to the addition of accelerator such as zinc acetate and ethyl alcohol [2]. Furthermore, a viscosity regulated agent e.g. brominol (brominated olive oil) and body forming agent e.g. ethyl alcohol are filled into some commercial available periodontal dressings (Coe-pak[®]) [2].

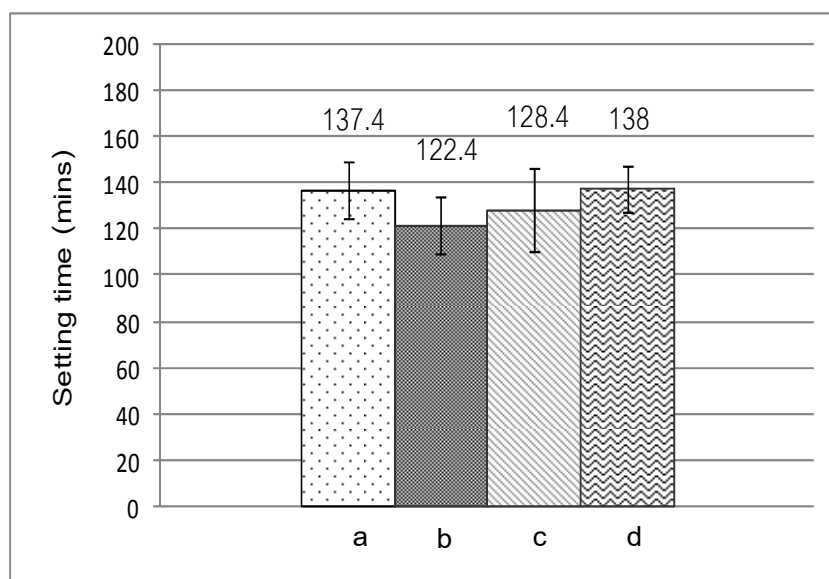


Figure 4.6 Setting time of sodium chitosan phosphate/zinc oxide complexes at mole ratios of chitosan to zinc oxide of (a) 1:0.25, (b) 1:0.5, (c) 1:1 and (d) 1:2, error bar represents n= 5.

4.4 Surface morphology

Figure 4.7 shows the dispersion of zinc oxide of the complexes. It was found that zinc oxide dispersed homogeneously throughout the polymeric matrices. However, when the mole of zinc oxide are less than that of polymer, thus, zinc oxide can embed into the polymer matrix and only small amount was bloomed on the surface. The higher amount of zinc oxide covering the surface of polymeric matrices was observed when increasing the mole ratios of zinc oxide to 1:1 or 1:2 equivalent mole. The disintegration of zinc oxide over the complex surface is found to influence to cytocompatibility that will be mentioned later.

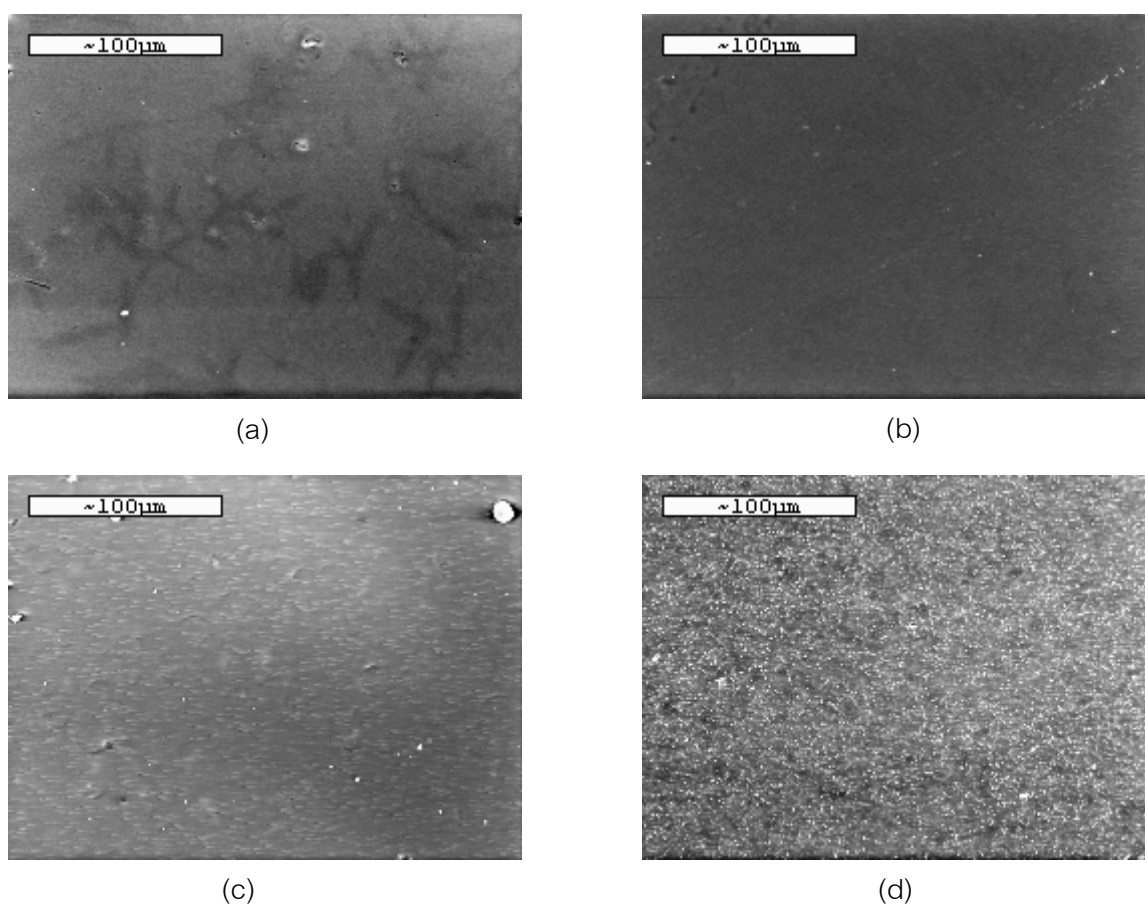


Figure 4.7 SEM images in mapping mode observing ZnO dispersion on the surface of the complexes at different ratios of PCTS/ZnO of (a) 1:0.25 (b) 1:0.5 (c) 1:1 (d) 1:2.

4.5 Hardness of PCTS/ZnO complexes

Table 4.3 shows the hardness of the complexes between sodium chitosan phosphate and zinc oxide at 1:0.25, 1:0.5, 1:1 and 1:2 equivalent moles. Hardness value increases when the content of zinc oxide increases, whereas material would be brittle when increasing zinc oxide. The hardness value is affected from the density of zinc oxide per surface area. The higher equivalent mole of zinc oxide gives rise to higher density of zinc oxide per surface area. As seen in Figure 4.7d, a large amount of zinc oxide covering complex surface leads to higher hardness value.

Table 4.3 Hardness value of PCTS/ZnO complexes at different PCTS/ZnO mole ratios

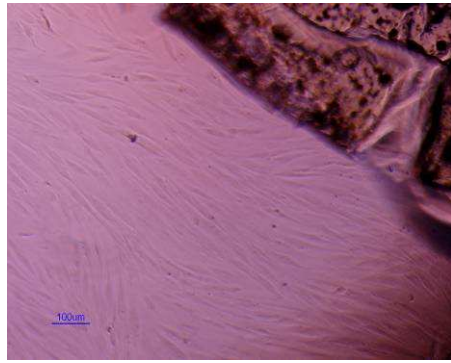
SD represents n=10

PCTS/ZnO complexes	Vicker hardness (HV)
1:0.25	1.18 ± 0.14
1:0.5	2.00 ± 0.45
1:1	2.75 ± 0.69
1:2	9.88 ± 1.18

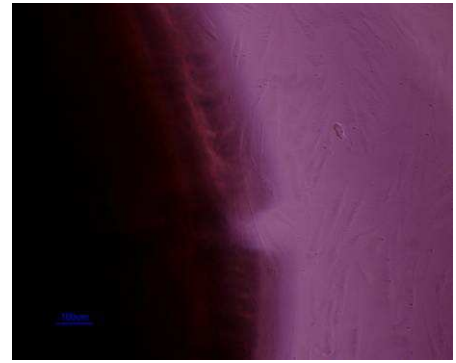
4.6 Cytocompatibility of PCTS/ZnO complexes

4.6.1 Direct contact test

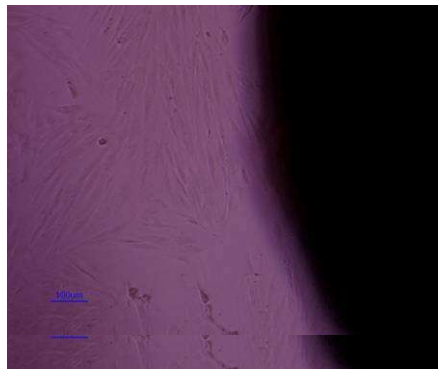
From Figure 4.8 the cytocompatibility of sodium chitosan phosphate/zinc oxide complexes at the various mole ratios were evaluated by directly contact on the monolayer of human gingival fibroblast (HGF) cell culture using sodium chitosan phosphate as control. Commercial periodontal dressing, Coe-pak[®], and rosin which is polymer having carboxylic groups mainly used as one component in Coe-pak[®] were also comparatively evaluated. Some cells death was observed at 24 hours for the complexes between sodium chitosan phosphate and zinc oxide at 1:1, 1:2 equivalent moles, rosin and Coe-pak[®], where cells death was not observed in sodium chitosan phosphate (control) and its complexes at sodium chitosan phosphate to zinc oxide of 1:0.25 and 1:0.5 equivalent moles. After 48 and 72 hours, the more cells death was observed in rosin, Coe-pak[®] and the complexes with mole ratios of 1:1 and 1:2 that cannot be observed for sodium chitosan phosphate (control) and its complexes at sodium chitosan phosphate to zinc oxide of 1:0.25 and 1:0.5. It should be noted from this result that sodium chitosan phosphate has the same phosphate groups as cell membrane of human gingival fibroblast, and, thus, exhibits cell biocompatibility. Therefore, sodium chitosan phosphate can be considered as good polymeric candidate for biocompatible periodontal dressing component. Furthermore, the complexes between sodium chitosan phosphate and zinc oxide at 1:0.25 and 1:0.5 do not show adverse effect on cell proliferation. Whereas, the complexes between sodium chitosan phosphate and zinc oxide at 1:1 and 1:2 show adverse effect, owing to high density of ZnO particles covering throughout the surface. Zinc oxide was found to be cytotoxic (data not shown, see in the appendices). Rosin and Coe-pak[®] could be reacted with the cell membrane of human gingival fibroblast due to carboxyl group, and aromatic rings of abietic acid [4].



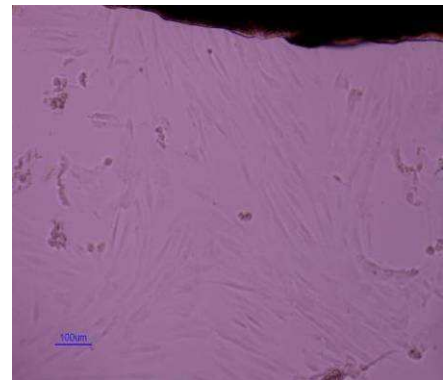
PCTS: ZnO, 1:0.25



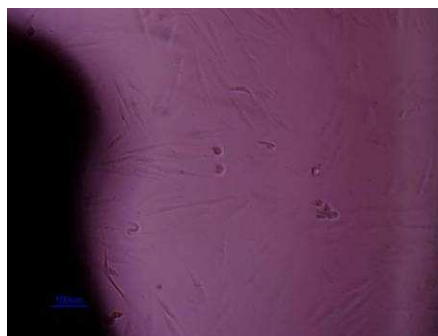
PCTS: ZnO, 1:0.5



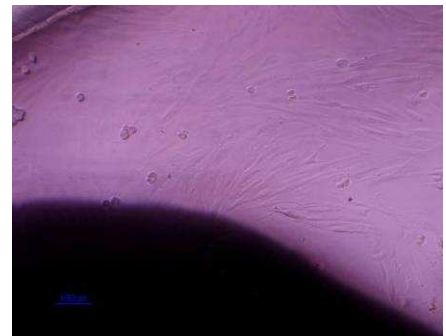
PCTS: ZnO, 1:1



PCTS: ZnO, 1:2



Rosin

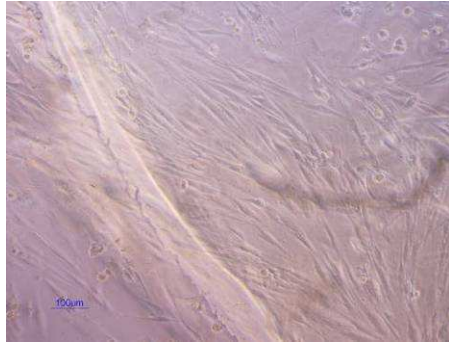


Coe-pak[®]

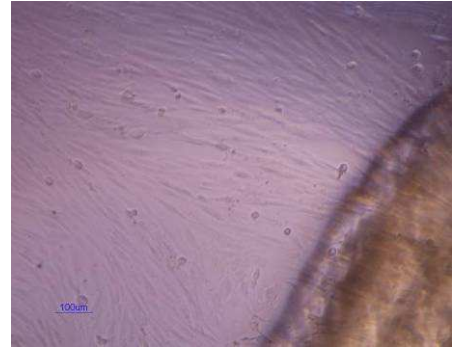


Sodium chitosan phosphate

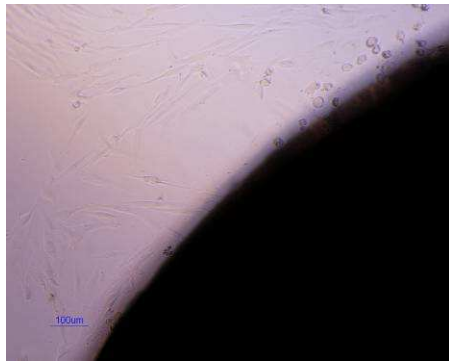
Figure 4.8 Direct contact test of materials placing on monolayer cell culture at 0 hr.



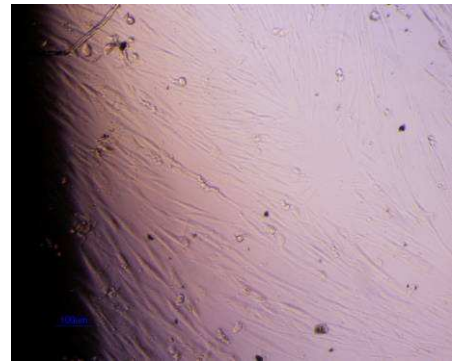
PCTS: ZnO, 1:0.25



PCTS: ZnO, 1:0.5



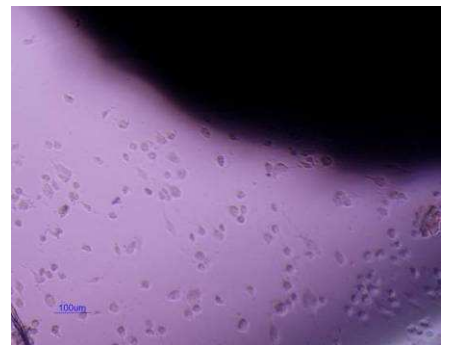
PCTS: ZnO, 1:1



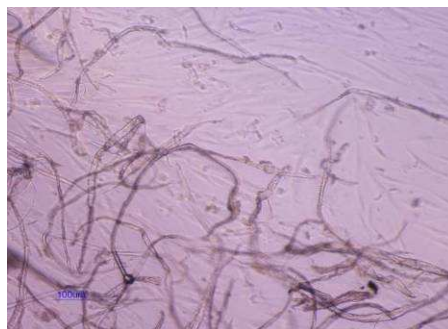
PCTS: ZnO, 1:2



Rosin

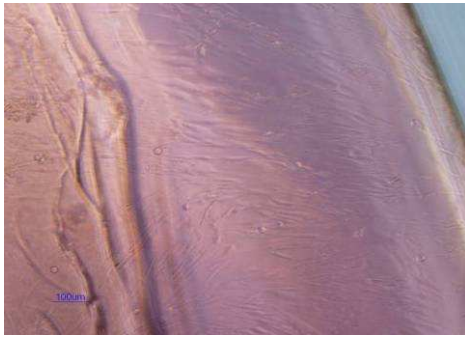


Coe-pak®

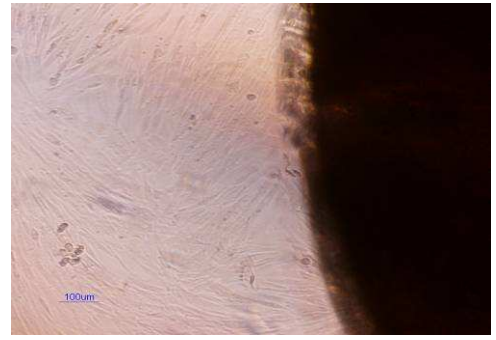


Sodium chitosan phosphate

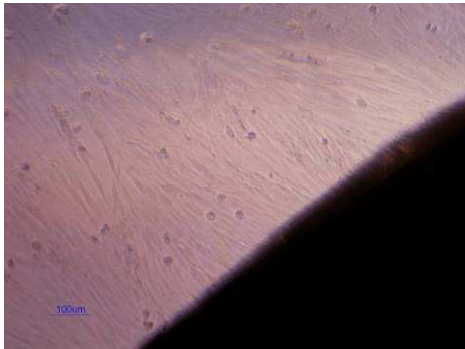
Figure 4.8 (conti.) Direct contact test of materials placing on monolayer cell culture after 24 hrs.



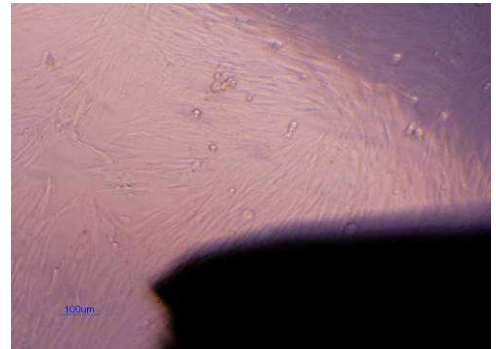
PCTS: ZnO, 1:0.25



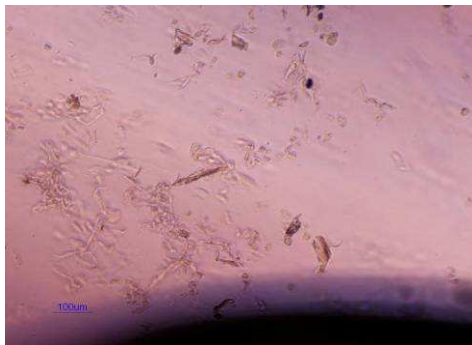
PCTS: ZnO, 1:0.5



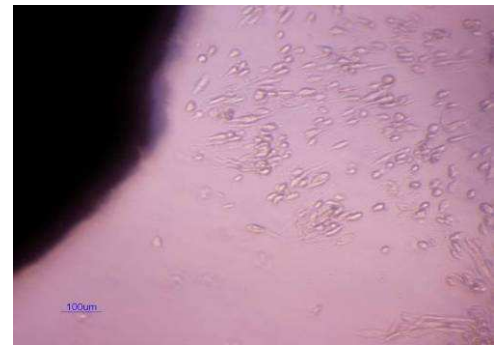
PCTS: ZnO, 1:1



PCTS: ZnO, 1:2



Rosin

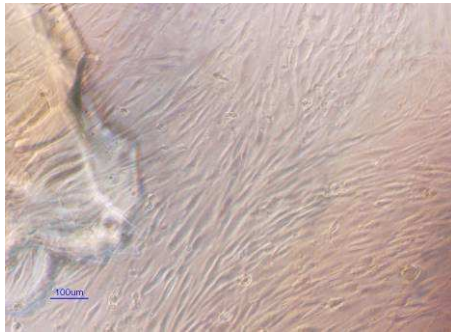


Coe-pak®

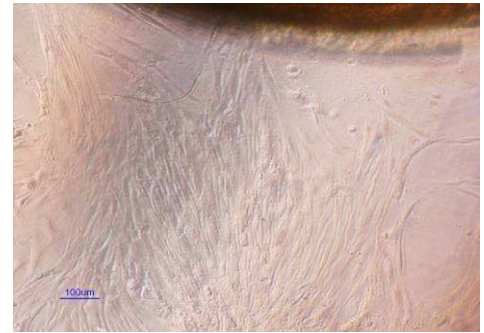


Sodium chitosan phosphate

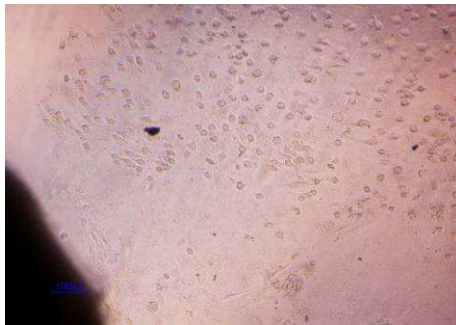
Figure 4.8 (conti.) Direct contact test of materials placing on monolayer cell culture after 48 hrs.



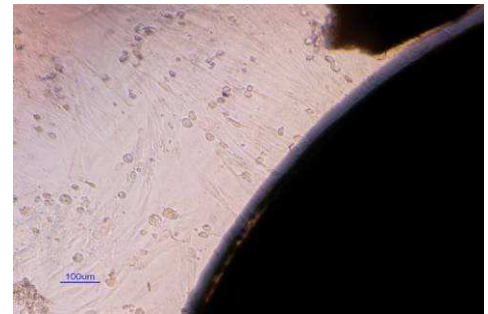
PCTS: ZnO, 1:0.25



PCTS: ZnO, 1:0.5



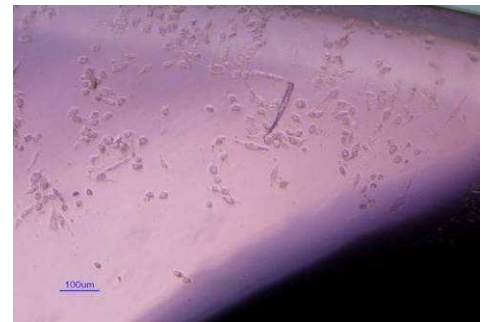
PCTS: ZnO, 1:1



PCTS: ZnO, 1:2



Rosin



Coe-pak®



Sodium chitosan phosphate

Figure 4.8 (conti.) Direct contact test of materials placing on monolayer cell culture after 72 hrs.

4.6.2 Indirect contact test

For indirect contact test, human gingival fibroblast was cultured with the extract solution. The extract solution was the fibroblast culture medium after samples immersion for 2 weeks and samples remove. Human gingival fibroblast was monolayer cultured for 24 and 48 hrs. The number of viable cell was determined using MTT assay. Vybrant[®] MTT Cell Proliferation Assay Kit provided a simple method for determination of cell number using standard microplate absorbance readers. The MTT assay involved the conversion of the water soluble MTT to an insoluble formazan. The concentration of formazan was measured as optical density (OD) at 570 nm as shown in Table 4.4.

Table 4.4 Optical density (OD) of PCTS, PCTS/ZnO complexes, rosin and Coe-pak[®] by MTT assay

Extract solutions from the specimens	Average optical density (OD _n) at 570 nm		
	Incubated after 24 hrs (OD ₂₄)	Incubated after 48 hrs (OD ₄₈)	OD ₄₈ / OD ₂₄
Positive control	0.46 ± 0.05	0.87 ± 0.09	1.89
PCTS	0.11 ± 0.02	0.14 ± 0.02	1.27
PCTS/ZnO, 1:0.25	0.22 ± 0.11	0.22 ± 0.07	1.00
PCTS/ZnO, 1:0.5	0.11 ± 0.06	0.18 ± 0.07	1.64
PCTS/ZnO, 1:1	0.12 ± 0.02	0.17 ± 0.07	1.42
PCTS/ZnO, 1:2	0.14 ± 0.05	0.22 ± 0.07	1.57
Rosin	0.08 ± 0.02	0.13 ± 0.07	1.63
Coe-pak [®]	0.10 ± 0.02	0.09 ± 0.01	0.90

The optical density is related to number of viable cells. A OD_{48}/OD_{24} value represent proliferation rate of HGF cells. From Table 4.4, cells culturing with each samples' extract solutions represent OD_{48}/OD_{24} value in the range of 0.90-1.64 which is closely to control with OD_{48}/OD_{24} value of 1.89. Cells in control groups proliferate in proper condition *in vitro*. Thus, cells culturing with each samples' extract solutions representing OD_{48}/OD_{24} value close to control, indicating normal cell growth. Therefore, extract solution of all complexes, rosin and Coe-pak[®] were not found to toxic with HGF cells culture. This can be implied that there are no toxic substances releasing from those samples.

CHAPTER V

CONCLUSIONS AND SUGGESTIONS

5.1 Conclusions

In this research, the complexes between sodium chitosan phosphate and zinc oxide at mole ratios of 1:0.25, 1:0.5, 1:1 and 1:2 equivalent moles were prepared for periodontal dressing application.

The possible structure of complexes between sodium chitosan phosphate/zinc oxide were confirmed by FTIR, XRD, TGA and DSC. The complexation between sodium chitosan phosphate and zinc oxide was successfully formed through transferring lone pair electron of amine groups, phosphate groups and hydroxyl groups of sodium chitosan phosphate to water molecules surrounding on zinc oxide surface. Owing to complex formation occurs at the surface of zinc oxide particle. Therefore, complexation does not change the structure of crystalline of zinc oxide.

The setting time of sodium chitosan phosphate/zinc oxide complexes was approximately 2 hours. Rate of complex formation should be the main factor to control setting time.

Zinc oxide was observed homogeneously throughout the complexes. The higher the amount of zinc oxide revealed the more zinc oxide covering the complexes surface.

From direct contact test to human gingival fibroblast, the complexes with mole ratios of 1:1 and 1:2 showed cytotoxicity to human gingival fibroblast due to a large amount of zinc oxide deposited on the surface of complexes, whereas the complexes with mole ratios of 1:0.25 and 1:0.5 were biocompatible as well as sodium chitosan phosphate. Moreover, indirect contact test, extract solutions of all complexes, rosin and Coe-pak[®] were not found to toxic with HGF cells culture. This can be implied that there are no toxic substances releasing from the specimens. Then, sodium chitosan phosphate was proved to be biocompatible polymer. Consequence, it can be consider as novel biocompatible polymer suitable for biomedical applications. In this research,

sodium chitosan phosphate was proved to be safe to replace some toxic component, e.g. polymeric resins having carboxyl groups, of periodontal dressing.

5.2 Suggestions

5.2.1 X-Ray Photoelectron Spectrometer (XPS) shall be measured for additional supporting data for prediction of the possible structure of the complexes by determining the bond energy of the coordinating bond.

5.2.2 The setting time of the complexes should be improved by adding accelerating agent. The setting time of some commercial periodontal dressings was about 3-5 minutes due to the addition of accelerator such as zinc acetate and ethyl alcohol. Furthermore, a viscosity regulated agent e.g. brominol (brominated olive oil) and body forming agent e.g. ethyl alcohol are filled into some commercial available periodontal dressings (Coe-pak[®]).

5.2.3 The elasticity properties of the complexes should be improved by adding some biocompatible body forming polymer such as poly(vinyl alcohol).

References

- [1] Newman, M. G., Takei, H. H., and Fermin, A. **Carranza's clinical periodontology**. 9th ed. Elsevier Health Sciences: W.B. Saunders, 2002.
- [2] Molnar, E. J. United states patent office. **Dental composition and process of making same**. US 3,028,247.
- [3] Alpar, B., Günay, H., Geurtsen, W. and Leyhausen G. Cytocompatibility of periodontal dressing materials in fibroblast and primary human osteoblast-like cultures. **Clin. Oral. Investi.** 3 (1999): 41–48.
- [4] Aranda, F. J. and Villalain, J. The interaction of abiestic acid with phospholipid membranes. **Biochimi. Et. Biophys. Acta.** 1327 (1997): 171-180.
- [5] Soderberg, T. A., Johansson, A. and Gref, R. Toxic effects of some conifer resin acids and tea tree oil on human epithelial and fibroblast cells. **Toxicol.** 107 (1996): 99-109.
- [6] Eugler, W.O., Ramfjord, S.P., and Hiniker, J.J. Healing following simple gingivectomy. A tritiated thymidine radioautographic study. I. Epithelialization. **J. Perio.** 37 (1966): 298-308.
- [7] Haugen, E. and Pettersen, A. H. In vitro Cytotoxicity of Periodontal Dressing. **J. Dent. Res.** 57 (1978): 495-499.
- [8] Sunzel, B., Soderberg, T.A., Johansson, A., Hallmans, G. and Gref, R. The protective effect of zinc on rosin and resin acid toxicity in human polymorphonuclear leukocytes and human gingival fibroblasts in vitro. **J. Biomed. Mater. Res.** 37 (1997): 20-28.
- [9] Hidebrand, C. N. and Derenzis, F.A. Effect of periodontal dressing on fibroblast in vitro. **J. Perio. Res.** 9 (1973): 114-120.
- [10] Koch, G., Magnusson, B., Nobreus, N., Nyquist G. and Soderholm, G. Contact allergy to medicaments and materials used in dentistry (IV). **Odont. Reby.** 24 (1973): 109-114.
- [11] Karlberg, A. T. and Magnusson, K. Rosin components identified in diapers. **Cont. Derm.** 34 (1996): 176-180.
- [12] Lysell, L. Contact allergy to rosin in a periodontal dressing A Case Report. **J. Oral.**

Med. 31 (1976): 24-25.

- [13] Tang E., Cheng G. and Ma X. Preparation of nano-ZnO/PMMA composite particles via grafting of the copolymer onto the surface of zinc oxide nanoparticles. **Pow. Tech.** 161 (2006) 209 – 214.
- [14] Varma, A. J., Deshpande, S. V. and Kennedy, J. F. Metal complexation by chitosan and its derivatives : a review. **Carbohydr. Polym.** 55 (2004): 77-93.
- [15] Sreenivasan, K. Thermal stability studies of some chitosan-metal ion complexes using differential scanning calorimetry. **Polym. Degrad. Stab.** 52 (1996): 85-77.
- [16] Peniche C. C., Jimenez, M. S., and Nunez, A. Characterization of silver-binding chitosan by thermal analysis and electron impact mass spectrometry. **Carbohydr. Polym.** 9 (1988): 249-256.
- [17] Wang, A., Zhou, J., and Yu, X. **Gaofenzi Xuebao.** 6 (2000): CA 133:231961.
- [18] Hall, L. D., and Kim, T. K. Studies of metal-sugar complexes in the solid state by the ¹³C-n.m.r. c.p.-m.a.s. method. **Carbohydr. Res.** 148 (1986): 13-23.
- [19] Sano, H., Shibasaki, K. I., Matsukubo, T. and Takaesu, Y. Comparison of the activity of four chitosan derivatives in reducing initial adherence of oral bacteria onto tooth surfaces. **Bull. Tokyo. Dent. Coll.** 42 (2001): 243-249.
- [20] Nishi, N., Maekita, Y., Nishimura, S.I., Hasegawa, O. and Tokura, S. Highly phosphorylated derivatives of chitin, partially deacetylated chitin and chitosan as new functional polymers : metal binding property of the insolubilized materials. **Int. J. Biol. Macromol.** 9 (1987): 109-114.
- [21] Netswasdi, N. **Preparation of chitosan/chitosan phosphate polyion complexes.** Master's Thesis, Department of Materials Science, Faculty of Science, Chulalongkorn University. 2007.
- [22] International organization for standardization, **Dental zinc oxide/eugenol cements and zinc oxide non-eugenol cements.** ISO 3107 (1988).
- [23] Japanese standards, **Knoop hardness test—Test method.** JISZ2251: (1998)
- [24] Sattayapornpipat C. **Biocompatibility of Chitosan Membrane for Guided Tissue Regeneration: *In vitro* Studies.** Graduate's Thesis, Department of Conservative Dentistry, Faculty of Dentistry, Prince of Songkla University. 2006.

- [25] Wenguang L., Shujun S., Zhiqiang C., Xin Z., Kangde Y., William W. L. and Luk K.D.K. An investigation on the physicochemical properties of chitosan/DNA polyelectrolyte complexes. **Biomat.** 26 (2005): 2705–2711.
- [26] Hiroki, T., Kenya, M., Akio, T. and Makoto, I. Mechanism of Hydroxylation of metal oxide surfaces. **J. Collo. Int. Sci.** 243 (2001): 202-207.
- [27] Hiroki T., Akio T., Ken-ya Mi. and Ryusaburo F. Surface Hydroxyl Site Densities on Metal Oxides as a Measure for the Ion-Exchange Capacity. **J. Collo. Int. Sci.** 209 (1999): 225–231.
- [28] Athena W., Merrill D. H. and David M. G. Metal complexation of chitosan and its glutaraldehyde cross-linked derivative. **Carbohy. Res.** 342 (2007): 1189–1201.
- [29] Trimukhe, K.D. and A.J. Varma. Metal complexes of crosslinked chitosans : Correlations between metal ion complexation values and thermal properties. **Carbohydr. Polym.** 75 (2009): 63–70
- [30] Liufu S. C., Xiao H. N. and Li Y. P. Thermal analysis and degradation mechanism of polyacrylate/ZnO nanocomposites. **Polym. Degrad. Stab.** 87 (2005): 103-110.
- [31] Yang T. C. K., Lin S. S. Y. and Chuang T. H. Kinetic analysis of the thermal oxidation of metallocene cyclic olefin copolymer (mCOC)/TiO₂ composites by FTIR microscopy and thermogravimetry (TG). **Polym. Degrad. Stab.** 78 (2002): 525-532.
- [32] Tang, L. G., and Hon, D. N. S. Chelation of Chitosan Derivatives with zinc ions. II. Association Complexes of Zn²⁺ onto O,N-Carboxymethyl Chitosan. **J. Appl. Polym. Sci.** 79 (2001): 1476-1485.
- [33] Wang, X., Du, Y. and Liu, H. Preparation, characterization and antimicrobial activity of chitosan-Zn complex. **Carbohydr. Polym.** 56 (2004): 21-26.
- [34] Ding, P., Huang, K. L., Li, G. Y. and Zeng, W. W. Mechanism and kinetics of chelating reaction between novel chitosan derivatives and Zn(II). **J. Hazard. Mater.** 146 (2007): 58-64.

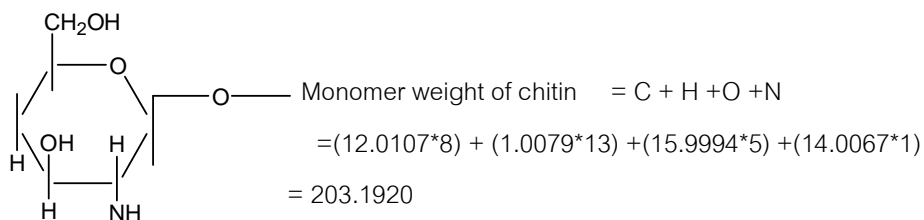
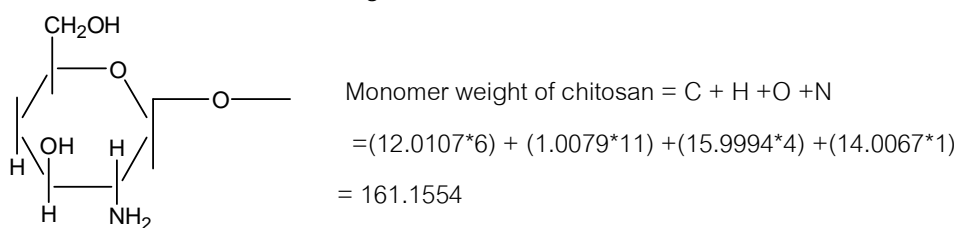
Appendices

Appendices I

A 1. The ratio of phosphorus pentoxide and chitosan

Mol ratios P ₂ O ₅ /unit of chitosan	Chitosan	P ₂ O ₅ (mol)	Degree of Substitution (DS)
2:1	0.024 mol	0.048	≅ 0.57*

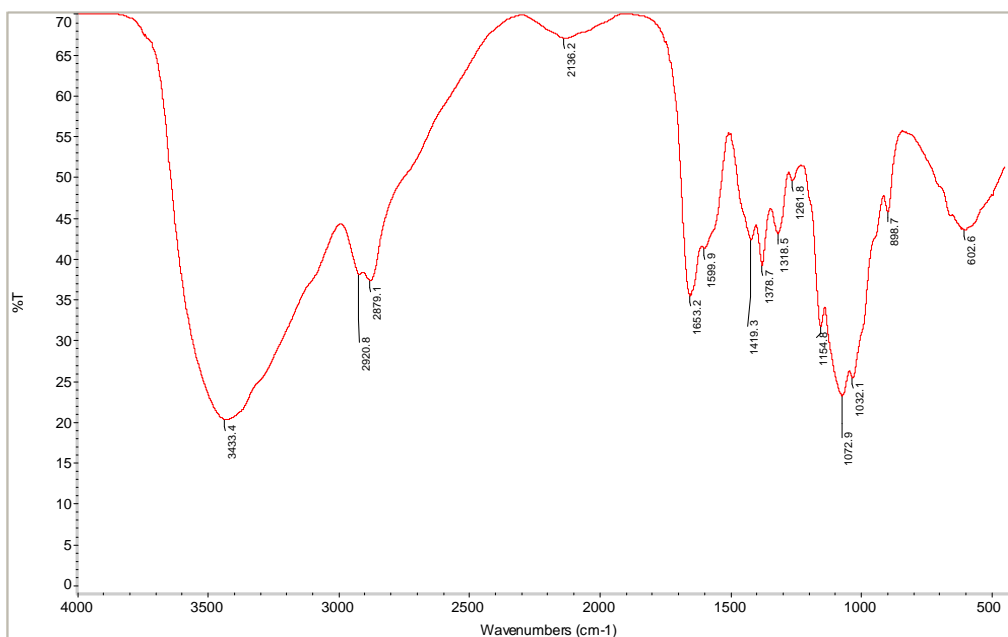
Calculation of molecular weight of chitosan



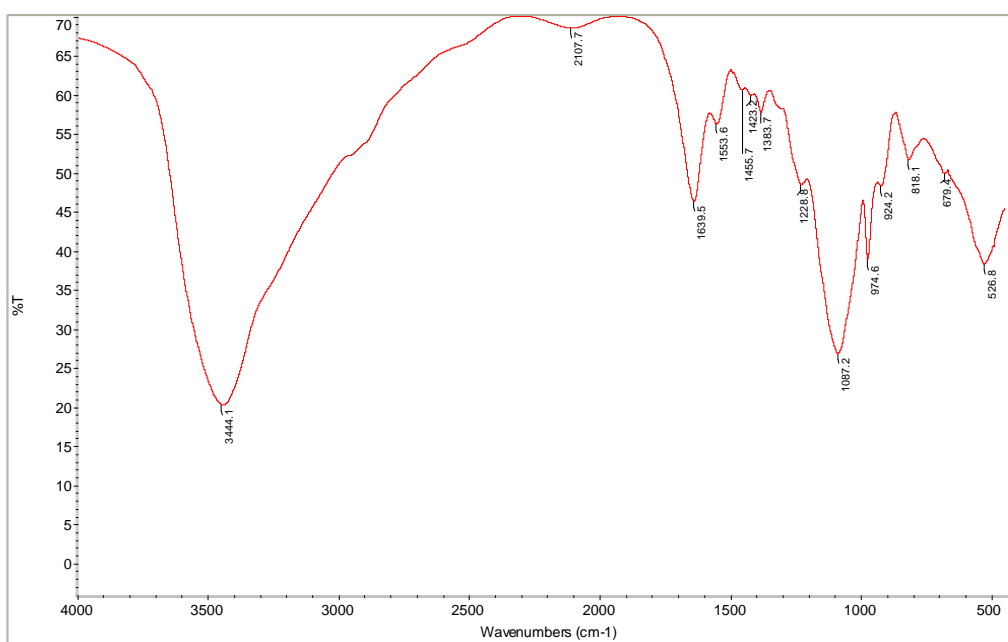
Molecular weight of chitosan (%DD = 85*) = $(0.85 \times 161.1554) + (0.15 \times 203.192)$
 $= 167.46$

Molecular weight of phosphorus pent oxide (P₂O₅) = $(31 \times 2) + (16 \times 5)$
 $= 142$

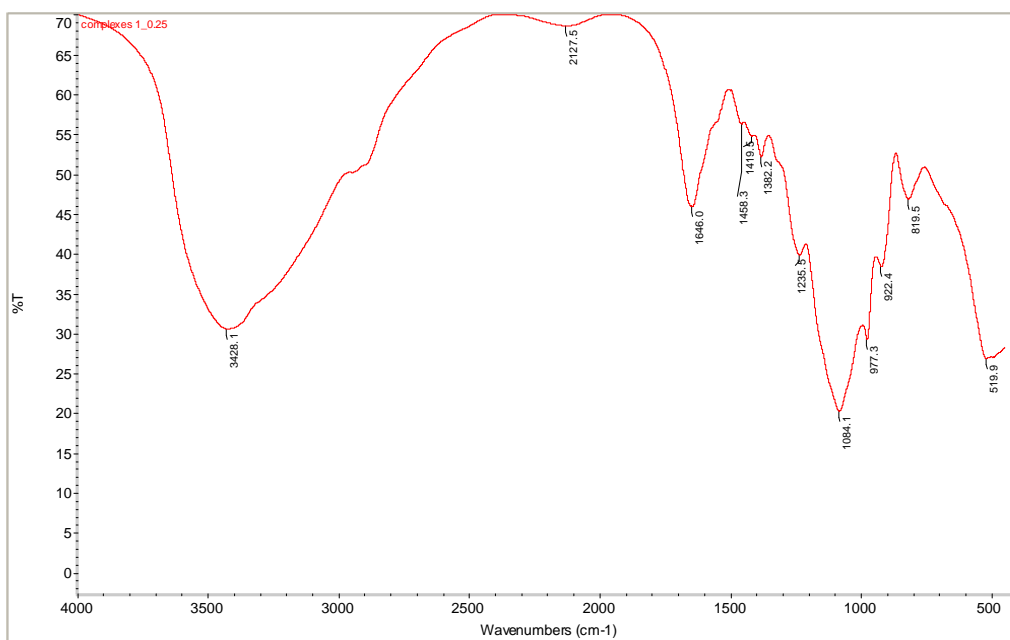
Appendix II



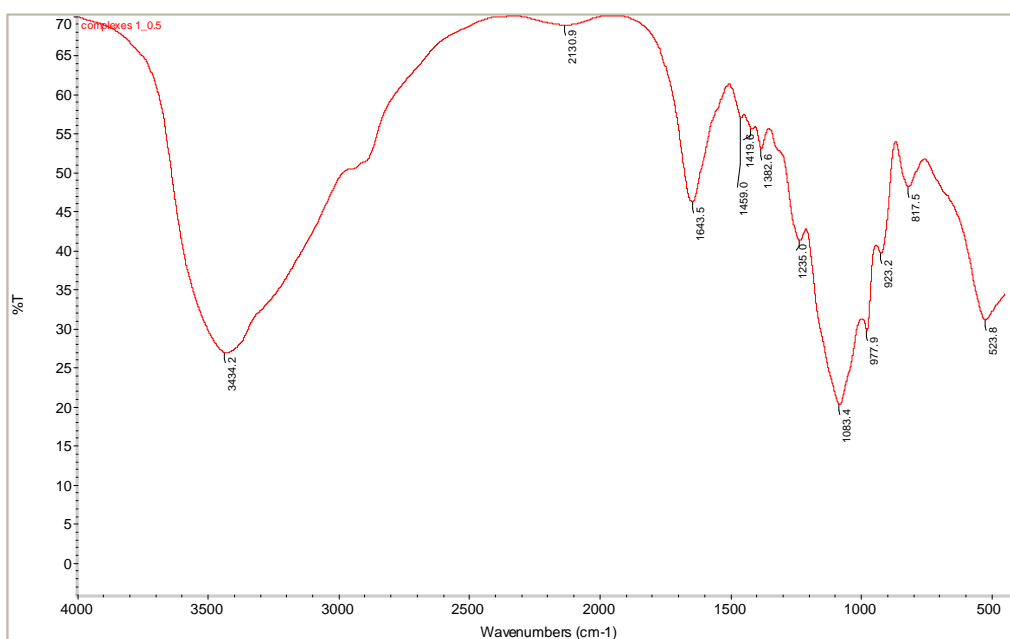
A 2. FTIR spectrum of chitosan.



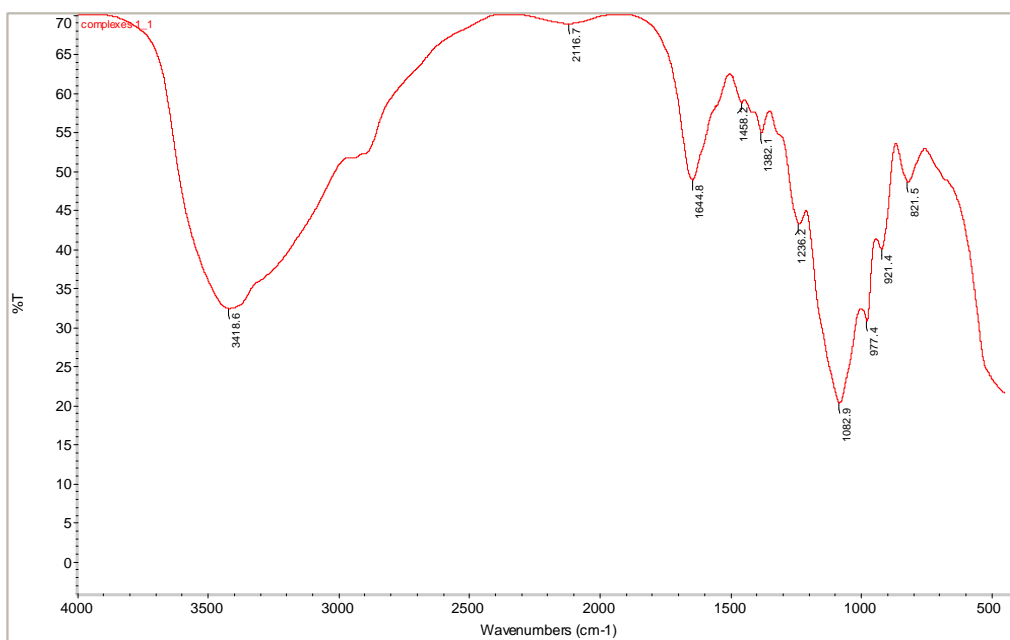
A 3. FTIR spectrum of sodium chitosan phosphate.



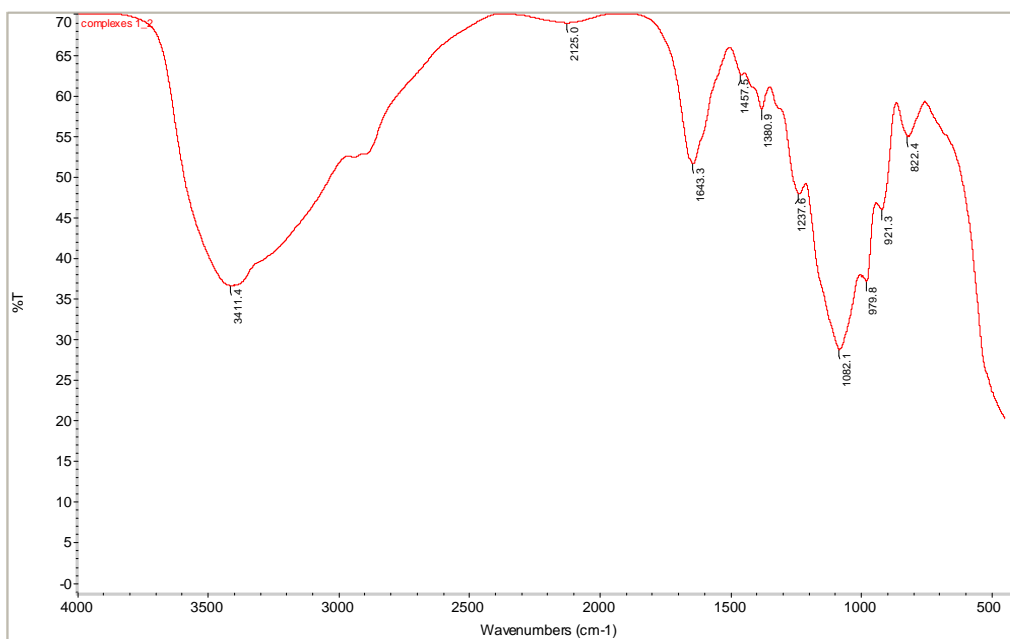
A 4. FTIR spectrum of the complexes at 1:0.25 equivalent moles.



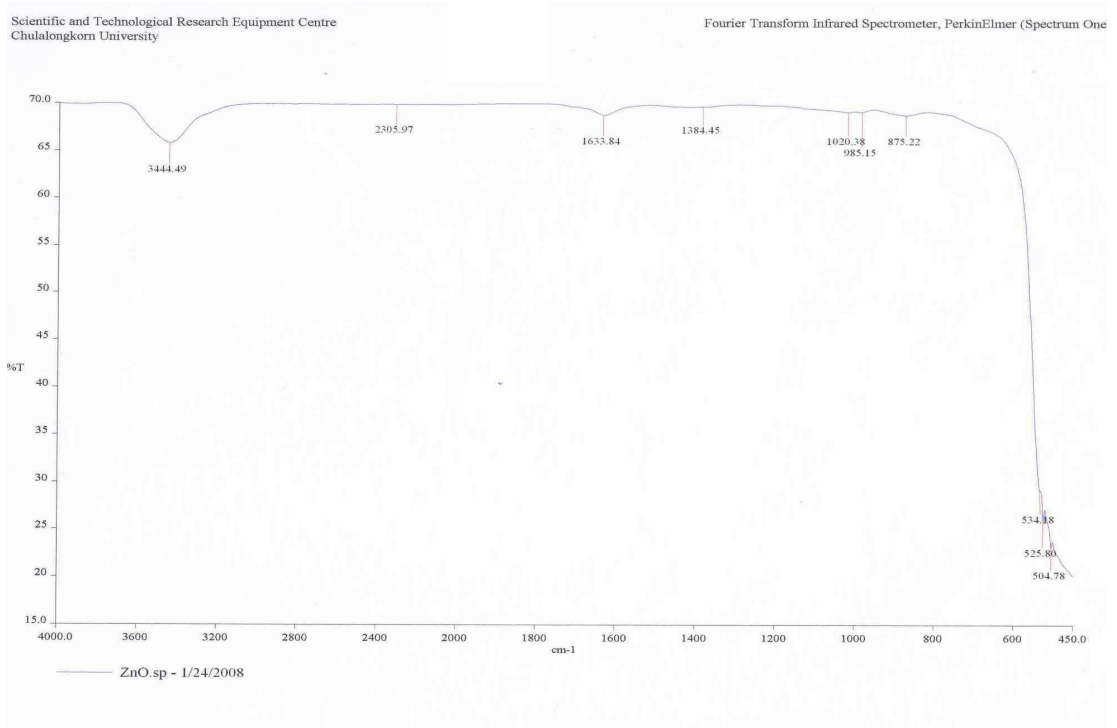
A 5. FTIR spectrum of the complexes at 1:0.5 equivalent moles.



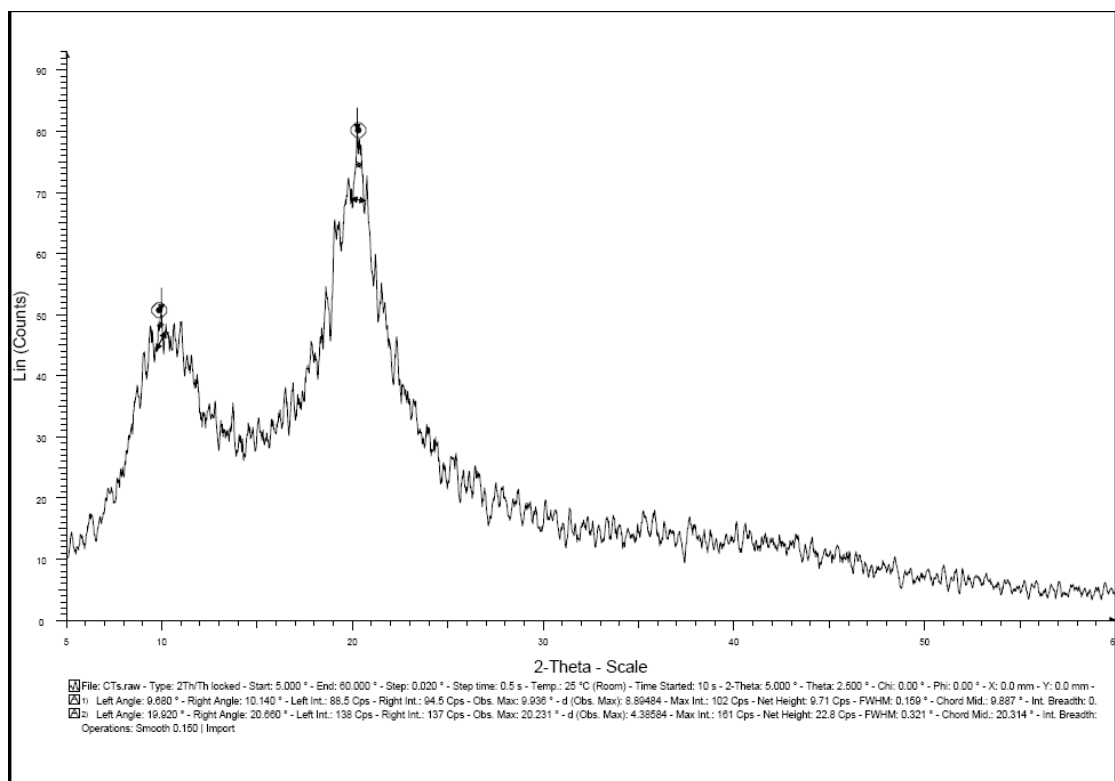
A 6. FTIR spectrum of the complexes at 1:1 equivalent moles.



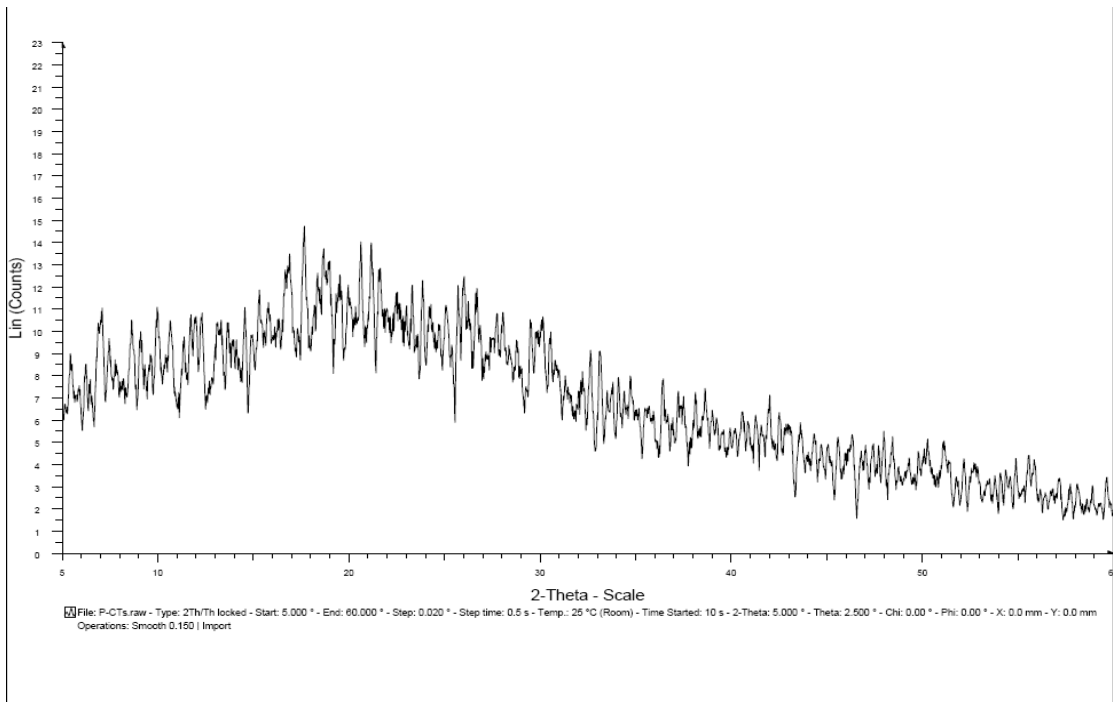
A 7. FTIR spectrum of the complexes at 1:2 equivalent moles.



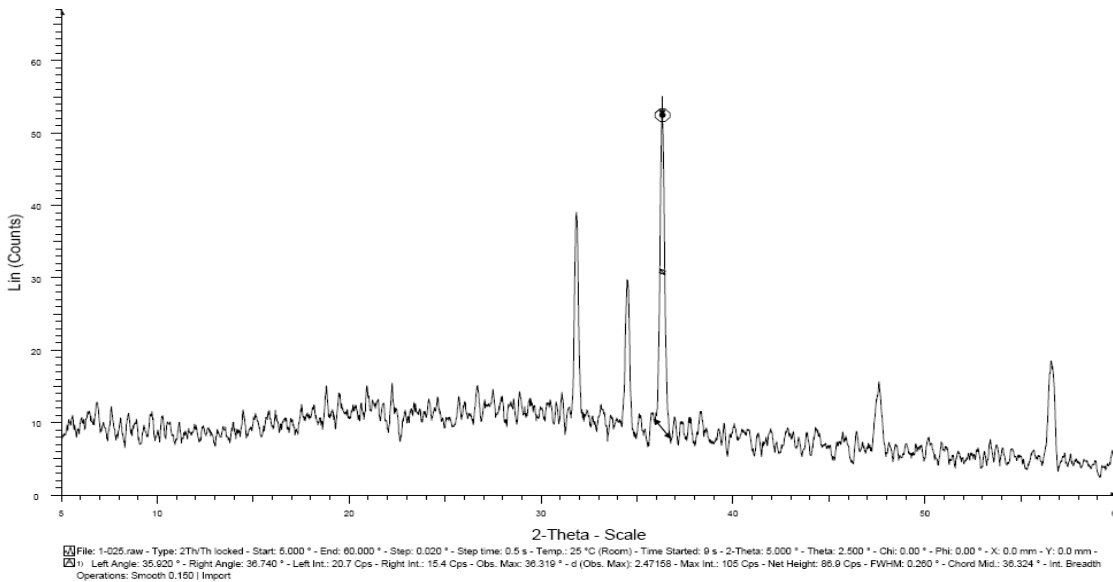
A 8. FTIR spectrum of ZnO.



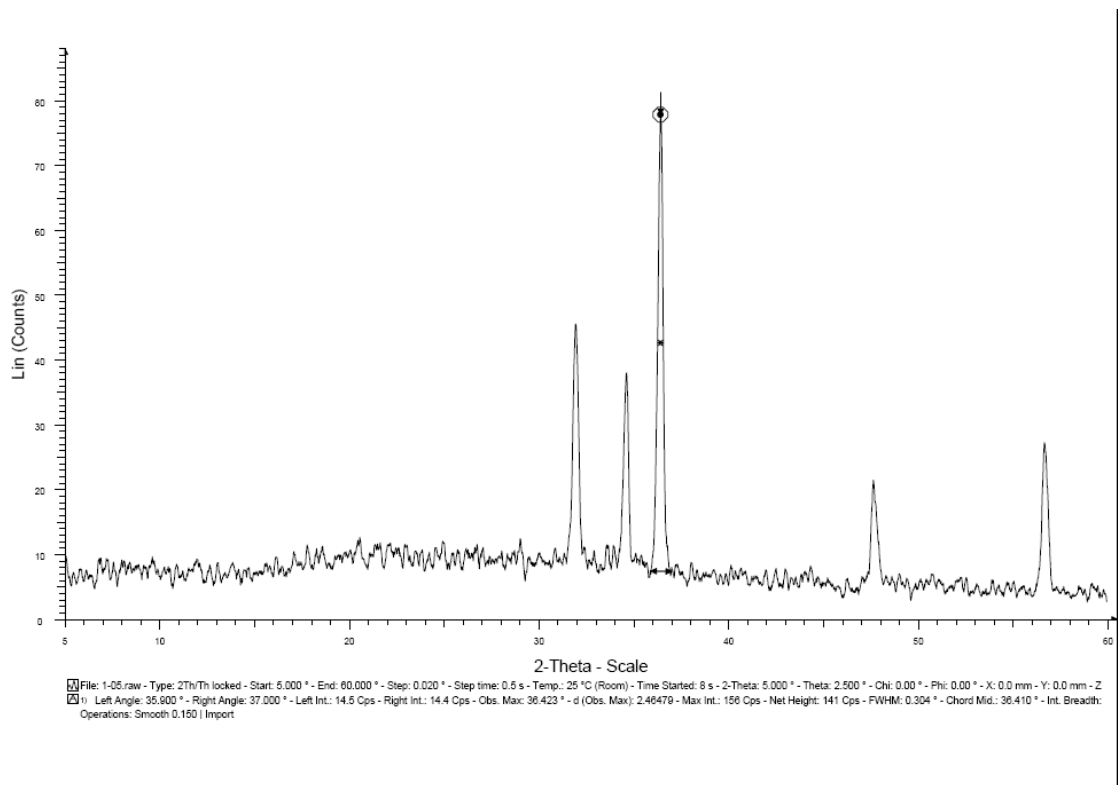
A 9. XRD pattern of chitosan.



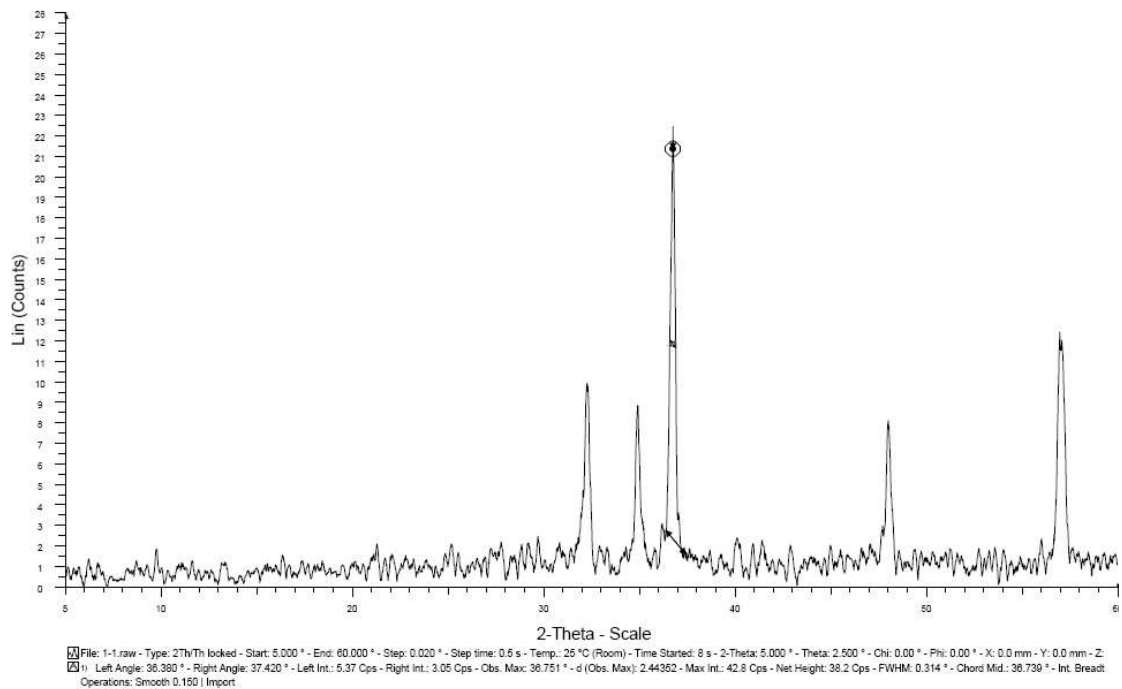
A 10. XRD pattern of sodium chitosan ρ



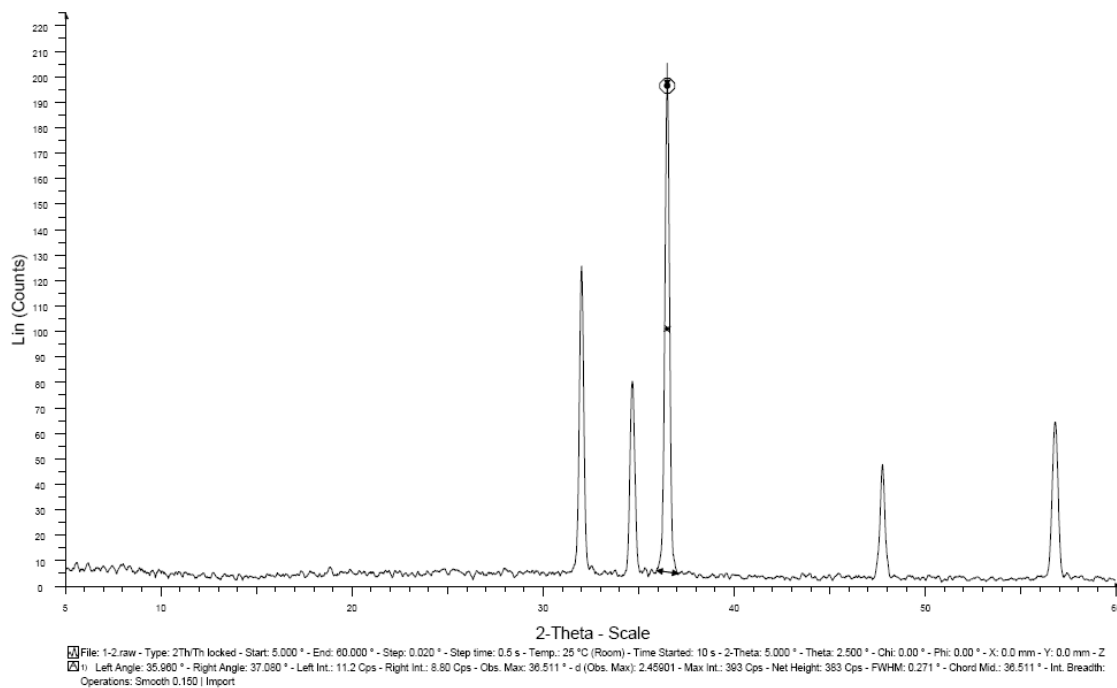
A 11. XRD pattern of PCTS/ZnO (1:0.25).



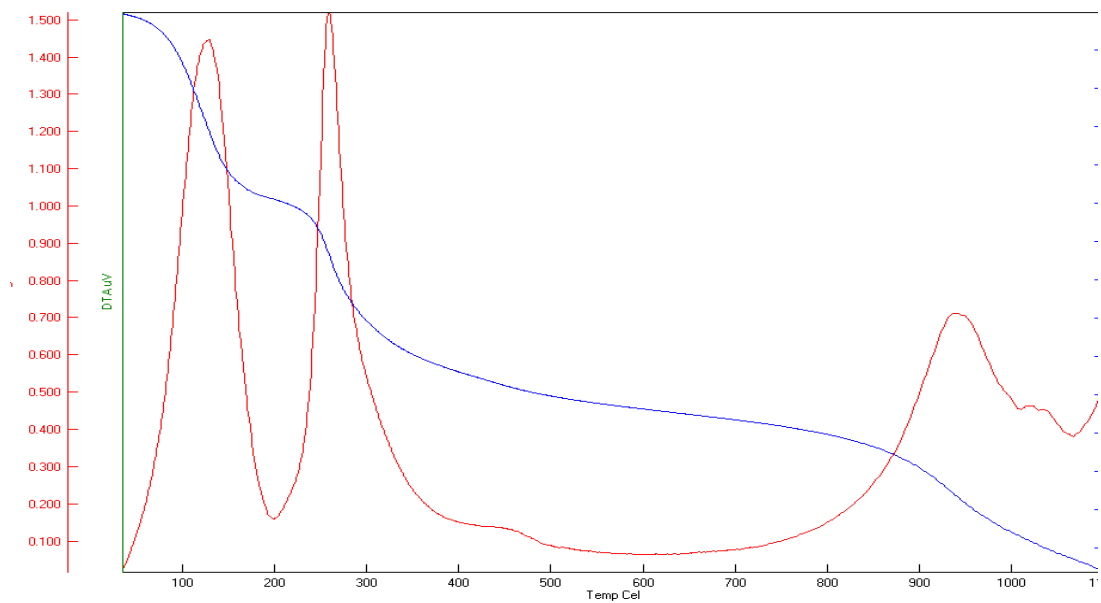
A 12. XRD pattern of PCTS/ZnO (1:0.5).



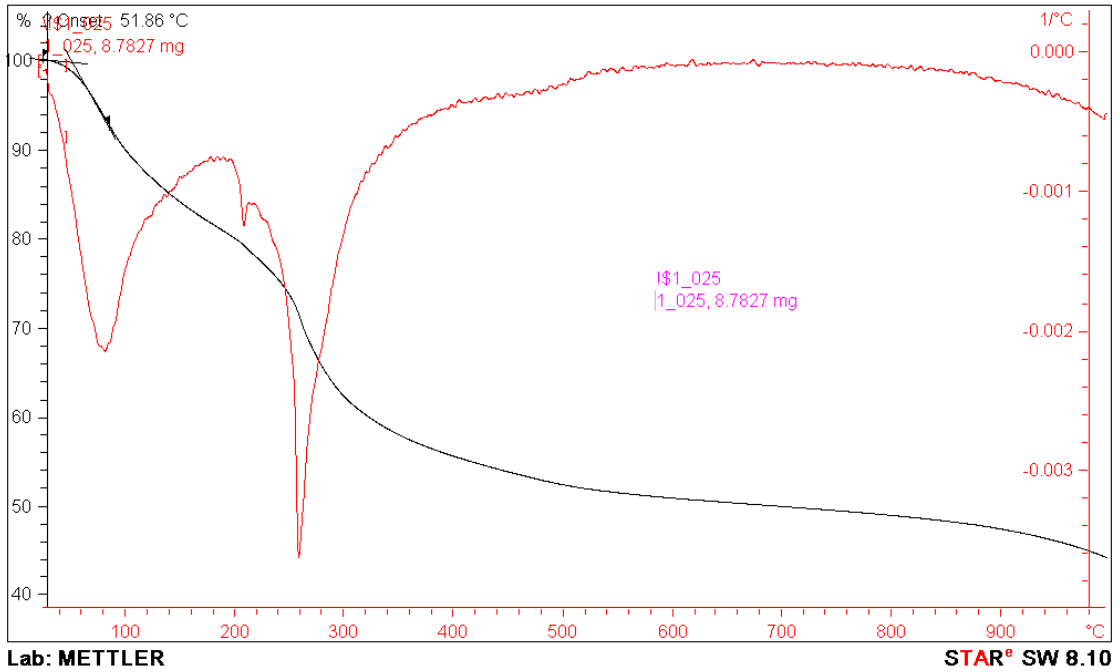
A 13. XRD pattern of PCTS/ZnO (1:1).



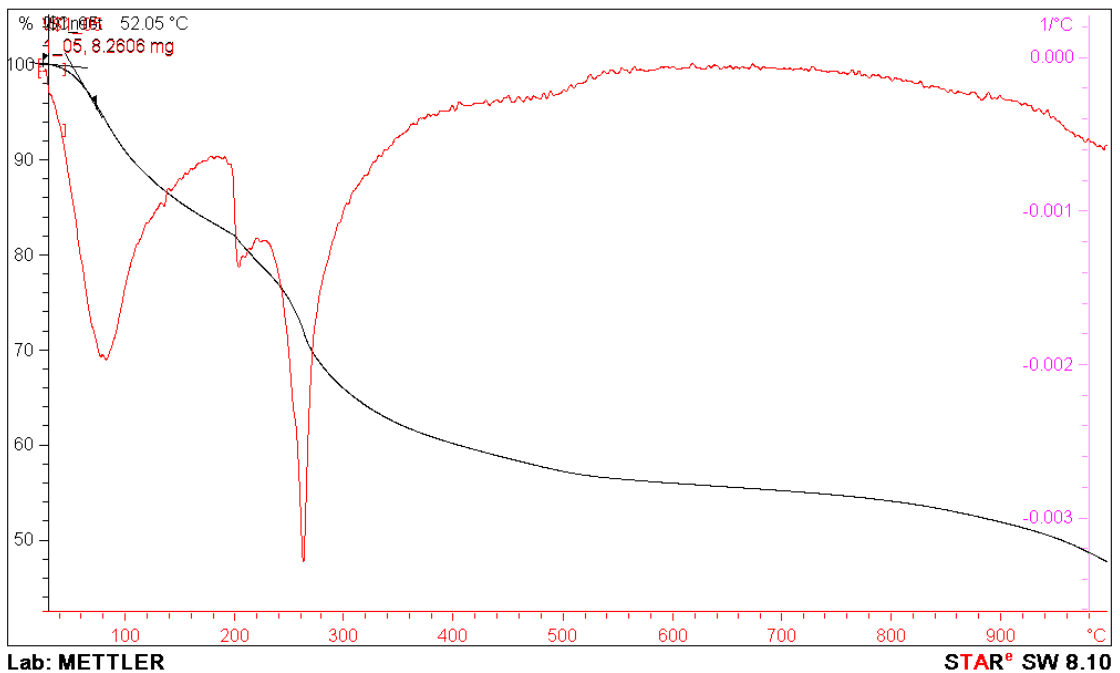
A 14. XRD pattern of PCTS/ZnO (1:2).



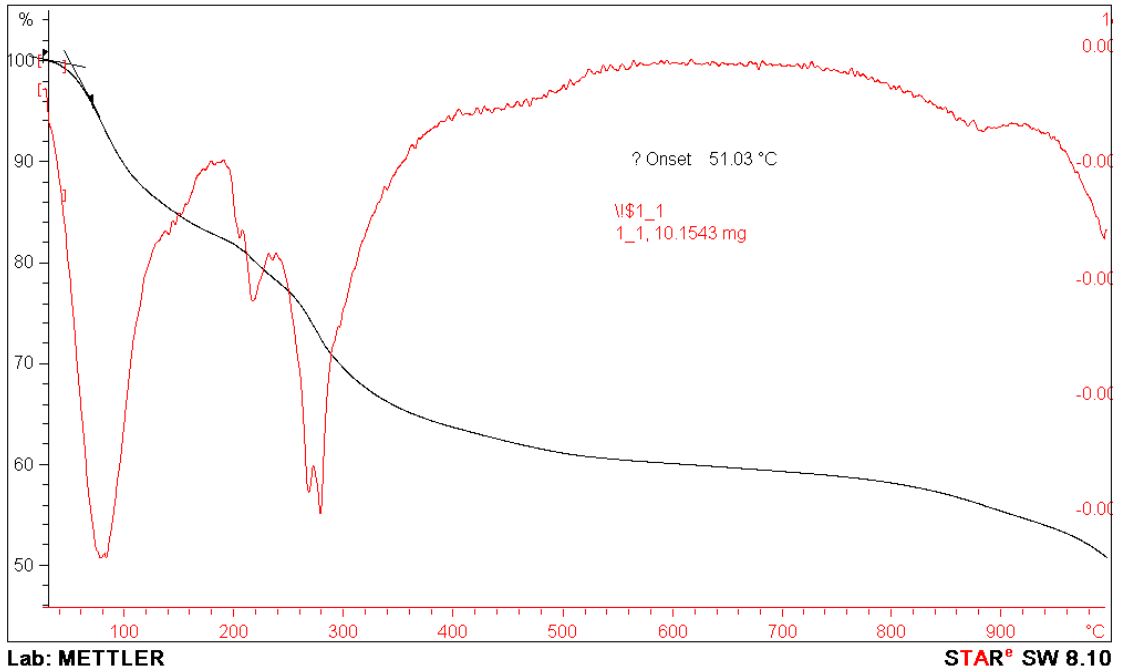
A 15. TGA diagram and Derivative thermal gravimetric (DTG) of sodium chitosan phosphate.



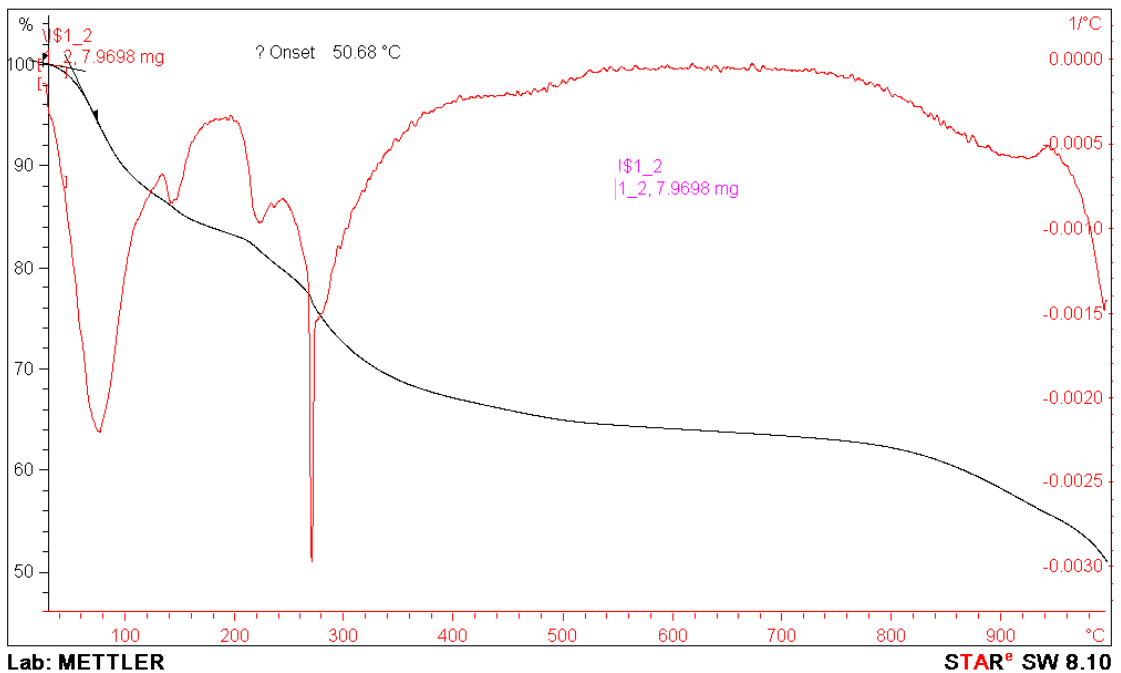
A 16. TGA diagram and Derivative thermal gravimetric (DTG) of sodium chitosan phosphate/zinc oxide complexes at 1:0.25 equivalent mole.



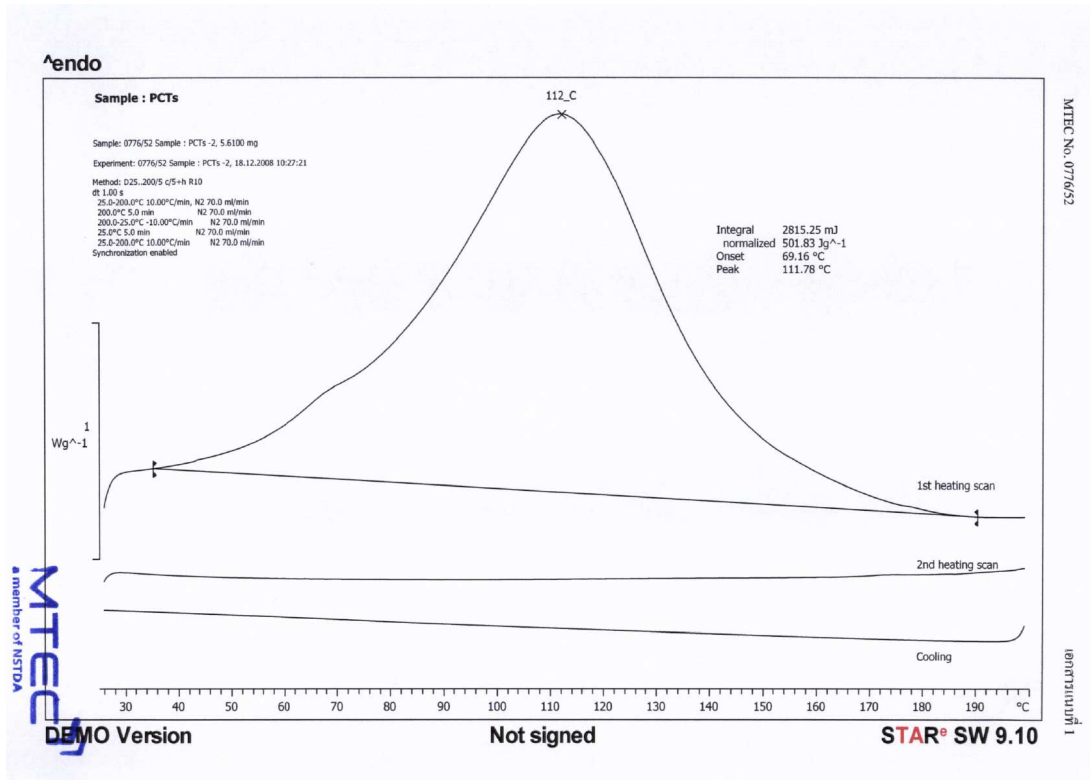
A 17. TGA diagram and Derivative thermal gravimetric (DTG) of sodium chitosan phosphate/zinc oxide complexes at 1:0.5 equivalent mole.



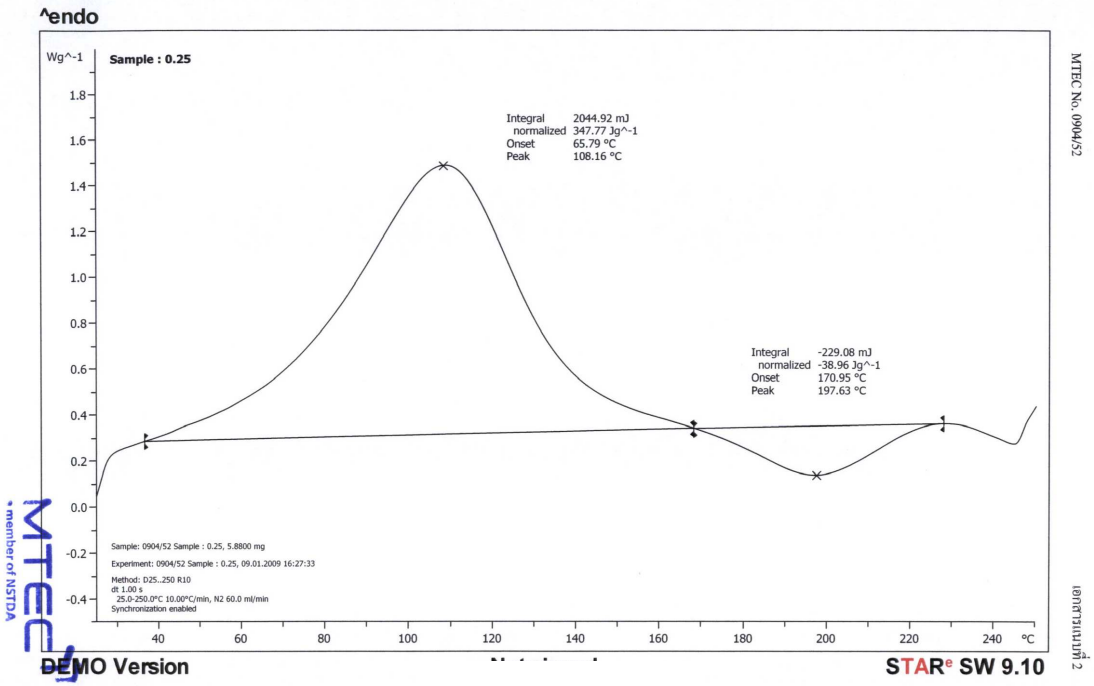
A 18. TGA diagram and Derivative thermal gravimetric (DTG) of sodium chitosan phosphate/zinc oxide complexes at 1:1 equivalent mole.



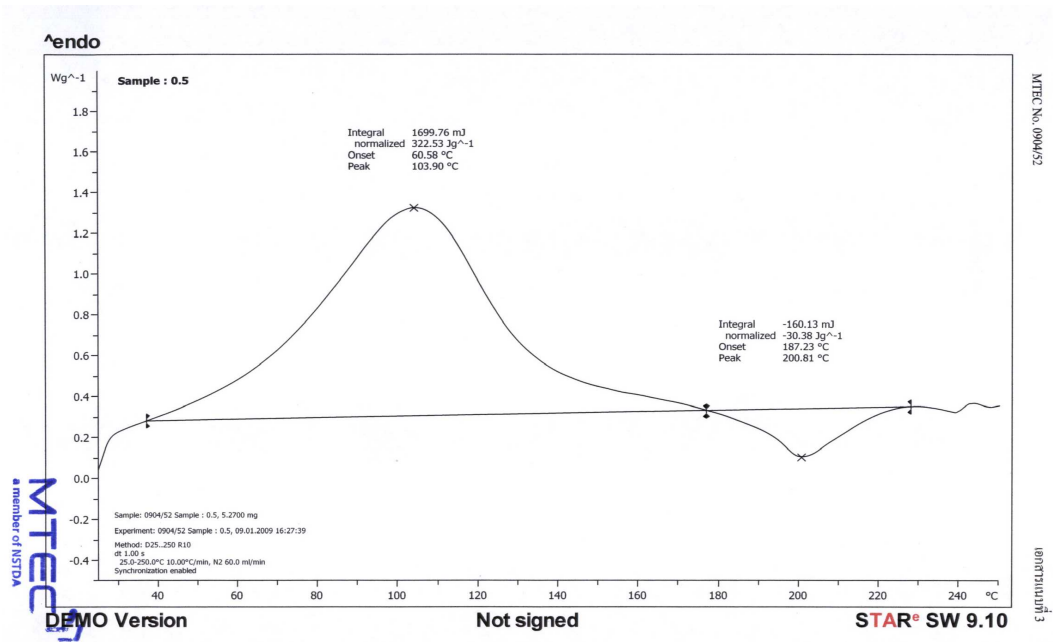
A 19. TGA diagram and Derivative thermal gravimetric (DTG) of sodium chitosan phosphate/zinc oxide complexes at 1:2 equivalent mole.



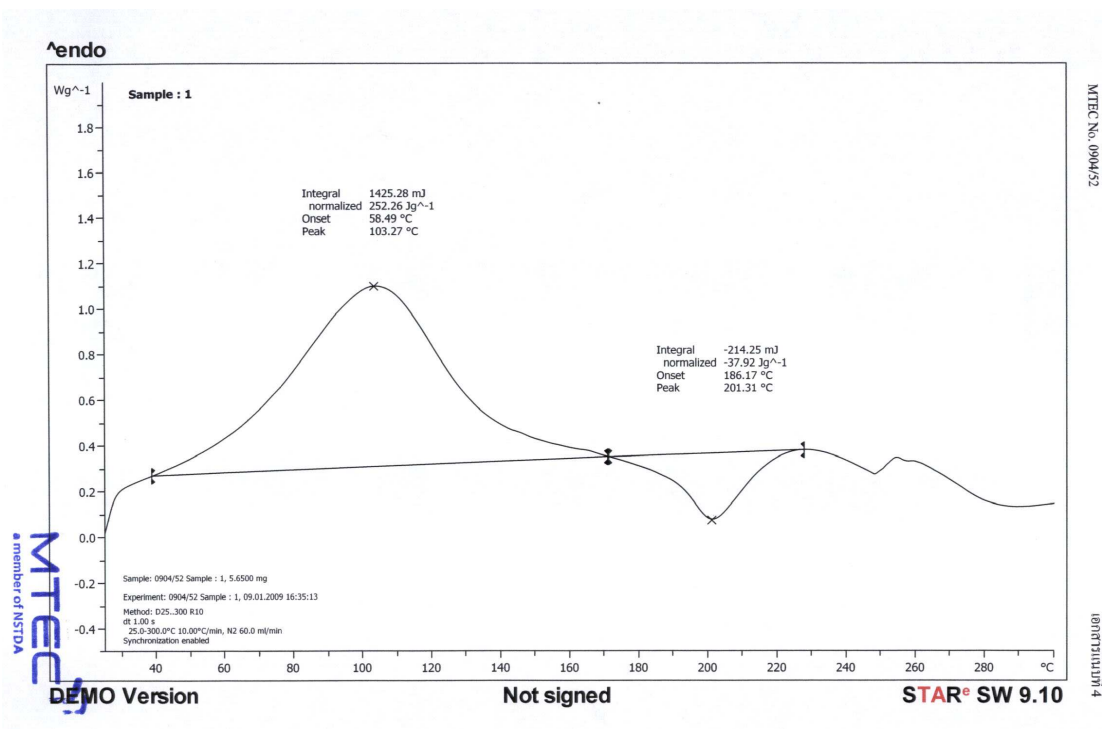
A 20. DSC curve of PCTS.



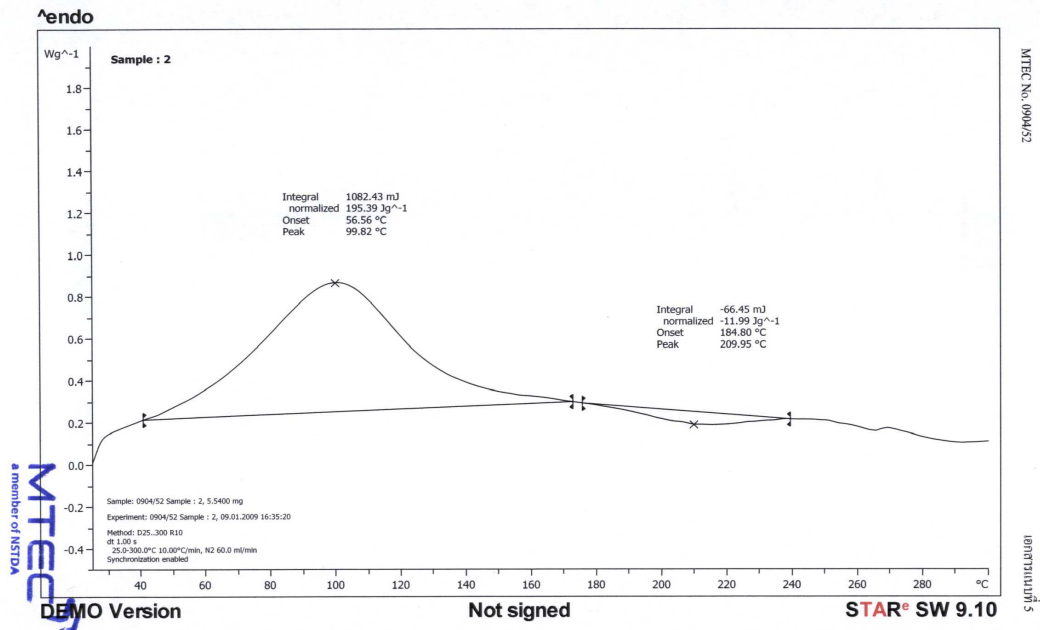
A 21. DSC curve of PCTS/ZnO (1:0.25).



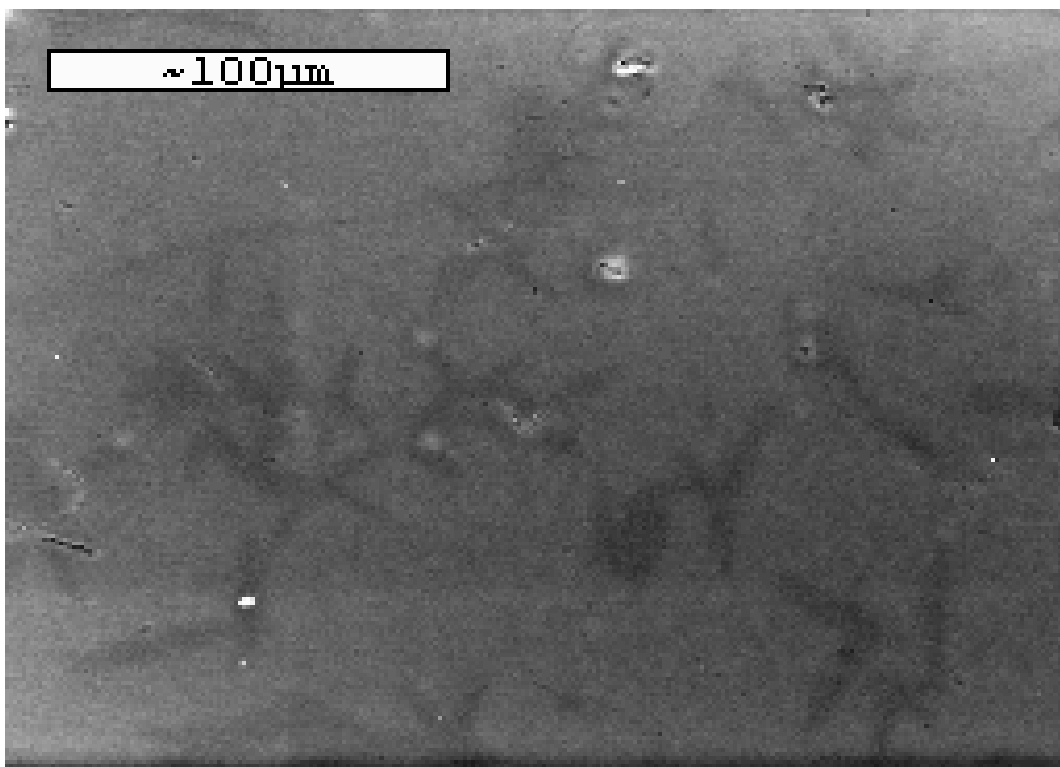
A 22. DSC curve of PCTS/ZnO (1:0.5).



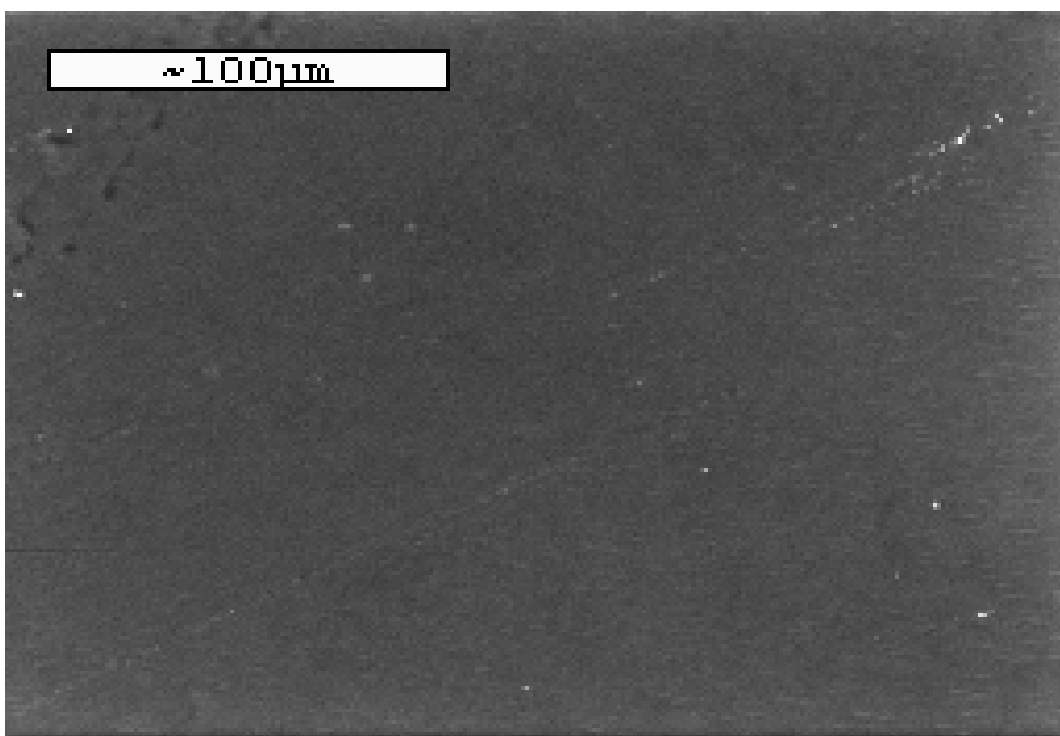
A 23. DSC curve of PCTS/ZnO (1:1).



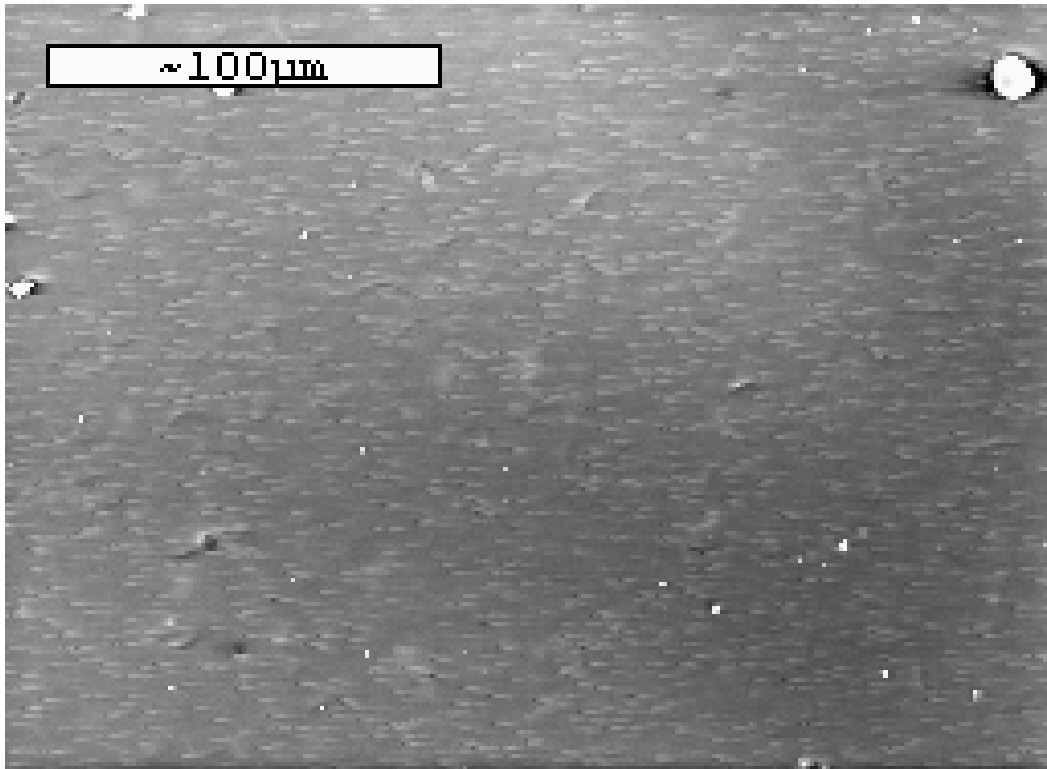
A 24. DSC curve of PCTS/ZnO (1:2).



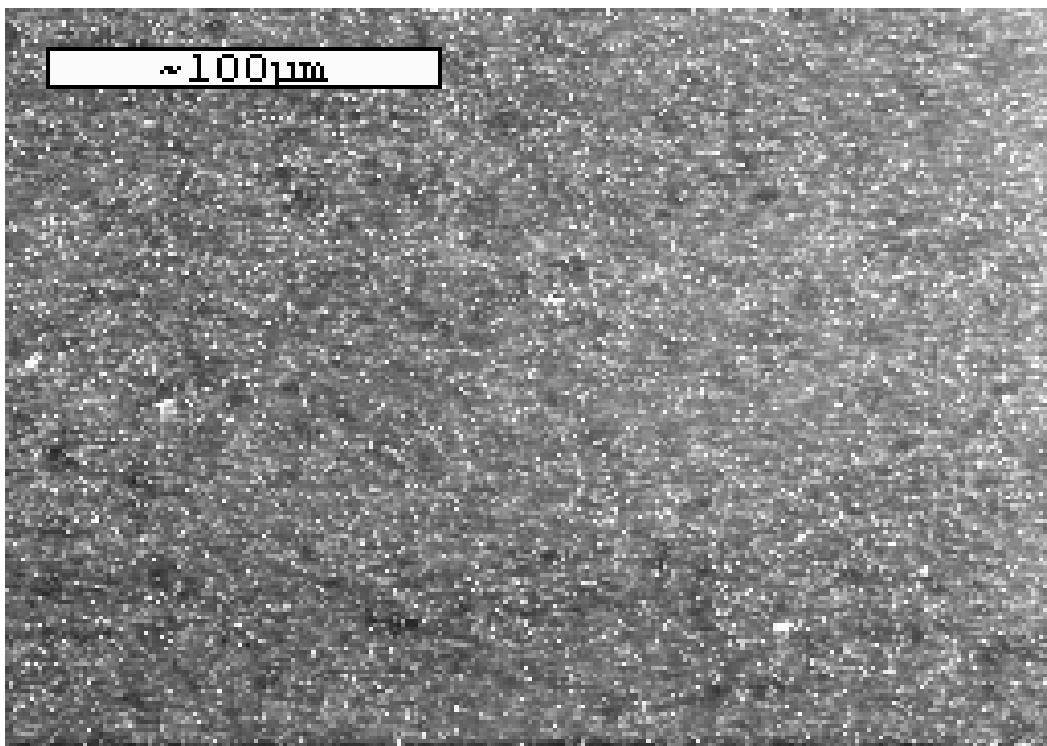
A 25. SEM images of the complexes at 1:0.25.



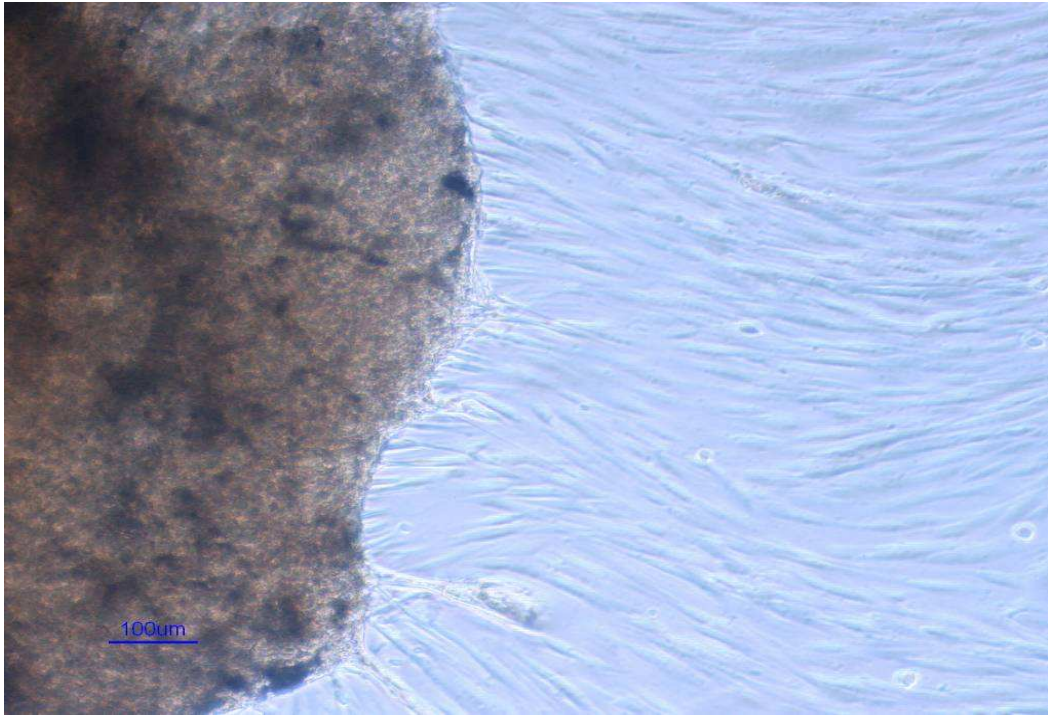
A 26. SEM images of the complexes at 1:0.5.



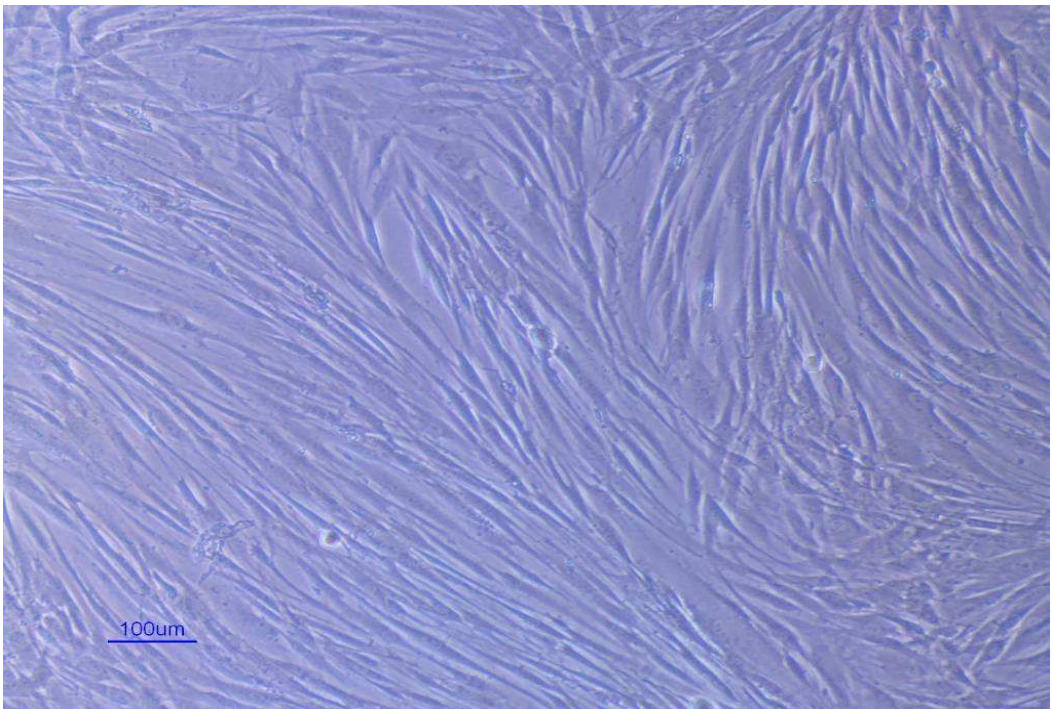
A 27. SEM images of the complexes at 1:1.



A 28. SEM images of the complexes at 1:2.



A 29. Human gingival fibroblast from gingival pieces.



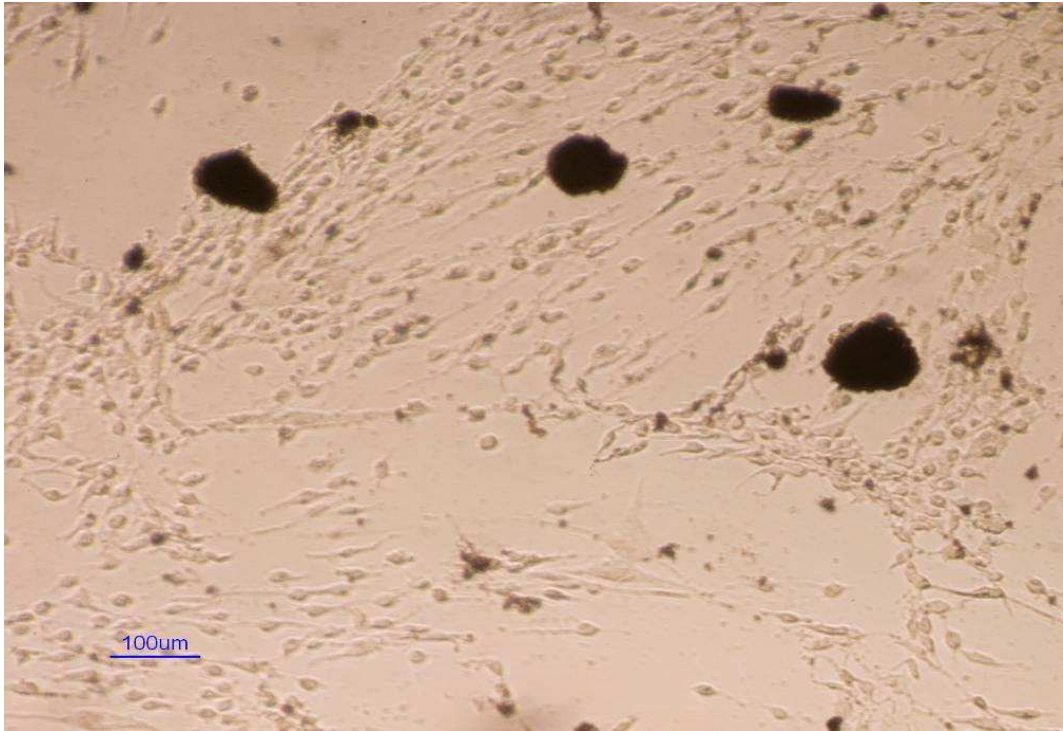
A 30. Human gingival fibroblast at passage 7.



A 31. Human gingival fibroblast at passage 1 in 75 ml plastic flask.



A 32. Immersion of materials into fibroblast media for 24, 48 and 72 hrs.



A 33. Death cells were contacted with zinc oxide.

BIOGRAPHY

Miss Veeranuch Srakaew was born on May 22, 1978 in Bangkok Thailand. She graduated with Bachelor Degree of Chemical Industry at King's Mongkut Institute of Technology North Bangkok in 1999. After that, she graduated with Master Degree in Polymer Technology at King's Mongkut Institute of Technology Ladkrabang in 2003. Next, she went to work at Thai Epoxy Resin Co., Ltd at Rayong for 3 months. In 2004, she went to work at Chandrakasem Rajabhat University during her work at here, she was admitted into Philosophy Doctor Program in Materials Science at Chulalongkorn University in 2005 and she received a scholarship from Chandrakasem Rajabhat University. She completed her study program of the Ph.D in Materials Science in 2008.